

2017

Home Sweet Home: Epigenetic Paths of Stem Cells In and Out of Their Niche

Rene C. Adam

Follow this and additional works at: http://digitalcommons.rockefeller.edu/student_theses_and_dissertations



Part of the [Life Sciences Commons](#)

Recommended Citation

Adam, Rene C., "Home Sweet Home: Epigenetic Paths of Stem Cells In and Out of Their Niche" (2017). *Student Theses and Dissertations*. 401.
http://digitalcommons.rockefeller.edu/student_theses_and_dissertations/401

This Thesis is brought to you for free and open access by Digital Commons @ RU. It has been accepted for inclusion in Student Theses and Dissertations by an authorized administrator of Digital Commons @ RU. For more information, please contact mcsweej@mail.rockefeller.edu.



**HOME SWEET HOME: EPIGENETIC PATHS OF STEM CELLS
IN AND OUT OF THEIR NICHE**

A Thesis Presented to the Faculty of
The Rockefeller University
in Partial Fulfillment of the Requirements for
the degree of Doctor of Philosophy

by

Rene C. Adam

June 2017

HOME SWEET HOME: EPIGENETIC PATHS OF STEM CELLS IN AND OUT OF THEIR NICHE

Rene C. Adam, Ph.D.

The Rockefeller University 2017

Adult stem cells reside in niches, which control their long-term ability to self-renew and produce the differentiated cell lineages necessary to regenerate and repair their tissues. Following injury, culture or transplantation, stem cells outside their niche often acquire broader plasticity in fates. In my graduate work, I showed that super-enhancers underlie the identity, lineage commitment and plasticity of adult stem cells *in vivo*. My chosen model is the hair follicle, where its stem cells (HFSCs), niche and master regulators are well-characterized. By mapping global chromatin domains of HFSCs in their native niche, and of committed progenitors, I discovered that super-enhancers and their dense clusters ('epicenters') of transcription factor binding sites change dramatically upon lineage progression. New fate is acquired by decommissioning old and establishing new super-enhancers, an auto-regulatory process that abates one master regulator subset while enhancing another. I showed that epicenters dictate tissue-specific and lineage-specific reporter expression *in vivo*, yielding powerful genetic tools to drive unprecedented lineage-specificity. Exploiting the ability to culture and transplant HFSCs, I found that intriguingly, when outside their niche and faced with a new environment, HFSCs dynamically remodel super-enhancers, including those driving master identity genes. *In vitro*, new super-enhancers emerge which drive genes induced upon wound-

healing *in vivo*. Cultured HFSCs adapt to this perceived wounding state by activating different epicenters within the super-enhancers of key SC-identity genes. Probing mechanism, I identified SOX9 as the crucial chromatin regulator of super-enhancers. While high levels maintain HFSC fate and absence results in alternative fates, low levels, e.g. during wound-repair, early lineage progression or culturing, permit fate plasticity. I showed that ectopically expressing SOX9 in epidermis activates polycomb-repressed super-enhancers of HFSC determinants, while sustaining SOX9 in the hair lineage prevents the super-enhancer lineage switch. Cultured HFSCs silence other super-enhancer-driven determinants, but retain low SOX9, endowing them with the plasticity to make both SOX9-negative epidermis and SOX9-positive HFs upon engraftment. Together, my findings expose super-enhancers as dynamic and dense transcription factor binding platforms which are exquisitely sensitive to master regulators. Furthermore, by harboring distinct epicenters, super-enhancers possess the ability to adjust reversibly to microenvironmental cues that transiently change transcriptional landscapes.

In a second line of research, I focused on functional analyses to uncover the role of super-enhancer regulated, putative stemness genes. I found that NFI transcription factors (NFIB and NFIX) act redundantly in mouse skin to maintain the undifferentiated state of progenitors in hair follicles, sebaceous glands and sweat glands. Combining gene expression and chromatin profiling, I discovered that NOTCH signaling, known to drive terminal differentiation in epidermis, is ectopically induced in NFI-deficient HFSCs. These findings provide novel insights into how progenitor status is maintained by a family of transcription factors ubiquitously active in skin appendages.

ACKNOWLEDGMENTS

There have been numerous people who have helped me during the course of my thesis and some of whom without which it simply would not exist.

First and foremost I owe an enormous debt of gratitude to my advisor Dr. Elaine Fuchs. Elaine has been a constant source of support and her intellectual input into this thesis is invaluable. I cannot imagine having a supervisor more suited to my personality. She always found the right balance between giving me an appropriate amount of freedom and making sure that I kept on track. I am so grateful that she continuously challenged me to tackle the most exciting problems, and no doubt her confidence in me has motivated and helped me become the scientist that I am today.

I have been fortunate to have good friends in the Fuchs lab who were always eager to discuss science during the progression of this thesis. In particular, I would like to thank Hanseul Yang and Yejing Ge. Both of them always had an open ear and engaged in lively discussions about new ideas. Together, we've always found a way to make things work. More importantly, they have always been supportive and have become good friends during graduate school. It's also been a pleasure to work next to Karen Tumaneng. I couldn't have asked for a better bay-mate. I thank Irina Matos for continuous training on the microscope and for being a constant source of wisdom when it comes to WNT signaling. I am also thankful to Lisa Polak, who managed my mouse lines and always found ways to solve the occasional problems with regard to animal experiments. I am grateful to Ya-Chieh Hsu, who mentored me when I first joined the lab and has been an incredible teacher. I would also like to thank my collaborator Deyou

Zheng for conducting bioinformatics analyses on my datasets. Without the support of all of the above, a substantial amount of this thesis would not exist.

While – unfortunately – it is not possible to mention everyone by name, I want to thank all other members of the Fuchs laboratory who provided integral support to this thesis and have made my time in the laboratory incredibly enjoyable.

The support from several Resource Centers at The Rockefeller University was invaluable to my progress. In particular, I would like to thank Svetlana Mazel, Stanka Semova, Selam Tadesse and Songyan Han at The Flow Cytometry Resource Center for their continuous support of isolating cells by FACS. I thank Christine Lai and Connie Zhao at the Genomics Core for assistance in high throughput DNA sequencing analysis. I thank the Comparative Bioscience Center for husbandry care of mice. Furthermore, I would like to thank Genomics Resources at Weill Cornell Medical College for assistance with RNA-sequencing experiments.

I also would like to acknowledge Rockefeller's Graduate Program and all the staff at the Dean's Office for supporting my studies. I thank my thesis committee Robert G. Roeder and C. David Allis, as well as my external examiner Angela Christiano for their suggestions, commitment of time, and help in preparing this thesis, as well as for their support in helping me move on to the next step in my career.

Finally it remains for me to thank my family and friends. I want to thank them for their loving support not only during this thesis, but throughout the duration of my studies. I am happy for the pride that they have taken in my work, and for their ongoing encouragement.

TABLE OF CONTENTS

Chapter 1: Introduction.....	1
Adult stem cells: The impact of the microenvironment on lineage choice.....	2
DNA methylation as epigenetic silencing mark.....	5
TET enzymes: novel epigenetic regulators in stem cell lineage progression.....	9
PcG-repressive complexes: safeguards against impromptu lineage choice.....	10
Lineage-specific enhancer selection by pioneer transcription factors.....	15
Transcriptional circuitries within Super-enhancers govern cellular identity.....	18
 Chapter 2: The impact of microenvironment on chromatin dynamics in stem cell plasticity and lineage choice.....	 19
Introduction.....	20
Results.....	21
<i>Super-enhancers govern cell identity genes in HFSCs in vivo.....</i>	<i>21</i>
<i>SEs are enriched in HFSC master transcriptional regulators.....</i>	<i>26</i>
<i>Dynamic remodeling of super-enhancers during lineage progression.....</i>	<i>29</i>
<i>Epicenters as accurate chromatin sensors.....</i>	<i>32</i>
<i>Environmental sensitivity of SEs allows SC adaptation and plasticity.....</i>	<i>36</i>
<i>SOX9 is a master regulator governing HFSC fate and plasticity.....</i>	<i>42</i>
Discussion.....	46
Materials and Methods.....	48
 Chapter 3: The role of Nuclear Factor I transcription factors NFIB and NFIX in the maintenance of skin appendages.....	 58
Introduction.....	59
Results.....	61
<i>Loss of Nfix does not yield overt phenotypes in hair follicles.....</i>	<i>61</i>
<i>NFIB and NFIX function redundantly in murine hair follicles.....</i>	<i>64</i>
<i>NFI-TFs maintain the function of multiple skin appendages.....</i>	<i>69</i>
<i>Molecular insights into HFSC behavior upon loss of Nfib and Nfix.....</i>	<i>71</i>
Discussion.....	76

Materials and Methods.....	81
Chapter 4: Summary and Perspectives.....	86
Dynamic super-enhancer remodeling facilitates lineage progression.....	87
Stem cell behavior and plasticity depends on their microenvironment.....	88
Home sweet home: the impact of niche signals on SC plasticity.....	91
Future Directions.....	92
Appendix.....	94
References.....	125

LIST OF FIGURES

1-1. Schematic of the mammalian hair follicle.....	3
1-2. Dynamic chromatin remodeling during stem cell lineage commitment.....	12
2-1. FACS purification strategy to isolate HFSCs.....	22
2-2. HFSC Super-enhancers are large clusters of active enhancers.....	23
2-3. Assignment of HFSC super-enhancers to corresponding genes.....	24
2-4. SE-associated genes are highly expressed and control transcriptional processes.....	25
2-5. Super-enhancers are enriched for HFSC master TFs.....	28
2-6. Dynamic super-enhancer remodeling facilitates lineage progression.....	30
2-7. Super-enhancer epicenters confer tissue, lineage and temporal specificity.....	33
2-8. Super-enhancer epicenter reporters for differentiating cell lineages.....	35
2-9. The sensitivity of SEs to environmental changes facilitates HFSC adaptation and plasticity.....	37
2-10. Dynamic gene expression changes in HFSCs in culture, upon wounding or transplantation	39
2-11. HFSCs activate different epicenters within super-enhancers to sustain expression of critical genes in different microenvironments.....	41
2-12. SOX9 is essential for HFSC specification and maintenance.....	43
2-13. SOX9 is a master regulator governing HFSC fate.....	44
2-14. Sustained Sox9 in committed progenitors perturbs lineage progression.....	45
3-1. NFIX expression pattern in skin during development.....	62
3-2. Ablation of Nfix in adult HFSCs does not perturb HF morphology or function.....	63
3-3. NFI-dKO mice show dramatic alterations in HF morphology.....	65
3-4. Ectopic epidermal differentiation in NFI-deficient hair follicles.....	67
3-5. Morphological and molecular changes in the NFI-dKO HFSC niche.....	68
3-6. Loss of NFI-TFs affects multiple skin appendages.....	70
3-7. RNA-seq analysis on NFI-dKO HFSCs.....	72
3-8. Changes in chromatin accessibility in NFI-dKO HFSCs.....	74
3-9. Activation of epidermal transcriptional regulators in NFI-dKO hair follicles.....	77
4-1. Super-enhancer epicenters represent accurate chromatin sensors.....	89

LIST OF TABLES

2-1. Selected list of HFSC super-enhancer regulated genes <i>in vivo</i>	26
2-2. Selected list of TAC super-enhancer regulated genes <i>in vivo</i>	31
2-3. Selected list of HFSC super-enhancer regulated genes <i>in vivo</i>	38
2-4. Complete list of super-enhancer regulated genes in HFSCs <i>in vivo</i>	94
2-5. Complete list of super-enhancer regulated genes in TACs <i>in vivo</i>	103
2-6. Complete list of super-enhancer regulated genes in HFSCs <i>in vitro</i>	112
3-1. Selected list of differentially expressed genes (WT vs. NFI-dKO).....	73

LIST OF ABBREVIATIONS

ATAC-seq	Assay for transposase-accessible chromatin using sequencing
ChIP	Chromatin immunoprecipitation
cKO	Conditional knockout
DP	Dermal papilla
dKO	double conditional knockout
EC	Epicenter
EGFP	Enhanced green fluorescent protein
Epi-SCs	Epidermal stem cells
FACS	Fluorescence-activated cell sorting
HFSCs	Hair follicle stem cells
HG	Hair germ
HS	Hair shaft
IP	Immunoprecipitation
IRS	Inner root sheath
KO	Knockout
LV	Lentiviral vector
NFI	Nuclear Factor I
ORS	Outer root sheath
PBS	Phosphate buffered saline
qPCR	Quantitative polymerase chain reaction
RFP	Red fluorescent protein
RNA-seq	RNA-sequencing
SE	Super-enhancer
TACs	Transit-amplifying cells
rtTA	Reverse tetracycline-controlled transactivator
TAM	Tamoxifen
TRE	Tetracycline response element
WT	Wild type
YFP	Yellow Fluorescent Protein

Chapter 1: Introduction

Adult stem cells: The impact of the microenvironment on lineage choice

Adult organisms rely on tissue stem cells for maintenance and repair. Tissue stem cells reside in specialized niches, which profoundly impact their activity and maintenance (Morrison and Spradling, 2008; Scadden, 2014). These cells are characterized by their ability to self-renew for long-term and to produce differentiated cell lineages. As such, they are used sparingly and their main function is regenerate tissue upon demand. During homeostasis, the concerted action of niche signals and epigenetic regulators establish stable gene expression patterns to ensure that stem cells are not lost over time. However, stem cells also provide host tissues with remarkable plasticity to respond to perturbations: The fate and multi-lineage potential of stem cells can change depending on whether a stem cell exists within its resident niche, whether it is mobilized to repair a wound, or whether it is challenged to *de novo* tissue morphogenesis after expansion in culture and following transplantation (Blanpain and Fuchs, 2014). Thus, cellular plasticity is the ability of stem cells to adapt to new microenvironments outside the niche and survive in limbo. Plasticity is not tested until cells are faced with a new microenvironment.

Skin is a great model system to illustrate and study features of plasticity. In most mammals, the epidermis has a dense array of hair follicles, which typically make negligible contribution to epidermal homeostasis. The stem cells in the hair follicle (HFSCs) reside in a specialized niche, termed the ‘Bulge’ of the follicle (Figure 1-1). During homeostatic regeneration, when HFSCs become transiently activated to regenerate new hair, HFSCs typically give rise to transit-amplifying progeny (‘Matrix’), which go on to differentiate and produce the mature hair and its channel. Thus, the main function of HFSCs is to produce hair (Figure 1-1).

Upon injury, however, hair follicle SCs (HFSCs) efficiently migrate out of their niche and into the epidermis, where they contribute long-term to wound repair. In the process, these stem cells lose hair follicle markers and adopt features of epidermal stem cells (Ito et al., 2005). Curiously, plasticity is not a feature that is limited to SCs.

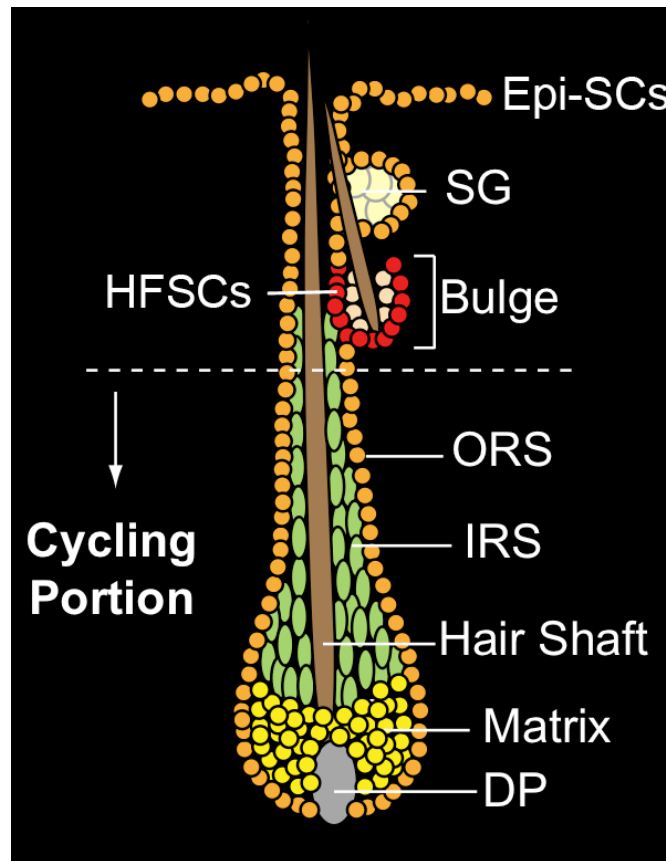


Figure 1-1. Schematic of the mammalian hair follicle. Hair follicle stem cells (HFSCs) are located in a niche called ‘the bulge’, in which they typically remain in a quiescent state (red cells). Upon activation of the hair cycle, HFSCs self-renew transiently and give rise to transit-amplifying ‘Matrix’ progenitors. Matrix cells, in turn, adopt one of seven fates and ultimately give rise to the mature hair (Hair Shaft) and its channel (Inner Root Sheath, IRS). Outer Root Sheath (ORS) cells are immediate HFSC progeny and form the barrier between epidermal and dermal lineages. Dermal Papilla (DP) cells serve as mesenchymal stimulus to coordinate multi-lineage hair growth. The sebaceous gland (SG) produces oil and keeps skin lubricated. Epidermal stem cells (Epi-SCs) replenish differentiating cells to provide the barrier function of the skin.

After ablation of epithelial stem cells, either by laser or using diphtheria toxin, the empty niche can recruit and induce normally committed cells to proliferate and revert back to a progenitor-like state. Indeed, HFSCs can be replaced by committed cells above the niche, while hair germ cells can be readily replenished if hair follicle stem cells are intact (Rompolas et al., 2013). Similarly in the intestinal crypt, loss of LGR5+ stem cells triggers dedifferentiation of committed precursor cells into functional stem cells, which then repopulate the crypt (van Es et al., 2012; Buczacki et al., 2013). Collectively, these studies have uncovered the dramatic plasticity within mammalian tissues following injury. Stem cells can acquire greater fate flexibility to replenish multiple lineages, whereas upon stem cell loss, their progeny and even differentiated cells may dedifferentiate to repair tissue damage.

Although plasticity is a well-described phenomenon across multiple SC populations, the mechanisms how adult SCs choose and acquire new fates are unknown. Changes in the niche microenvironment allow SCs to exit the niche and make tissue and/or repair wounds. However, this poses a dilemma for SCs: how can they retain their ability to survive outside the niche, how do they choose appropriate fates and what defines the point of reversibility versus commitment to differentiation? The notion that stem cells acquire greater fate flexibility after injury or transplantation suggests that besides the impact imposed on stem cells by their native niche, additional mechanisms must be in place to govern stem cell identity, fate decisions and plasticity.

While genome-wide chromatin mapping of cultured embryonic SCs and other cell types have provided new insights into cellular states, *in vitro* mRNA and protein expression profiles have long been known to differ quite dramatically from their *in vivo*

tissue counterparts. Such observations suggest that gene expression, and likely chromatin dynamics, of stem cells will also be highly dependent upon their native niche microenvironment. If so, tackling the mechanisms underlying chromatin dynamics and their physiological relevance will necessitate *in vivo* analyses. This is especially important for adult stem cells, where there are often multiple steps in lineage commitment that cannot be easily understood or recapitulated outside the confines of the tissue. Indeed, even with the handful of recent *in vivo* studies conducted thus far, it is already clear that cell-intrinsic, dynamic chromatin modifications play major roles in adult stem cells, which make lineage choices by integrating changes in niche signals with transcriptional circuitries that determine cell identity.

In this chapter, I explore the emerging role of chromatin modifiers and master transcription factors in adult stem cell fate decisions and plasticity, which ensure that selective lineage choices are only made when environmentally cued. By focusing on various adult stem cell populations, I will summarize recent advances on chromatin dynamics that have contributed to the emergence of new concepts in stem cell biology.

DNA methylation as epigenetic silencing mark

Although the full complexity of epigenetic regulation is only starting to unveil, DNA methylation is of particular relevance for tissue homeostasis. DNA methylation provides a means for functional variability while maintaining the information content of the nucleotide: In mammals, the fifth carbon of the pyrimidine ring of CpG dinucleotides can become methylated (5mC) (Bergman and Ceder, 2013). Due to the spontaneous deamination of 5mC, C→T transitions at CpG dinucleotides account for >30% of all

point mutations in human genetic disorders.

During development, CpG methylation is established by *de novo* DNA methyltransferases DNMT3A and DNMT3B (Smith and Meissner, 2013). The 5mC pattern is then faithfully preserved by DNMT1, which is targeted to hemimethylated DNA by UHRF1 during DNA replication (Sharif et al., 2007). While the majority of cytosine residues within CpG dinucleotides are methylated, CpG islands at promoters remain mostly unmethylated, a feature that has long been surmised to create a permissive environment for transcription initiation (Schuebeler, 2015). CpG islands are short sequences of DNA with over-representation of CG dinucleotides compared to the genomic average. 40–70% of human promoters contain CpG islands.

Indeed historically, DNA methylation has been considered a stable silencing mark, ensuring tissue-specific gene expression in a heritable manner throughout development. As such, DNA methylation is critical for control of gene transcription, establishment of cellular identity, silencing of transposon elements, parental imprinting and X-chromosome inactivation (Smith and Meissner, 2013).

The presence of 5mC is thought to inhibit transcriptional activation by preventing the binding of many transcription factors to DNA and by recruitment of methyl-binding proteins (e.g. MeCP2 or MDB1) and histone deacetylases, which ultimately generate a repressed chromatin environment (Klose and Bird, 2006). However, recent evidence suggests that DNA methylation is more dynamic than hitherto appreciated. Although 5mC can be lost passively through imperfect maintenance, the discovery of ten-eleven translocation (TET) family enzymes provided a compelling means for catalyzed active demethylation (Tahilani et al., 2009). TET enzymes first convert 5mC into 5-

hydroxymethylcytosine (5hmC), which can subsequently be reverted to cytosine through iterative oxidation and thymine DNA glycosylase (TDG)-mediated base excision repair (He et al., 2011; Ito et al., 2011; Zhang et al., 2011).

Dynamic DNA methylation is achieved by the interplay between DNMT and TET enzymes, and becomes a powerful strategy to regulate gene activity, as was recently found for stem cell lineage progression. Even though global changes are modest, dynamic DNA methylation/de-methylation in adult stem cells occurs specifically in regulatory regions of developmental genes and correlates with the presence of cell-type specific transcription factors (Stadler et al., 2011; Ziller et al., 2013). Hence, differentiation-associated gene promoters are frequently methylated in blood or skin stem cells, yet lose this repressive mark upon fate commitment. Concomitantly, regulatory elements of other lineages become increasingly methylated to lock cells in their differentiated fate (Khavari et al., 2010; Bock et al., 2012; Hodges et al., 2011).

Although DNA methyltransferases are dispensable for self-renewal of embryonic stem cells (Tsumura et al., 2006), DNMT1 is essential for the maintenance of epithelial (Sen et al., 2010; Li et al., 2012; Pathania et al., 2015), mesenchymal (Tsai et al., 2012) and hematopoietic stem cells (Broske et al., 2009; Trowbridge et al., 2009). Depletion of DNMT1 from skin stem cells causes aberrant differentiation due to marked de-repression of epidermal differentiation genes (Sen et al., 2010; Li et al., 2012). Mice conditionally targeted for *Dnmt1* also exhibit progressive alopecia owing to self-renewal defects and increased apoptosis in hair follicle stem cells (Li et al., 2012). *Dnmt1*-null hematopoietic stem cells similarly show premature exhaustion (Broske et al., 2009; Trowbridge et al., 2009). Despite global hypomethylation, DNMT1-deficient hematopoietic stem cells

selectively induce myeloid-progenitor transcription factors and display a skewed distribution towards myeloid fates, at the expense of the lymphoid lineage (Broske et al., 2009). In contrast, loss of *de novo* DNA methyltransferase DNMT3A results in hematopoietic stem cell expansion and impaired differentiation (Challen et al., 2011). Combined loss of DNMT3A/DNMT3B is synergistic, resulting in enhanced hematopoietic stem cell self-renewal and greatly exacerbated defects in differentiation (Challen et al., 2014). Collectively, these studies indicate that DNA methyltransferases have distinct functions in adult stem cells. DNMT1 may serve to balance alternative fates by protecting stem cells from premature activation of predominant differentiation programs, whereas DNMT3A/B appear to license the differentiation program.

The impact of DNMTs on adult stem cell lineage progression has long been attributed to a generally repressive function of DNA methylation, irrespective of position and density of CpG motifs (Schuebeler, 2015). Recent evidence adds new dimensions to this traditional view. Similar to hematopoiesis, neurogenesis critically depends on DNMT3A, which exerts a dual role in neural stem cells (Wu et al., 2010). On the one hand, DNMT3A represses glial-differentiation genes by methylating CpG islands. On the other hand, it promotes the expression of neurogenic genes by functionally antagonizing Polycomb-mediated gene silencing by methylating non-proximal promoter elements, including gene bodies (Wu et al., 2010). Indeed, recent advances in genome-scale mapping have demonstrated that intragenic methylation is quite prevalent in actively transcribed genes, where it is thought to promote transcriptional elongation, suppress alternative promoters and potentially influence splicing (Jones, 2012; Maunakea et al., 2010; Maunakea et al., 2013). *De novo* methylation of active genes is coupled with

H3K36me₃, a histone modification associated with transcriptional elongation, which can directly be recognized by DNMT3B via its PWWP domain (Ambrosi et al., 2017; Neri et al., 2017; Baubec et al., 2015). These findings have nurtured our understanding that the impact of DNA methylation on transcriptional activity is more nuanced than previously appreciated.

TET enzymes: novel epigenetic regulators in stem cell lineage progression

DNA methylation must be dynamic to ensure tissue homeostasis. The discovery of TET enzymes provided the long-sought demethylases that remove CpG methylation marks on DNA (Tahilani et al., 2009; He et al., 2011; Ito et al., 2011; Zhang et al., 2012). The specific enrichment of 5hmC in mammalian brain suggests that TET-mediated hydroxymethylation, providing an intermediate step in DNA demethylation, is particularly critical for neuronal development and brain function: When *Tet1* is conditionally targeted for ablation in mice, neural stem cell expansion is impaired due to promoter hypermethylation of pro-proliferative genes, which in turn leads to impaired hippocampal neurogenesis and cognitive disorders (Zhang et al., 2013).

In contrast, TET2-deficiency in the hematopoietic lineage increases stem cell self-renewal, endowing them with a competitive advantage. The outcome is reduced lineage progression and accumulation of premalignant clones (Moran-Crusio et al., 2011; Kunitomo et al., 2012; Ko et al., 2011; Li et al., 2011; Quivoron et al., 2011). Despite the seemingly opposing actions of TET1/2 in different stem cell compartments, these results suggest that tissue-specific de-methylation is indispensable for stem cells to embark upon cellular differentiation programs. However, specific 5hmC readers have now been

identified, suggesting that 5hmC might be more than a de-methylation intermediate but also an epigenetic regulator itself (Mellen et al., 2012; Sprujit et al., 2013). 5hmC is also enriched at lineage-specific enhancers, which are dynamic and frequently become demethylated upon gene activation (Hon et al., 2014).

Although these studies have established a critical role for dynamic DNA methylation in adult stem cells, there is a relative paucity of CpG in the mammalian genome: the majority of CpG islands remain unmethylated during development and stem cell differentiation (Bergman and Cedar, 2013; Smith and Meissner, 2013). If DNA methylation alone regulated chromatin dynamics, there would be a more permissive transcriptional environment than the <50% of genes that are actively expressed in any mammalian cell type. In reality, many genes with unmethylated CpG islands are inactive, either due to a lack of the appropriate transcription factors, or the existence of other epigenetic mechanisms, such as the Polycomb complex, that achieve chromatin silencing (Bergman and Cedar, 2013).

Polycomb-repressive complexes as safeguards against impromptu lineage choice

Polycomb-group (PcG) proteins form multi-subunit chromatin remodeling complexes known as Polycomb repressive complexes (PRC) that orchestrate the sequential modification and compaction of chromatin, resulting in potent repression of target genes (Schwartz and Pirrota, 2013).

The mammalian PRC2 complex consists of EZH2, EED, SUZ12 and RBAP48 subunits. The methyltransferase EZH2 then catalyzes the tri-methylation of histone H3 lysine 27 (H3K27me3) at target gene promoters, which is associated with transcriptional

repression (Schwartz and Pirrota, 2013). Subsequently, the PRC1 complex, comprising CBX, RING1A/B, PH and BMI1 subunits, deposits a mono-ubiquitination mark on histone H2A lysine 119, a modification that impedes RNA polymerase II elongation and promotes chromatin compaction and silencing (Schwartz and Pirrota, 2013). The ability of PRC1 subunit CBX to recognize H3K27me3 facilitates the concerted action of PRC2/1 and thus warrants potent gene silencing, although variant PRC1 complexes can be recruited to initiate silencing in the absence of PRC2 (Tavares et al., 2012; Blackledge et al., 2014) (Figure 1-2).

Since PRC2 is recruited to a large cohort of developmental genes in embryonic stem cells, it has been proposed that PcG-silencing is critical to regulate lineage fidelity by preventing unscheduled induction of non-lineage and differentiation genes. Histone methylation profiles in adult stem cells further support this notion. In skin stem cells, genes associated with stemness are decorated with activating H3K4me3 and H3K79me2 marks, while non-epidermal and differentiation genes are H3K27me3-repressed. Conversely, committed short-lived progeny acquire high levels of H3K27me3 on stemness genes, while differentiation genes lose the repressive mark (Figure 1-2) (Lien et al., 2011). This indicates that, in addition to DNA methylation changes, stem cell lineage progression is governed by the dynamic regulation of PcG-silencing. In contrast to embryonic stem cells, where key developmental genes exist in a bivalent state and display both activating H3K4me3 and PcG-repressive H3K27me3 marks, adult stem cells have very few genes exhibiting this ‘poised’ behavior (Lien et al., 2011). Thus, bivalency may be less critical once tissue lineages have been selected and cell type options have been restricted.

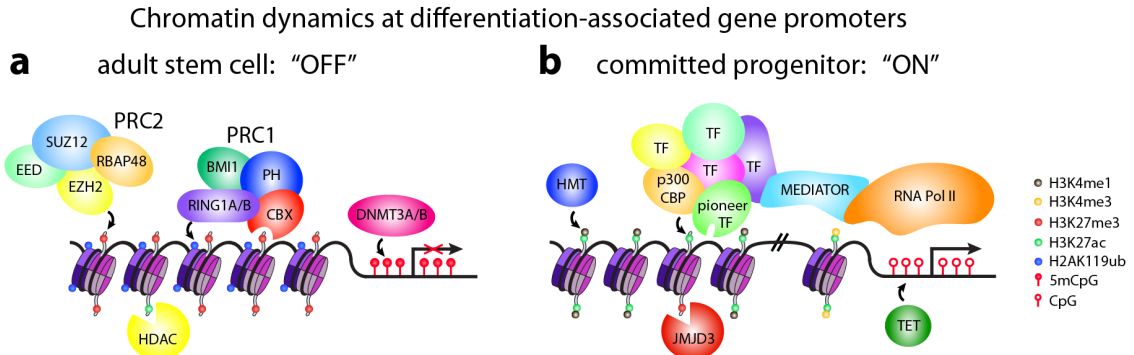


Figure 1-2. Dynamic chromatin remodeling during stem cell lineage commitment.

a, In adult stem cells, differentiation-associated gene promoters are frequently silenced by the concerted action of Polycomb-repressive complexes (PRC) and DNA methyltransferases (DNMT3A/B). The PRC2 component EZH2 deposits the silencing mark H3K27me₃, which can be recognized by the PRC1 moiety CBX. This facilitates PRC1 recruitment and allows for RING1A/B mediated deposition of H2AK119ub, which further leads to chromatin compaction. DNMT3A/B can methylate CpG islands at promoters and contribute to gene silencing, while histone deacetylases (HDACs) remove active chromatin marks (e.g. H3K27ac). This ultimately results in condensed chromatin and potent repression of gene expression.

b, Upon stem cell lineage commitment, dynamic chromatin remodeling is required to induce a program of differentiation. TET enzymes remove 5mCpG through iterative oxidation, whereas histone demethylases (e.g. JMJD3) eliminate repressive chromatin marks (e.g. H3K27me₃). On the other hand, histone methyltransferases (HMTs) establish a permissive chromatin environment, for example by deposition of the H3K4me₁ (at enhancers) or H3K4me₃ (at promoters) marks. Upon external niche stimuli, pioneer factors engage their target sites in silent chromatin, and recruit histone acetyl transferases (p300/CBP, which deposit H3K27ac) as well as other transcription factors. Although the temporal order of chromatin remodeling is unclear, transcription factors at enhancers can eventually be recognized by the Mediator co-activator complex, which recruits RNA Polymerase II to gene promoters, resulting in de-repression of gene activity and the induction of stem cell differentiation.

The expression of PcG proteins highly correlates with developmental stage. Several PRC1/2 subunits are robustly expressed in epidermal and neural progenitors, but their expression wanes in committed cells (Ezhkova et al., 2009; Pereira et al., 2010), which cease proliferation and switch to a program of differentiation. However, fate commitment requires relief of PcG-repression on differentiation gene promoters, a process that depends on the H3K27me3 demethylase JMJD3 (Sen et al., 2008; Park et al., 2014). A similar switch is observed during tissue regeneration after injury, which relies on stem cells and their ability to choose appropriate fates. Upon skin wounding, PRC subunits are repressed, whereas JMJD3 is upregulated at the wound site as the genes needed for repair are rapidly induced (Shaw and Martin, 2009).

Genetic studies have substantiated these roles of PcG-silencing in governing stem cell function. Although loss of EZH2 in embryonic stem cells reduces global H3K27-methylation levels, H3K27me3 on key developmental genes is surprisingly intact. This has been attributed to the activity of EZH1, which can functionally compensate for EZH2 in embryonic stem cells (Shen et al., 2008). Evidence from adult stem cells further support the notion that alternative PRC2 complexes have evolved as safeguards to reinforce cellular identity in mammalian organisms (Ezhkova et al., 2011; Hidalgo et al., 2012). The activation of aberrant lineage fate genes that occurs upon EZH1/2 loss of function is not nearly as high as that normally seen within the proper lineage itself, revealing the combined role of lineage-specific transcription factors and relief of PcG-repression in regulating fate determination (Ezhkova et al., 2011).

In embryonic epidermis, EZH2 controls the proliferative potential of basal progenitors by preventing the premature recruitment of AP1 transcription factors to genes

required for epidermal differentiation (Ezhkova et al., 2009). Intriguingly in adult mice, *Ezh2* deletion has no apparent consequence to skin integrity. In contrast, complete loss of PRC2 function by *Ezh1/2* double conditional knockout in skin abolishes the H3K27me3 mark and severely compromises hair follicle formation and maintenance (Ezhkova et al., 2011; Frye and Benitah, 2012). Although hair follicle stem cell specification is unaffected, PRC2 loss of function specifically affects stem cell self-renewal and hence tissue regeneration and wound repair. Deletion of EZH2 in blood progenitors similarly compromises fetal liver hematopoiesis but not the self-renewal capacity of adult hematopoietic stem cells in bone marrow (Mochizuki-Kashio et al., 2011). Instead, adult hematopoietic stem cells rely more on EZH1, which promotes a slow cycling state and prevents differentiation and senescence (Hidalgo et al., 2012). Insights obtained from EZH2-deficient neural and muscle stem cells further support the critical role of PcG-repression in stem cell self-renewal (Hwang et al., 2014; Juan et al., 2011).

Mechanistically, the inability of PcG-deficient adult stem cells to proliferate is deeply rooted in untimely activation of the *Ink4a/Arf/Ink4b* locus (Ezhkova et al., 2011; Hidalgo et al., 2012; Hwang et al., 2014; Juan et al., 2011), which encodes tumor-suppressor proteins that arrest the cell cycle. Genetic deletion or shRNA-mediated suppression of the *Ink4a/Arf* locus restored the proliferation and survival of adult stem cells defective in PcG components (Ezhkova et al., 2011; Hidalgo et al., 2012; Hwang et al., 2014). While these studies have exposed the sensitivity of the *Ink4a/Arf/Ink4b* locus to PcG-repression, it is noteworthy that unlike in embryonic stem cells (Chi and Bernstein, 2009), the global loss of H3K27me3 does not result in widespread differentiation defects. Even though PcG-silenced genes are transcriptionally activated in

hair follicle stem cells in the absence of EZH1/2, the amplitude of non-epidermal/hair follicle differentiation programs are too low to overcome already established stem cell fates (Lien et al., 2011; Ezhkova et al., 2011). Similarly, stable knockdown of SUZ12, a core subunit critical for PRC2 assembly and function, leads to precocious activation of terminal differentiation markers, but is insufficient to cause phenotypic fate switches in intestinal stem cells (Benoit et al., 2012). Thus, even though PcG-silencing places a molecular threshold on the irreversible transition from a multipotent activated stem cell to a differentiation-committed cell, the absence of phenotypic fate switches in PcG-deficient stem cells underscore the importance of additional epigenetic modifiers that have evolved to ensure the reinforcement and maintenance of lineage programs in adult tissues. Indeed, adult SCs seem to couple PcG-silencing with a requirement for cell-type specific transcriptional activators, to ensure that cell identity is robustly maintained during homeostasis and selective lineage choices can only be made when environmentally cued.

Lineage-specific enhancer selection by pioneer transcription factors

Transcription factors shape the precise gene expression pattern required for a cell to perform its unique functions. They dictate cell fates by activating genes critical for the identity of particular cells while concurrently antagonizing lineage-inappropriate genes (Cantor et al., 2008; Pongubala et al., 2008; Schaffer et al., 2010; Qi et al., 2013). Genome-wide studies have demonstrated that the majority of transcription factor binding sites are located in distal ‘enhancers’ (Heinz et al., 2015). Enhancers are functionally defined as short DNA sequences with the potential to increase basal transcription levels from a distance and independently of orientation on DNA. They were initially identified

by studies using viral SV40 DNA in the 1980s, which revealed that sequences remote from gene promoters can readily boost transcription levels (Banerji et al., 1981). Mechanistically, transcription factor binding at enhancers activates a cascade of epigenetic events initiating from recruitment of transcriptional co-activators, to covalent modification (e.g. methylation and acetylation) of histone tails, loss of 5mC levels, and culminating in increased transcriptional output (Figure 1-2) (Hon et al., 2014; Heinz et al., 2015). Thus, enhancers are characterized by nucleosomal depletion, DNaseI hypersensitivity and enrichment of histone acetyltransferase p300/CBP occupancy, suggesting an overall open chromatin structure (Heinz et al., 2015).

Although active promoters and enhancers typically possess H3K27ac, enhancers are characteristically enriched in H3K4me1, in contrast to H3K4me3 found at promoters (Creyghton et al., 2010; Ernst et al., 2011; Heintzman et al., 2009; Rada-Iglesias et al., 2011). Therefore, enhancers can readily be distinguished from promoters by their unique epigenetic modification signatures. That said, recent evidence suggests that promoters and enhancers share common sequence structures and operational characteristics. Enhancers are also enriched for RNA Polymerase II, resulting in active transcription of enhancer-associated RNAs (eRNAs) (Heinz et al., 2015).

Although mammalian genomes contain a vast number of putative enhancers, only a fraction is active within a given cell, raising the question how unique enhancer repertoires are selected. Earlier studies suggest that cell-type specific enhancer selection involves the binding of lineage-determining transcription factors that “prime” enhancers. These so-called ‘pioneer factors’ have the unique ability to engage target sites in condensed chromatin, upon which they trigger nucleosomal remodeling to grant

chromatin access to additional factors (Zaret and Carroll, 2011). As such, pioneer factor binding occurs prior to lineage commitment and employs a chromatin-opening step to establish competence for gene activation. However, pioneer factor binding is also dependent on the chromatin environment. Although certain pioneer factors can bind methylated DNA, H3K9me3 heterochromatic domains represent a barrier and may provide a means for cells to stably retain their fate (Soufi et al., 2012). Thus, histone/DNA modifications and pioneer factors are likely to function synergistically to establish competence for transcription. Well-characterized pioneer factors include forkhead box A (FOXA) factors, GATA-binding (GATA) factors and PU.1 (Zaret and Carroll, 2011), and a recent study established a pioneer factor role for pluripotency factors OCT4, SOX2 and KLF4 (Soufi et al., 2015).

However, most transcription factors, including pioneer factors, are not lineage-specific *per se*. Despite their broader expression pattern, transcription factors may exhibit entirely different binding patterns and regulate non-overlapping sets of target genes in different cell types and tissues (Heinz et al., 2010; Meredith et al., 2013; Gertz et al., 2013; Pimkin et al., 2014), because they often bind concomitantly to DNA as multi-protein complexes, whose composition is typically cell-type specific (Junion et al., 2012; Yan et al., 2013; Wilson et al., 2010; Liu et al., 2014). On the flip side, chromatin accessibility, DNA methylation patterns and enhancer usage are highly variable across different cell types (Rada-Iglesias et al., 2012; Wamstad et al., 2012). As a consequence, cellular identity is the result of the combinatorial action of distinct transcription factor complexes on lineage- and cell-type- specific enhancers.

Transcriptional circuitries within Super-enhancers govern cellular identity

Recent evidence suggests that genes specifying cell identity and function are associated with densely spaced clusters of active enhancers referred to as ‘super-enhancers’ (SEs), which recruit much of the cell's transcriptional apparatus (Whyte et al., 2013; Loven et al., 2013; Hnisz et al., 2013; Suzuki et al., 2017). Initially identified in embryonic SCs, super-enhancers were found to control the expression of genes particularly important in stem cell behavior (Whyte et al., 2013). Although small in number (<5% of total enhancers), super-enhancers differ from typical enhancers by their exceptional size (>10kb) and their particular enrichment for factors generally associated with enhancer activity. These include a high density of H3K27ac and H3K4me1 modifications, increased Mediator subunit MED1 and RNA polymerase II occupancy, enrichment of RNA from transcribed enhancers (eRNA), elevated binding of histone acetyltransferases p300/CBP, as well as generally increased chromatin accessibility as measured by DNase-seq (Hnisz et al., 2013). Importantly, super-enhancers are also characterized by their high density of sequence motifs for cell stage-specific transcription factors. This allows for their concomitant binding, thereby rendering super-enhancer regulated genes particularly sensitive to the key transcription factor cohort. Notably, the genes encoding lineage-specific transcription factors often themselves harbor super-enhancers (Whyte et al., 2013; Adam et al., 2015). The wiring of cell-type specific transcription factors as self-reinforcing circuits within super-enhancers allows for robust maintenance of specific transcriptional landscapes and thus governs cell identity.

Chapter 2:
The impact of microenvironment on chromatin dynamics in
stem cell plasticity and lineage choice

Introduction

Adult stem cells are essential to maintain tissues during homeostasis and wound repair (Blanpain and Fuchs, 2014). They reside in niches, which control their long-term ability to self-renew and produce the differentiated cell lineages necessary to regenerate and repair their tissues (Morrison and Spradling, 2008; Scadden, 2014). Following injury, culture or transplantation, stem cells outside their niche often acquire broader plasticity in fates (Lopez-Garcia et al., 2010; Lu et al., 2012; van Es et al., 2012; Stange et al., 2013; Blanpain and Fuchs, 2014). Thus, although changes in the microenvironment allow stem cells to exit the niche and build or repair tissue, they pose a dilemma for these cells: how can stem cells survive outside their niche, and what defines the point of reversibility versus commitment to differentiation?

Due to their synchronized bouts of quiescence and tissue regeneration, their extraordinary capacity to regenerate tissue, their documented plasticity *in vitro* and in wound repair, and their abundance, hair follicle stem cells (HFSCs) represent a particularly attractive system to address the impact of microenvironment on stem cells and tissue dynamics. Quiescent HFSCs reside in a specialized niche ('bulge'), where they become transiently activated to self-renew and fuel new hair growth with each new hair cycle (Hsu et al., 2014). Prior studies had suggested that hair follicle lineage progression is governed in part by dynamic regulation of Polycomb (PcG)-mediated repression/de-repression typified by a trimethylation mark on lysine 27 of histone H3 (H3K27me3) (Ezhkova et al., 2011; Lien et al., 2011). However, HFSC identity and function are mainly independent of PcG-regulated genes, indicating that additional epigenetic mechanisms underlie the governance of critical cell identity genes.

Although the physiological relevance remained largely unexplored, recent *in vitro* studies on a wide variety of cultured cells suggested that genes controlling unique cellular identities are driven by so-called ‘super-enhancers’ (SE) (Whyte et al., 2013; Loven et al, 2013; Hnisz et al, 2013; Parker et al, 2013). Super-enhancers represent only a fraction of total enhancers, but they encompass exceptionally large chromatin domains that are occupied by a high density of cell-type specific transcription factors (TFs) called ‘master regulators’. The high density of motifs enables transcription factors to bind concomitantly, rendering super-enhancer regulation sensitive to their concentration (Whyte et al., 2013). Super-enhancer domains are also typified by their high density of H3K27 acetylation, rendering them mutually exclusive for PcG-repression. They are also marked by H3K4me1 and regulated by Mediator, a multiprotein complex which brings super-enhancers to promoters to initiate transcription (Whyte et al., 2013; Loven et al., 2013). Since super-enhancers drive the expression of a cell’s most critical genes, I hypothesized that super-enhancer profiling is a promising approach to understand how stem cell identity is maintained *in vivo* and dynamically altered by changes in microenvironment. At the time I began this endeavor, this notion was unexplored.

Results

Super-enhancers govern cell identity genes in HFSCs *in vivo*

To test the potential *in vivo* importance of super-enhancers in adult stem cell dynamics, I began by conducting genome-wide chromatin mapping on quiescent HFSCs purified directly from skin by fluorescence activated cell sorting (FACS) (Fig. 2-1). The Fuchs lab’s prior *in vivo* Chromatin Immunoprecipitation followed by next-generation

sequencing (ChIP-seq) had revealed the identity of a) promoter regions (by their binding of RNA polymerase II and H3K4me3); b) transcribed or silenced genes (by their respective histone modifications H3K79me2 or H3K27me3) (Lien et al., 2011); and c) specific binding sites for HFSC TFs TCF3, TCF4, LHX2, SOX9, NFIB and NFATc1 (Lien et al., 2014; Folgueras et al., 2013; Kadaja et al., 2014; Chang et al., 2013; Keyes et al., 2013). To identify super-enhancers, I additionally mapped HFSC chromatin binding sites for Mediator subunit MED1, H3K4me1 and H3K27ac (Creyghton et al., 2010).

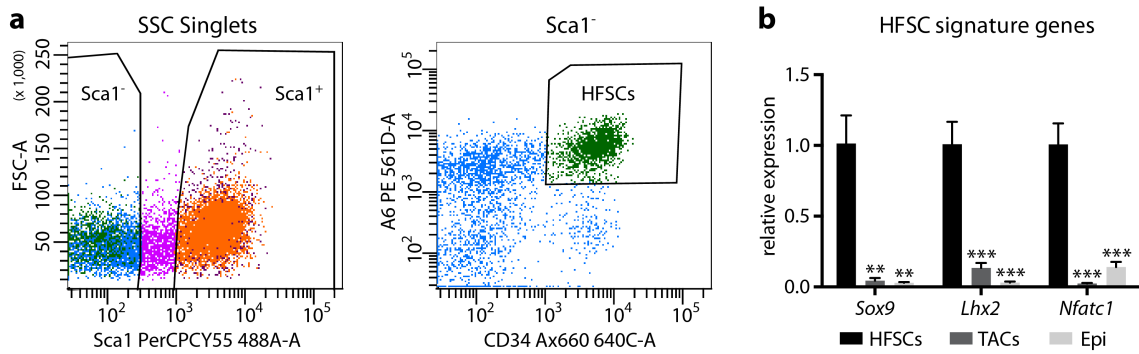


Figure 2-1. FACS purification strategy to isolate HFSCs. a, FACS purification of WT HFSCs for ChIP-Seq according to established markers $\alpha 6^{\text{high}}$ and CD34⁺ (Blanpain et al., 2004). Sca1 was used to remove basal epidermal cells. **b**, qRT-PCR to verify the FACS sorting strategy and measure enrichment of cell-type specific marker genes.

H3K27ac peaks in HFSC chromatin resided within promoters (± 2 kb of annotated genes) (40%) and within distal elements, considered enhancers (60%). Super-enhancers were identified by ranking these enhancers according to increasing H3K27ac occupancy (Whyte et al., 2013). The general features of the 377 HFSC super-enhancers resembled those of cultured embryonic stem cells (Whyte et al., 2013). They spanned ~ 28 kb and were composed of ≥ 5 H3K27ac-enriched clusters (Fig. 2-2).

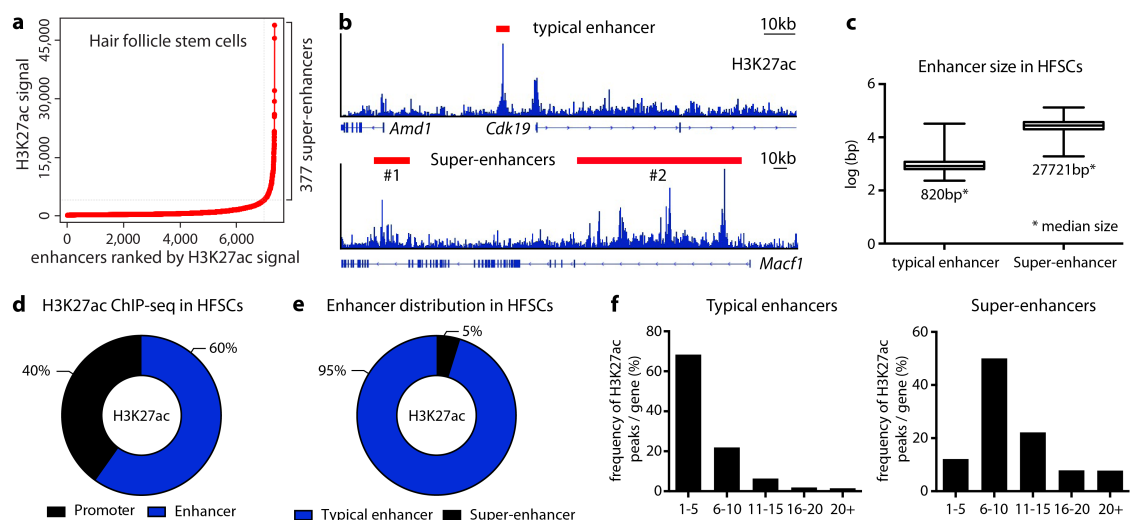


Figure 2-2. HFSC Super-enhancers are large clusters of active enhancers. **a**, Distribution of H3K27ac ChIP-seq signal across all enhancers in HFSCs reveals 377 super-enhancers with exceptionally high levels of H3K27ac. **b**, H3K27ac ChIP-seq occupancy at the *Cdk19* and *Macf1* loci in HFSCs. Red bars denote the location of enhancers. **c**, Enhancer size distribution in HFSCs. Super-enhancers are substantially larger than typical enhancers. **d**, Distribution of H3K27ac ChIP occupancy at promoter and enhancer elements in HFSCs. **e**, Distribution of typical and super-enhancers in HFSCs. Note that super-enhancers represent a small fraction of total enhancers. **f**, Number of individual H3K27ac peaks per gene. Super-enhancers are clusters of H3K27ac peaks and mainly consist of more than 5 peaks per gene. Note: Super-enhancer identification *in silico* performed by Dr. Deyou Zheng.

I then focused on assigning genes to the corresponding super-enhancers. Definitive ChIA-PET analyses of embryonic stem cells established that >80% accuracy in gene assignments for super-enhancers can be achieved simply by applying optimized algorithms that employ RNA-seq and proximity (Downen et al., 2014). Therefore, I began by carrying out these analyses on HFSC super-enhancers. Most of the ambiguities arising from assignments in the absence of ChIA-PET data appeared to involve multiple

expressed genes in close proximity of a super-enhancer (Dowen et al., 2014). I was able to resolve most such ambiguities without ChIA-PET by requiring that the super-enhancer genes must a) exhibit H3K4me3 and H3K79me2 activating marks and lack H3K27me3 repressive histone modifications; and b) maintain a strict correlation between super-enhancer and candidate expression in three different states: HFSCs and their committed progenitors *in vivo*, as well as HFSCs *in vitro* (Fig. 2-3, and see below).

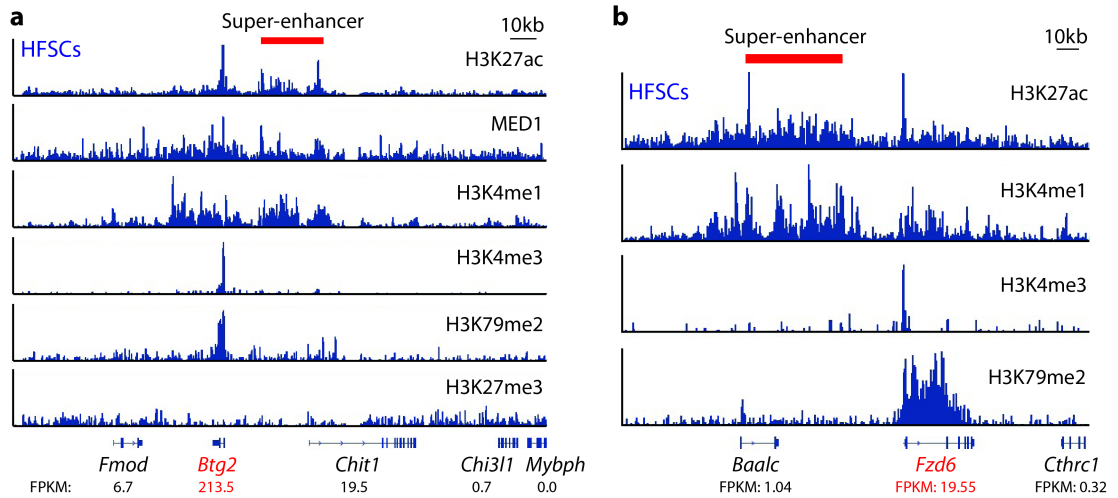


Figure 2-3. Assignment of HFSC super-enhancers to corresponding genes.

Enhancer-gene assignments were done using proximity, as well as additional histone modifications and RNA-seq data. Examples shown are from the *Btg2* (a) and *Fzd6* (b) super-enhancers in HFSCs. MED1, Mediator subunit 1; H3K4me1, poised and active enhancers; H3K4me3, Transcription start site; H3K79me2, elongated transcripts; H3K27me3, Polycomb-group repressive mark. FPKM, fragments per kilobase of transcript per million mapped reads (RNA-seq).

Typical enhancers (1-2kb) governed expression of >90% of HFSC genes, encompassing a large cohort of housekeeping and broadly expressed skin epithelial

genes. By contrast, the small group of Super-enhancer driven genes were highly transcribed in HFSCs and reflected many unique features of their niche microenvironment (Fig. 2-4, Table 2-1).

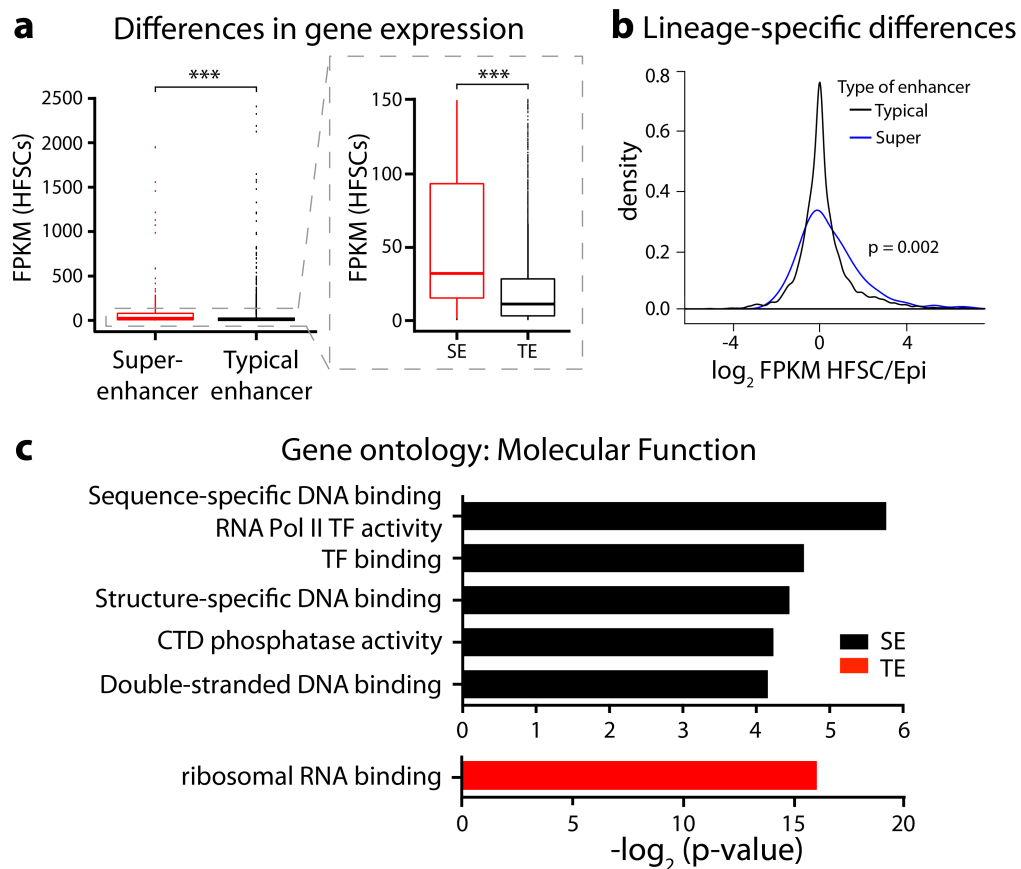


Figure 2-4. Super-enhancer associated genes are highly expressed and control transcriptional processes. **a**, Box and whisker plots showing differences in expression for genes driven by super-enhancers and typical enhancers. SE, super-enhancer; TE, typical enhancer; *** $p < 0.001$. **b**, Density plot, comparing the expression of typical- versus super-enhancer-associated genes in HFSCs compared to epidermal progenitors. Note cell type-specific differences in expression for HFSC genes controlled by super-enhancers but not typical enhancers. **c**, Gene Ontology analysis of genes controlled by HFSC super-enhancers and typical enhancers.

Thus for example, *Bmp6* and its effectors *Bmpr1a*, *Id1* and *Id3* all displayed super-enhancers, consistent with high BMP6 levels in the quiescent HFSC niche (Kandyba et al., 2013). Similarly, WNT inhibitor genes *Sfrp1* and *Dkk3* were regulated by super-enhancers, reflective of the WNT-silenced microenvironment of the quiescent HFSC niche (Lien et al., 2014, Lo Celso et al., 2004). Critical stemness genes such as *Itga6*, *Itgb4* and *Cd34*, were also featured, as were genes linked to human skin disorders (McGrath et al., 1995; Whittock et al., 2002; Schramek et al., 2014).

Table 2-1. List of selected super-enhancer-associated genes in HFSCs

Category	Super-enhancer associated genes in HFSCs <i>in vivo</i>
Transcription, Chromatin	<i>Sox9, Lhx2, Nfatc1, Nfib, Id1, Id3, Trp63, Tfp2a, Grhl2, Barx2, Atf3, Hoxa7, Bcl11b, Nfix, Irx2, Casz1, Tcf12, Klf6, Klf13, Rfx2, Hopx, Zfp36l2, Kat2b, Aff1, Chd2, Chd6, Hdac4, Mll5, Arid5b</i>
Signaling	<i>Bmp6, Bmpr1a, Dkk3, Fzd6, Fgfr2, Fst, Gpsm2, Egfr, Cxcl14, Rac1, Ece1, Src, Ddr1, Aqp3, Prkch, Ctgf, Sfrp1, Ephb6, Shisa2</i>
Cell adhesion, cytoskeleton	<i>Cd34, Macf1, Cdh1, Actn4, Ahnak, Cd9, Actn1, Prickle2, Kank1, Dlgap4, Mllt4, Cd44, Arpc2, Pxn, Mical2</i>
skin disease	<i>Itga6, Itgb4, Myh9, Col17a1, Dsp, Bcl11b, Ttc7, Perp, Fam83g, Nfkb1a, Rin2, Itpr3, Vdr, Rxra</i>

Genes in **blue** have a reported functional role in skin

Super-enhancers are enriched in HFSC master transcriptional regulators

Unbiased gene ontology (GO) analysis further distinguished the list of super-enhancer regulated genes by its preponderance of transcriptional regulators (Fig. 2-4, Table 2-1). *Sox9*, *Lhx2*, *Nfatc1* and *Nfib* were of particular interest to me, since prior genetic studies revealed their roles in maintaining stemness, quiescence and/or crosstalk within the HFSC niche (Kadaja et al., 2014; Folgueras et al., 2013; Keyes et al., 2013; Chang et al., 2013). Moreover, my analyses of *in vivo* HFSC ChIP-seq data revealed that these factors,

and in particular SOX9, bound at high frequency (87%) to super-enhancers, thus serving an autoregulatory role (Fig. 2-5). Notably WNT-effector TCF3 also bound within the majority (92%) of all HFSC super-enhancers, although the *Tcf7l1* enhancer fell just below the assignment cut-off. In fact, >60% of super-enhancers were occupied by ≥ 5 different HFSC-TFs (Fig. 2-5). By contrast, typical enhancers often encoded strong but more broadly expressed genes, and HFSC transcription factor binding events were not similarly distributed within their open chromatin, as evidenced by arbitrarily selecting and analyzing three different cohorts of 377 typical enhancers (and flanking sequences to normalize for their smaller size). Remarkably, the absolute number of transcription factor binding events was stunningly higher in super-enhancers than in size-matched chromatin encompassing typical enhancers. These results suggest that binding of HFSC-specific transcription factors is not dictated by open chromatin per se, but rather by the presence of super-enhancers, which control critical cell identity genes, including themselves.

Along with MED1, the cohort of HFSC-TFs bound within small (1-2kb) chromatin domains scattered across the super-enhancer (Fig. 2-5). Sequence analyses confirmed that these ‘epicenters’ were also richly concentrated with corresponding consensus binding motifs. This clustering of master regulator binding sites within super-enhancers resembled the recently described ‘hotspots’ within SEs of cultured adipocytes (Siersbaek et al., 2014). Notably, only 15 typical enhancers had even one such cluster of HFSC-TF binding motifs, where most super-enhancers had five. Concomitant binding of TFs within these chromatin epicenters, coupled with their repetition over large stretches of chromatin, likely endows these super-enhancers with powerful transcriptional driving activity, and also makes them highly sensitive to transcription factor concentration levels.

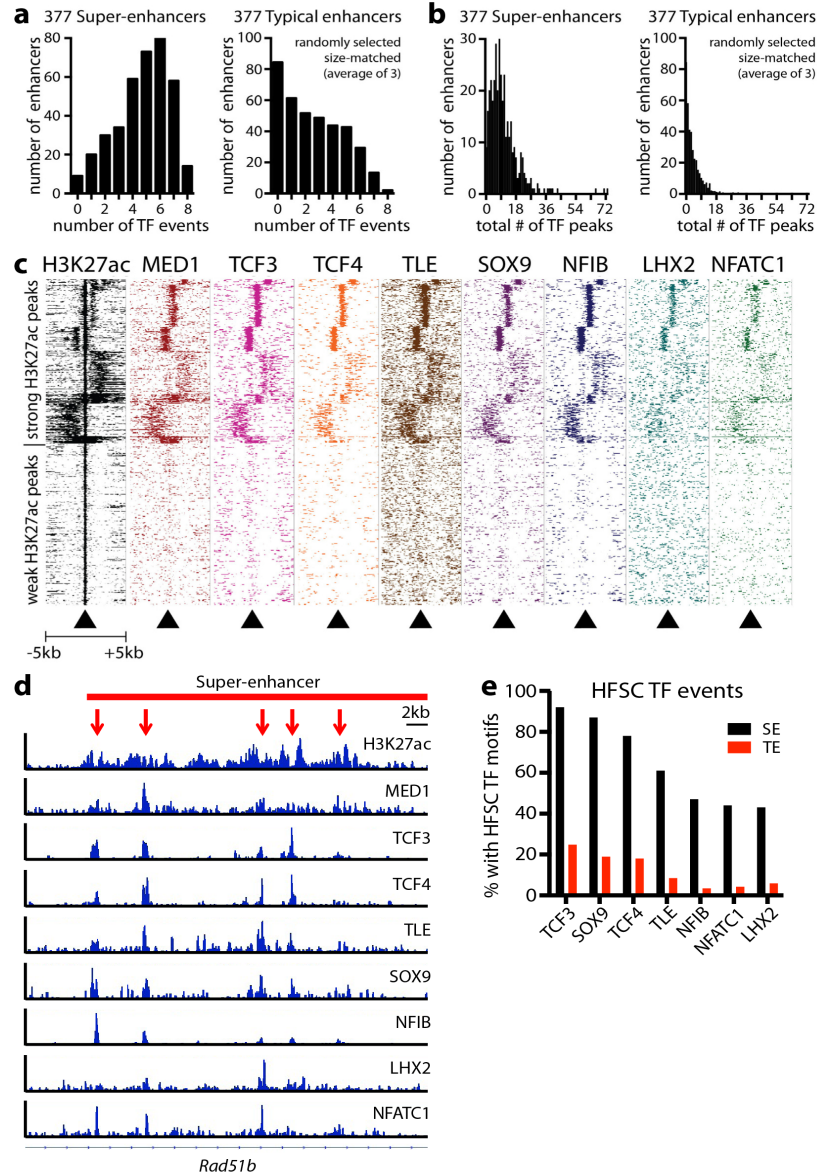


Figure 2-5. Super-enhancers are enriched for HFSC master TFs. **a, b**, Enrichment of HFSC TFs within chromatin of super-enhancers, but not typical enhancers. Comparisons were made with 377 randomly selected typical enhancers and their flanking sequence extended 5' and 3' to match the average kilobase length of super-enhancers (average of 3 analyses is shown). **c**, Heatmap showing ChIP-seq read densities (from -5kb to +5kb of peak center) across H3K27ac peaks located in the super enhancers. **d**, ChIP-seq gene tracks at the *Rad51b* locus illustrate that HFSC-TFs cluster in 'epicenters' (denoted by arrows) within super-enhancers. **e**, Occupancy (ChIP-seq) of HFSC-TFs within SEs. Note: Bioinformatics performed by Dr. Deyou Zheng.

Dynamic remodeling of super-enhancers during lineage progression

Given the auto-regulatory mechanism for the transcription factors of super-enhancers (Whyte et al., 2013), I posited that extensive enhancer remodeling must take place to progress along a lineage and that expression of HFSC TF genes will be lost as a cohort during progression. I tested this hypothesis by FACS-purifying transit-amplifying cells (TACs) and developing genome-wide maps of H3K27ac, H3K4me1 and MED1 occupancy. 381 TAC super-enhancers surfaced which were largely distinct from those of HFSCs (Fig. 2-6). Moreover, HFSC-specific TF genes lost their super-enhancer in TACs, while transcription factor genes linked to the hair lineage gained super-enhancers (Fig. 2-6). Notably, my unbiased analysis revealed that TAC super-enhancers were markedly enriched for binding motifs of many of these TFs (Fig. 2-6). These results added *in vivo* relevance to *in vitro* evidence that differential usage of super-enhancers dictate cell identity (Downen et al., 2014). This was important, since prior collective *in vivo* findings suggested a model whereby typical enhancers are activated or silenced in lineage-specific fashion, but super-enhancers remain open as stem cells progress throughout a lineage (Lien et al., 2011; Luyten et al., 2014; Kim TH et al., 2014).

Like HFSCs, TAC SEs controlled transcription factors and signaling pathways (Table 2-2). TACs use WNT and BMP to govern the seven lineages afforded to TACs, which form the hair and its channel. However, reflective of their distinctive usage of these signaling pathways, TAC and HFSC super-enhancers marked distinct subsets of genes involved in these pathways. Moreover, TAC super-enhancers highlighted cell-cycle related genes, reflective of their highly proliferative state, and NOTCH pathway genes involved in early execution of commitment along a terminal differentiation pathway.

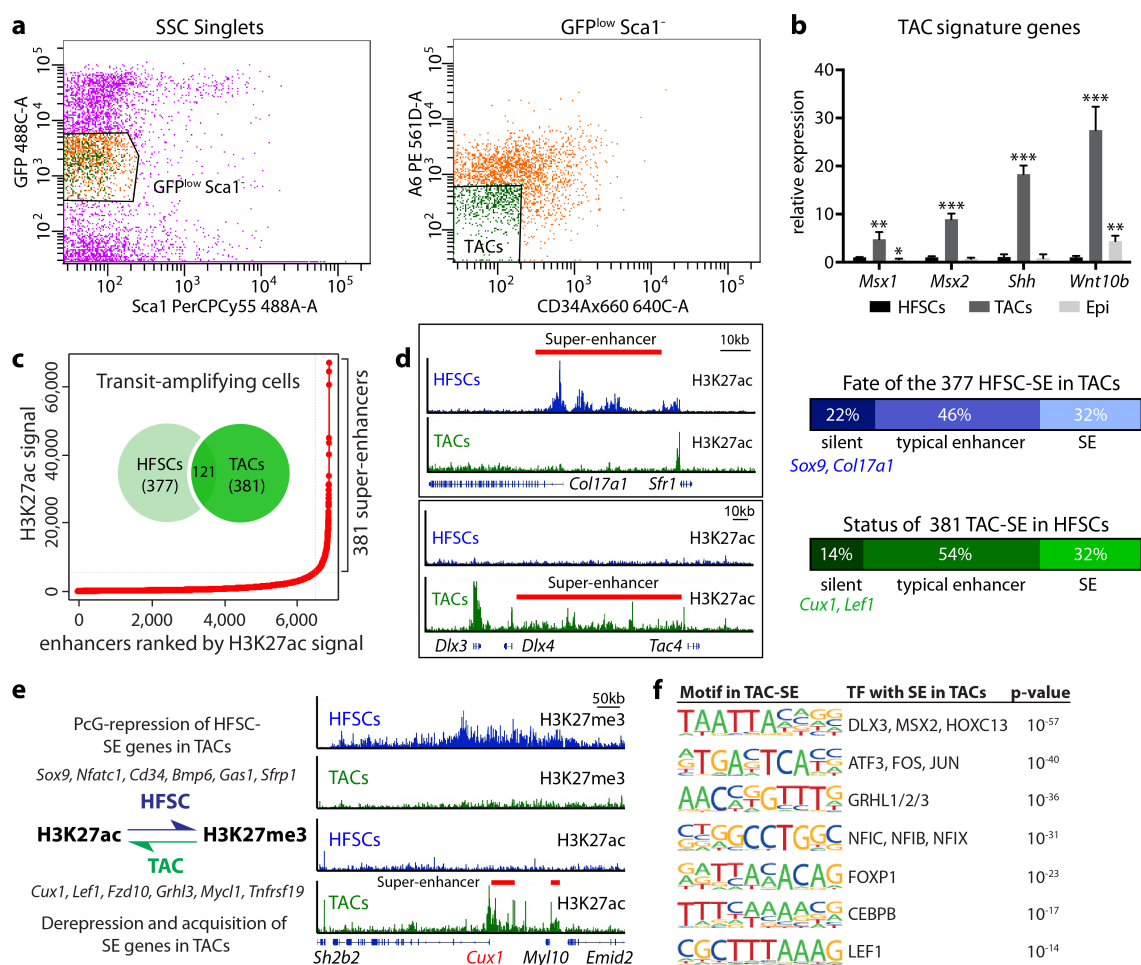


Figure 2-6. Dynamic super-enhancer remodeling facilitates lineage progression. **a**, FACS purification of TACs from *Krt14-H2B-GFP* mice. TACs were GFP^{low} Sca1⁺ α6^{low/-} CD34⁻. **b**, qRT-PCR to verify the FACS sorting strategy and measure enrichment of cell-type specific marker genes. **c**, Distribution of H3K27ac ChIP-seq signal across all enhancers in TACs reveals 381 super-enhancers that share little overlap with HFSC super-enhancers. **d**, Tracking the fate of HFSC and TAC super-enhancers during lineage progression from HFSCs→TACs. **e**, The balance between PcG-repression (H3K27me3) and super-enhancer (H3K27ac) remodeling facilitates lineage progression. Representative example (*Cux1*) showing this swap in H3K27 modifications that occurs upon TAC fate commitment. **f**, Motif analysis of TAC super-enhancers for putative TF binding sites reveals that they are regulated by a new cohort of transcriptional regulators.

Intrigued by the paucity of overlap between HFSC and TAC super-enhancers, I probed the enhancer remodeling that occurs during lineage progression. Only 32% of HFSC super-enhancers persisted, while half were reduced to typical enhancers, suggestive of more subordinate roles in TAC biology. 22% of HFSC super-enhancers became entirely decommissioned in TACs, while many new super-enhancers appeared (Fig. 2-6).

Table 2-2. List of selected super-enhancer-associated genes in TACs

Category	Super-enhancer associated genes in TACs
Transcription	<i>Cux1, Lef1, Msx2, Dlx3, Hoxc13, Hr, Foxn1, Foxp1, Ovol1, Rxra, Mafk, mir31, Cebpb, Fos, Jun, Fosl2, Rara, Runx1, Egr3, Grhl3, Rreb1, Zmiz1</i>
Signaling	<i>Notch1, Notch2, Jag1, Ptch2, Wnt10a, Bmp7, Smad7, ErbB2, Fgfr3, Hes1, Fzd7, Fzd10, Ptk7, Smad6, Rgmb, EphA2, Nrarp, Dazap2</i>
Cell adhesion, cytoskeleton	<i>Jup, Vangl2, Cdc42, Macf1, Pvr1, Itgb5, Amotl2, Dlgap4, Ptpfr, Trio, Mtap7, Emp2, Mical2, Actn4, Pkp4, Kif21a, Pxn, Lad1</i>
Cell cycle	<i>Cdkn1a, Cdkn1b, E2f2, Aurkb, Birc5</i>
skin disease	<i>Tnfrsf19, Nfkb1a, Rin2, Gab1, Gja1, Gjb2, Ets2, Ripk4, St14, Krt17</i>

Genes in green have a reported functional role in skin

Among the HFSC super-enhancers that were decommissioned in TACs were genes that dictate HFSC fate (e.g. *Sox9, Nfatc1, Cd34*) (Fig. 2-6). For this select cohort, the absence of H3K27ac modification was accompanied by H3K27me3 (Lien et al., 2011), which appeared to silence these super-enhancers in TACs (Fig. 2-6). Conversely, specific TAC fate determinant genes (*Cux1, Lef1, Fzd10, Mycl1*) became de-repressed by losing the PcG-catalyzed H3K27me3 marks over a large chromatin domain while simultaneously gaining H3K27ac to expose a new super-enhancer (Fig. 2-6). Another intriguing facet is that 54% of lineage genes that gained a super-enhancer in TACs were already expressed in HFSCs, where they were driven by typical enhancers (Fig. 2-6). For

these genes, lineage progression appeared to be dependent on the dynamics of super-enhancers but independent of PcG-mediated changes. Notably, overall gene expression levels correlated well with super-enhancer dynamics. Genes with novel super-enhancers in TACs were more highly expressed in TACs than in HFSCs. In this way, SEs can provide an epigenetic readout to gauge transcriptional levels within a lineage.

Epicenters as accurate chromatin sensors

To address the functionality of this dynamic regulation *in vivo*, I focused on the super-enhancers' epicenters, and tested their ability to drive reporter gene expression in a cell-state and lineage-specific manner in skin. For my paradigm, I chose the 1.2kb hotspot within the *Cxcl14* super-enhancer, since it was occupied by seven HFSC transcription factors as well as MED1 (Fig. 2-7). I then produced high-titer lentivirus harboring the *Cxcl14* SE-driven eGFP-reporter and *Pgk-H2B-mRFP1*, and virus was then injected into the amniotic sacs of E9.5 embryos. This method resulted in stable transduction and sustained H2B-mRFP1 expression throughout the entire adult skin epithelium (Beronja et al., 2010). Notably however, I found that eGFP reporter activity was highly restricted to the quiescent HFSCs residing in the outer layer of the resting-phase (telogen) bulge (Fig. 2-7). I observed similar eGFP expression patterns when HFSC super-enhancer epicenters from *Nfatc1* or *miR205* were used as drivers (Fig. 2-7).

As HFSCs became activated to initiate a new round of hair growth (anagen), the HFSC super-enhancer reporters showed activity in both HFSCs and their early progeny in the upper/mid outer root sheath (ORS) (Fig. 2-7), whose cells retain stemness, express the

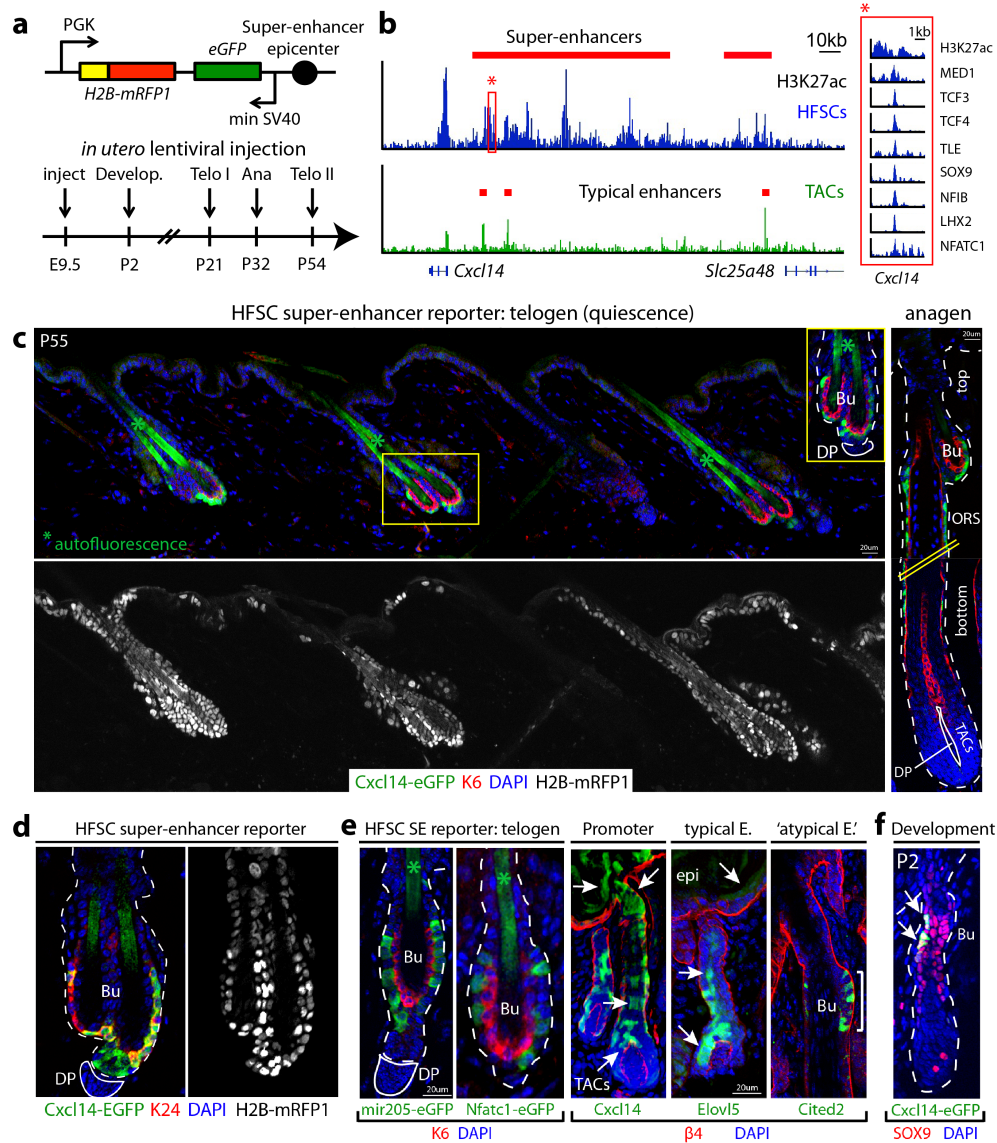


Figure 2-7. Super-enhancer epicenters confer tissue, lineage and temporal specificity. **a**, Lentiviral SE-reporter and analysis scheme. **b**, H3K27ac ChIP-seq occupancy at the *Cxcl14* locus in HFSCs and TACs. Red box highlights an epicenter of the HFSC-super-enhancer that was cloned for reporter assays. **c**, *Cxcl14-SE-eGFP* expression in H2B-mRFP1 epidermis is limited to HFSCs and early SC progeny along upper ORS in anagen (right). **d**, *Cxcl14-SE-eGFP* co-localizes with K24+ HFSCs. **e**, HFSC-specific targeting by *mir205*- and *Nfatc1*-epicenters, whereas the *Cxcl14* promoter and *Elov15* typical-enhancer display broader activity. Atypical *Cited2* enhancer binds all seven HFSC-TFs and drives HFSC-specific targeting. **f**, Temporal activation of *Cxcl14-SE-eGFP* in SOX9+ cells, concomitant with HFSC niche establishment at P2.

HFSC transcription factors and form the new HFSC niche for the next hair cycle (Hsu et al., 2014). By contrast, the reporter was silent in lower ORS, TACs and hair cells, consistent with the suppression of HFSC transcription factors during lineage progression and differentiation. Finally, this HFSC-specific super-enhancer epicenter was also faithful in its temporal regulation, as illustrated by emerging *Cxcl14*-reporter activity at postnatal day 2 (Fig. 2-7), concomitant with niche establishment and functional contribution of SOX9-, TCF3- and LHX2- expressing HFSCs to hair production and wound-repair (Nowak et al., 2008).

The restricted specificity of super-enhancer epicenter fragments was intriguing, since *mir205* and *Cxcl14* are also expressed in the epidermis. I found that their restricted specificity appeared to be dependent upon the dense clustering of HFSC transcription factor binding sites, since HFSC-specific reporter activity was also obtained with *Cited2*'s enhancer, among the few typical enhancers that bound the majority of HFSC transcription factors. By contrast, the typical enhancer of *Elovl5* drove more general expression in skin epithelia, as did expression of the 1.5kb promoter fragment of *Cxcl14* (Fig. 2-7). This was notable, since the H3K27ac peak over this domain was stronger than those throughout the *Cxcl14* super-enhancer, indicating that it is the overall properties of the super-enhancer, and not merely strength of H3K27ac signal, that drives specificity.

My studies suggested that by focusing on the epicenters that bind transcription factors driven by super-enhancers, I can tease apart the cell-stage specific regulatory elements from those driving broader expression elsewhere. If so, prior knowledge of cell-stage-specific master regulators should not be required to exploit the cell-type and lineage specificity of super-enhancers. To test this, I focused on the TAC-super-enhancer

controlled gene *Cux1*, whose promoter lacked most of the motifs for such TAC transcription factors, but whose super-enhancer contained a MED1-bound epicenter rich in motifs for super-enhancer regulated TAC transcriptional factors. Indeed, *in vivo*, the *Cux1* epicenter-driven reporter was largely restricted to a subset of TACs that generate the hair channel (inner root sheath, IRS), where despite broader expression elsewhere, it is known to be essential for proper hair growth (Fig. 2-8) (Ellis et al., 2001). Together, these results unveil two important findings: first, that super-enhancers and their epicenters reflect comprehensively the molecular status of the stem cell and its progenies, and second, that they house powerful and highly specific epigenetic drivers that can be exploited for developing new genetic tools with unprecedented cell-type and lineage specificity.

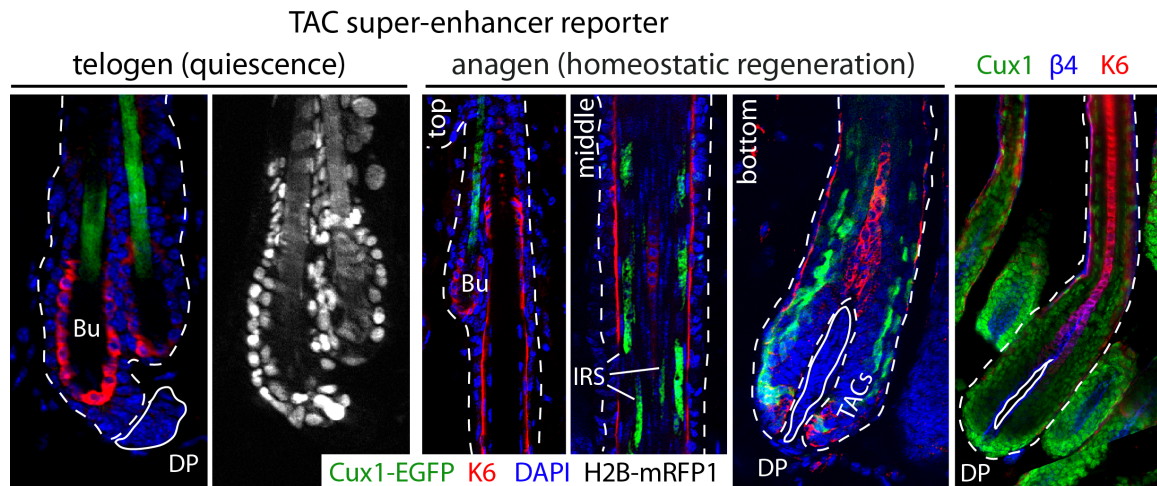


Figure 2-8. Super-enhancer epicenter reporters for differentiating cell lineages. The TAC epicenter from the *Cux1* super-enhancer is silent in HFSCs and ORS, but active in a subset of TACs and the early differentiating progeny of the IRS lineage. DP, dermal papilla, the mesenchymal stimulus of the HF; IRS, inner root sheath; ORS, outer root sheath. White dashed lines denote the epidermal-dermal border; solid lines delineate DP.

The environmental sensitivity of SEs allows HFSC adaptation and plasticity

Given their cell-type, lineage and temporal specificity, I wondered the extent to which super-enhancers reflect a cell's intrinsic identity versus its microenvironment. I mentored a then rotation student, Hanseul Yang, and together, we addressed this important question by exploiting the ability of primary HFSCs to retain stemness long-term *in vitro* under proliferative conditions. We FACS-purified and infected HFSCs with lentiviral *Cxcl14*-HFSC-SE reporter (Fig. 2-7). Despite efficient transduction (evidenced by H2B-mRFP1) the *Cxcl14*-SE reporter was silent in cultured HFSCs (Fig. 2-9).

Since *Cxcl14*-SE faithfully reported HFSC transcription factor activity *in vivo*, its suppression *in vitro* suggested that one or more key HFSC regulators were repressed. qPCR showed downregulation of all SE-associated HFSC-TF genes *in vitro*, with some silenced completely (Fig. 2-9). Curiously, these alterations in transcription factor expression could be restored upon *de novo* HF morphogenesis of engrafted cultured HFSCs (Fig. 2-9). Together, my findings illustrated the sensitivity of epicenters to HFSC-TF expression, their dependency on HFSC's microenvironment and their reversibility.

The impact of microenvironment on super-enhancer dynamics became graphically apparent upon performing H3K27ac ChIP-seq on cultured HFSCs. Only 26% overlap existed between *in vivo* vs. *in vitro* SEs of HFSCs (Fig. 2-9). 28% of *in vitro* SEs had been silent in HFSCs *in vivo*, suggesting they became de-repressed in culture. Only ~3% of "signature genes" of proliferating HFSC (Hsu et al., 2014) displayed SEs *in vitro*, indicating that SE dynamics reflected environmental adaptation more than proliferative status. Further bolstering this point was the complete *in vitro* decommissioning of *Lhx2*, *Nfib*, *Cd34*, and *Sfrp1*, all features of HFSC niche microenvironments *in vivo* (Fig. 2-9).

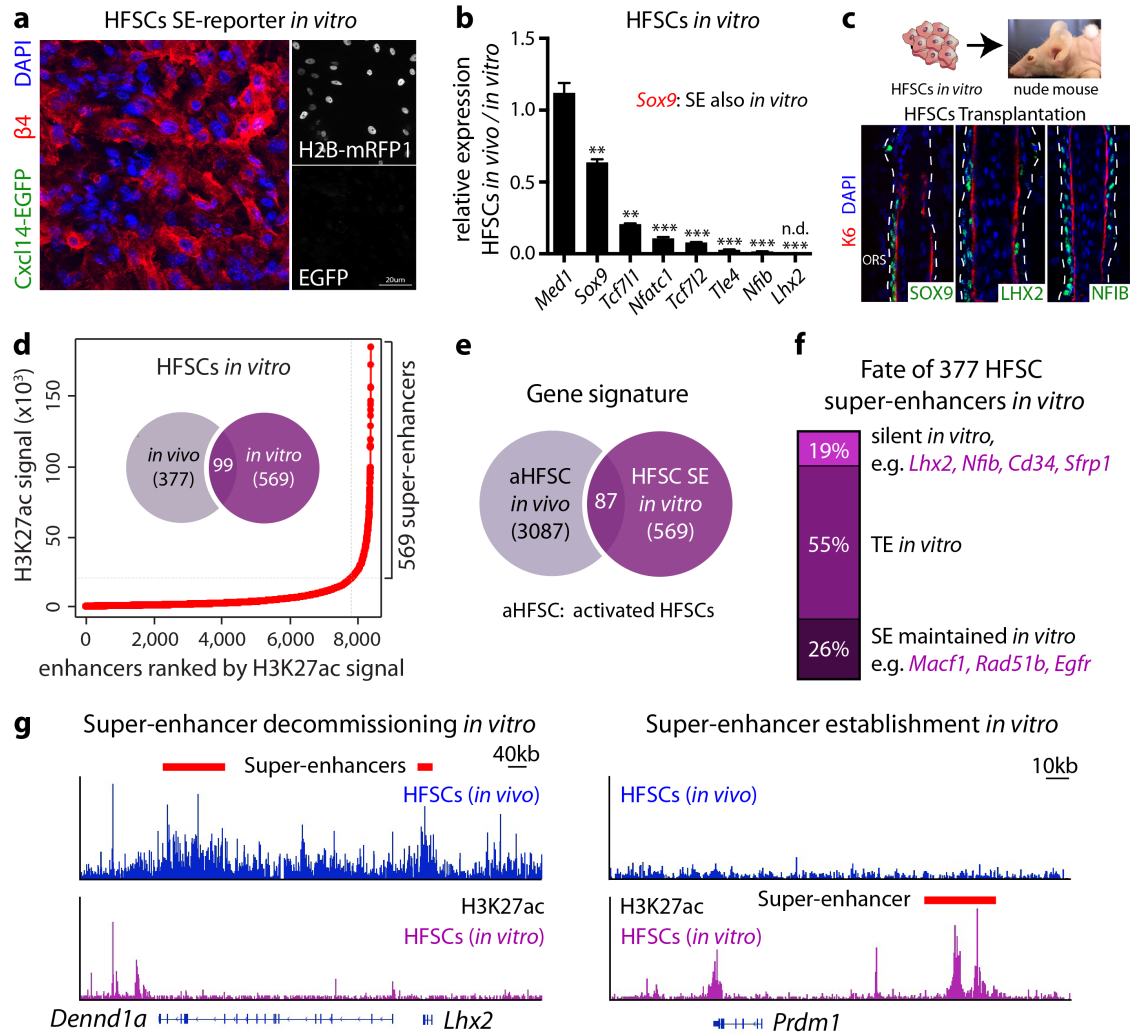


Figure 2-9. The sensitivity of super-enhancers to environmental changes facilitates HFSC adaptation and plasticity. **a**, Absence of *Cxcl14-eGFP* reporter activity in transduced cultured HFSCs. **b**, qRT-PCR demonstrates strong repression of HFSC transcription factor mRNAs *in vitro*. **c**, Cultured HFSCs regenerate HFs upon transplantation. Immunofluorescence shows that the ORS has regained the expression of HFSC-TFs. **d**, Distribution of H3K27ac ChIP-seq signal in cultured HFSC chromatin reveals 569 super-enhancers that share little overlap with HFSC SEs *in vivo*. **e**, HFSCs *in vitro* are molecularly distinct from activated HFSCs (aHFSC) *in vivo*. **f**, Tracking the fate of HFSC SEs in culture indicates striking enhancer remodeling. **g**, H3K27ac ChIP-seq occupancy at the *Lhx2* and *Prdm1* loci in HFSCs *in vivo* and *in vitro*. Note: Super-enhancer analyses of cultured HFSCs were performed by Hanseul Yang and myself.

We noticed that some genes acquiring super-enhancers *in vitro* were epidermal genes, while others have been implicated in wound-repair (Table 2-3). This was intriguing because when epidermis is damaged but underlying HFSCs remain, HFSCs participate long-term in re-epithelialization (Nowak et al., 2008). Additionally, when engrafted, cultured HFSCs can also generate epidermis (Blanpain et al., 2004). To further pursue the notion that the SE dynamics occurring upon culturing HFSCs may reflect a transition to a wound-repair and eventual epidermal state, we tested whether SE-regulated genes change as HFSCs exit the niche and migrate into a wound bed. To accomplish this, we fluorescently marked niche HFSCs, introduced a shallow wound onto the animal's back, and then analyzed the migrating HFSC progeny by immunostaining for proteins whose genes had displayed a change in super-enhancer status *in vitro* (Fig. 2-10).

Table 2-3. List of selected super-enhancer-associated genes in cultured HFSCs

Category	Super-enhancer associated genes in cultured HFSCs
Gene regulation	<i>Klf5</i> , <i>Foxo3</i> , <i>Ahr</i> , <i>mir-21</i> , <i>Hif1a</i> *, <i>Runx1</i> *, <i>Zfp361</i> *, <i>Klf6</i> *, <i>Mitf</i> *, <i>Aff1</i> *, <i>Dcps</i> *, <i>Aebp2</i> , <i>Vdr</i> , <i>Ehf</i> , <i>Prdm1</i> , <i>Grhl1</i> , <i>Barx2</i>
Signaling	<i>Fhl2</i> *, <i>Tgfa</i> , <i>Calml3</i> , <i>Lgals3</i> , <i>Prl2c4</i> , <i>Ripk4</i> , <i>Fam129b</i> , <i>Hmox1</i> , <i>Thbd</i> , <i>Lrp1</i> , <i>SerpinB2</i> , <i>Asprv1</i> , <i>Arg1</i> , <i>Ppfibp2</i> *, <i>Mcl1</i> *, <i>Prrg4</i>
Adhesion, migration	<i>Perp</i> , <i>Itgb4</i> , <i>Sdc1</i> , <i>Cd9</i> , <i>Cd44</i> , <i>Kank1</i> , <i>Macf1</i> , <i>Arf6</i> , <i>Iqgap1</i> , <i>Mllt4</i> , <i>Ezr</i> , <i>Hspb1</i> , <i>Ppl</i> , <i>Gan</i> , <i>Dsg3</i> , <i>Cldn4</i> , <i>Pvrl1</i> , <i>Dstn</i> , <i>Tjp2</i>

Genes in **purple** have a reported role in wound healing
 * reported role in HFSC self-renewal (Chen et al., 2012)

As HFSCs exited their niche and migrated upward in response to the wound, they induced non-HFSC genes such as *Fhl2* and *Prrg4* which had acquired super-enhancers *in vitro*. Conversely, super-enhancer-marked HFSC transcription factor genes were markedly down-regulated in the migrating HFSCs (Fig. 2-10).

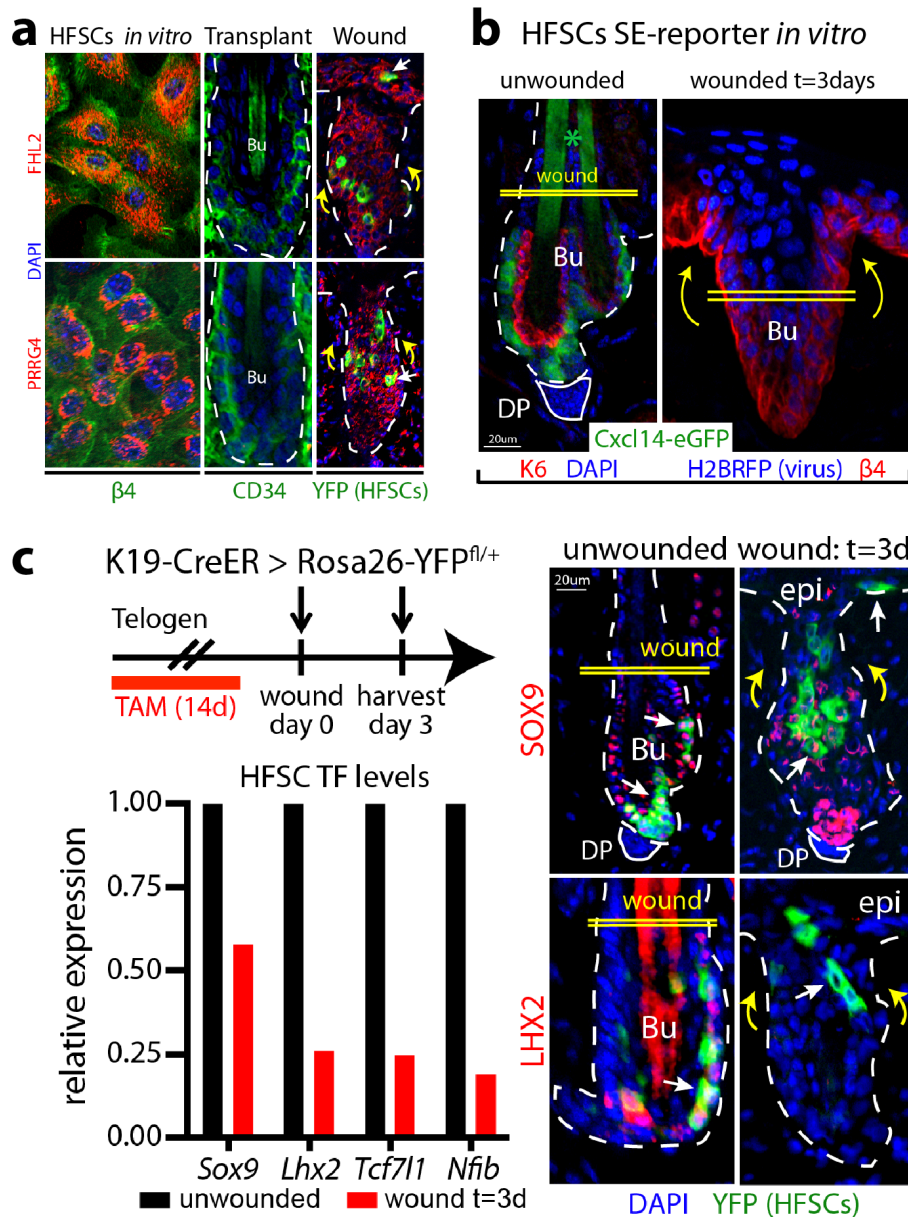


Figure 2-10. Dynamic gene expression changes in HFSCs in culture, upon wounding or transplantation. **a**, *Fhl2* and *Prrg4* display super-enhancer mediated activity *in vitro*. Upon transplantation, HFSCs silence *in vitro*-induced genes concomitant with hair follicle regeneration. However, during wounding, HFSCs (lineage marked with K19-CreER/R26YFP) regain expression of *Fhl2* and *Prrg4*. **b**, *Cxcl14-SE-eGFP* reporter is repressed in wound-activated HFSCs. **c**, Suppression of HFSC transcription factors during wound-repair in *K19-CreER*(HFSC-specific)/*R26YFP* mice.

Directly focusing on super-enhancer dynamics, we next tested the behavior of the *Cxcl14*-eGFP reporter to a wound response. Although *Cxcl14*-eGFP was still detected in those HFSCs that remained in their native niche, it was dramatically down-regulated in the migrating HFSCs (Fig. 2-10), thereby recapitulating what I had seen when HFSCs were cultured. These findings reveal an exquisite sensitivity of super-enhancers to their microenvironment and demonstrate the physiological relevance of their dynamic shifts between *in vivo* and *in vitro* to wound-repair and fate plasticity.

A small cohort of genes, including those surfacing in a self-renewal screen for cultured HFSCs (Chen et al., 2012), maintained super-enhancers *in vitro*. Seeking to understand of how super-enhancers remain active in culture when many HFSC-TF genes are suppressed, we noticed that epicenters of broadly active SEs differed between the two states (Fig. 2-11). As illustrated by *Macf1*, a gene essential for HFSCs to migrate and repair epidermal wounds (Wu et al., 2011), only *in vivo* epicenters were enriched for HFSC-TF motifs, while *in vitro* epicenters were enriched for motifs of the AP1/KLFs/GRHL families, typically up-regulated not only during wound-healing but also in epidermis (Fig. 2-11). Using reporter assays, we tested the functional relevance of epicenter shifts. None of *in vivo* epicenters exhibited luciferase activity in culture, but *in vitro* epicenters were robustly active (Fig. 2-11). Finally, we tested *in vitro* epicenters as reporter drivers *in vivo*. Interestingly, we observed no activity of these epicenters in the HFSC niche, but did see appreciable expression in epidermis and upon wound-repair (Fig. 2-11). These tantalizing findings suggest that by shifting epicenters, HFSCs maintain the expression of certain key genes even in the face of dramatic changes in the transcriptional landscape outside their native niche.

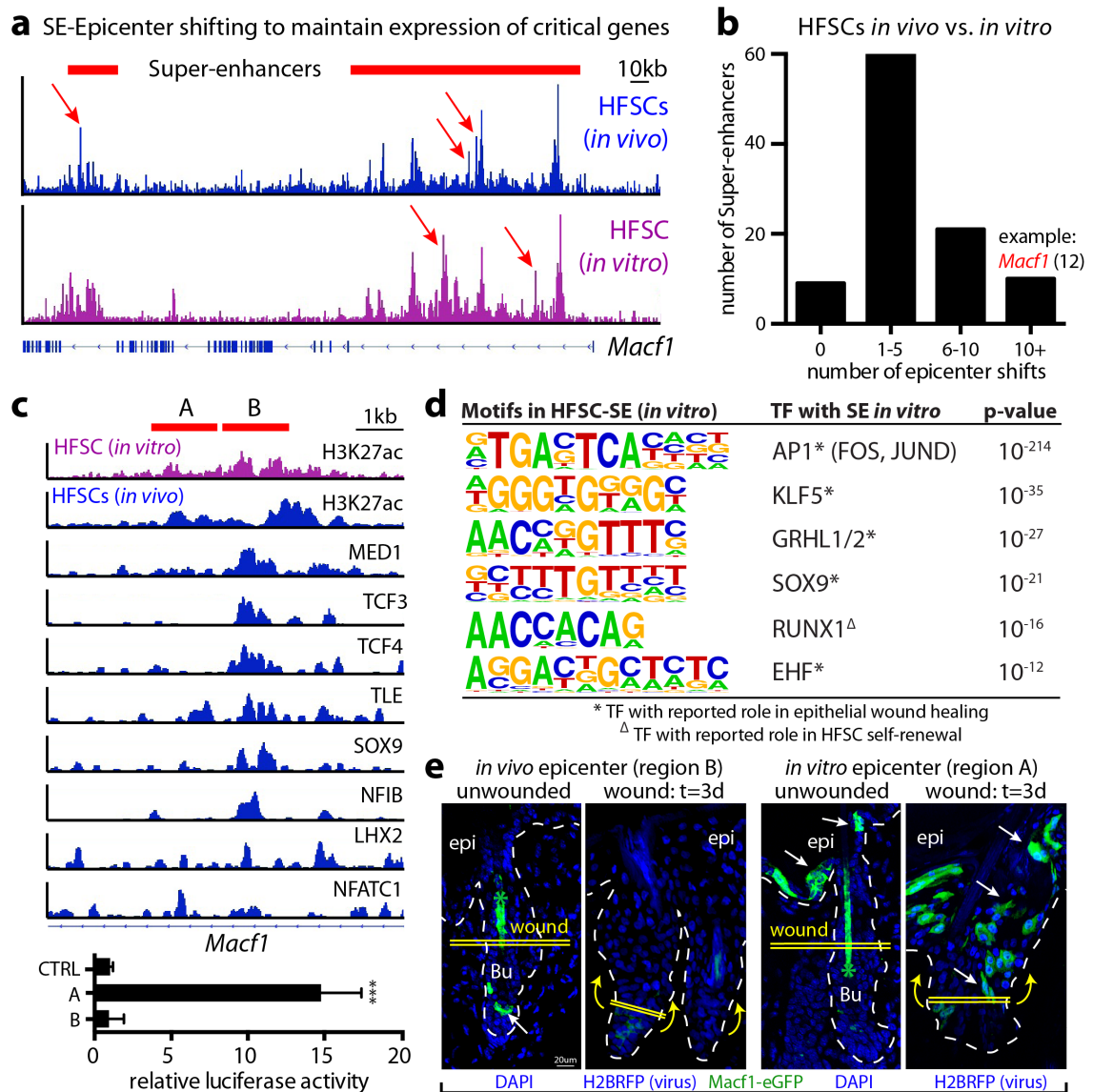


Figure 2-11. HFSCs activate different epicenters within super-enhancers to sustain expression of critical genes in different microenvironments. **a**, H3K27ac ChIP-seq occupancy at *Macf1* locus in HFSCs *in vivo* vs. *in vitro*. Arrows denote differences in peak distributions. **b**, Frequency of epicenter shifts in HFSC-SEs (*in vivo* versus *in vitro*). **c**, Region B marks an epicenter active *in vivo*, bound by HFSC transcription factors; adjacent region A is a novel epicenter that emerged *in vitro*. Relative luciferase activities were driven by the 1-1.5kb encompassing these two epicenters. *** $P < 0.001$; Error bars indicate standard deviation. **d**, Motif analysis for TF binding sites of cultured HFSC-SEs. **e**, Functional validation of epicenter shifts in mice transduced with *Macf1-SE-eGFP* reporters. *Note*: Hanseul Yang assisted with luciferase assays.

SOX9 is a master regulator governing HFSC fate and plasticity

To understand how HFSCs might exploit super-enhancer dynamics to elicit the plasticity that allows them to repair wounds and regenerate skin, I was drawn to SOX9, since its loss *in vivo* results in the transformation of the HFSC niche into an epidermal cyst (Kadaja et al., 2014). *Sox9* was also the only HFSC-TF gene that maintained a super-enhancer *in vitro*, where it is expressed at ~60% of its *in vivo* level (Fig. 2-9). I therefore addressed whether SOX9 might behave as master regulator, enabling HFSCs to adapt and maintain stemness at low levels (either *in vitro* or during initial migration from the bulge niche) while delineating fates when either elevated (HFSCs) or absent (epidermal SCs).

To test this hypothesis, Meelis Kadaja, a postdoctoral fellow in the lab, had ablated *Sox9* in HFSCs and examined the consequences to colony formation *in vitro*. In contrast to their SOX9+ heterozygous counterparts, SOX9-deficient HFSCs formed very few colonies *in vitro* (Fig. 2-12). We observed similar striking defects when lentiviral-Cre was used to ablate *Sox9* in actively growing *Sox9^{fl/fl};Rosa26-YFP^{fl/+}* HFSC cultures, which were then imaged live to monitor and quantify colony growth (Fig. 2-12). Moreover, prior studies had shown that when SOX9 expression is blocked during embryogenesis, LHX2, TCF3/4 and NFATc1 are not turned on, and functional HFSCs failed to form (Fig. 2-12) (Nowak et al., 2008). These findings suggest that without SOX9, other super-enhancer driven HFSC-TF genes are not likely to be activated.

To explore the role of SOX9 further, I transgenically raised SOX9 levels in cultured basal epidermal progenitors, which *in vitro* as *in vivo*, did not express appreciable levels of HFSC transcription factors (Fig. 2-13). Of HFSC transcription factors, *Lhx2* was most sensitive to SOX9 levels, showing >80X induction in

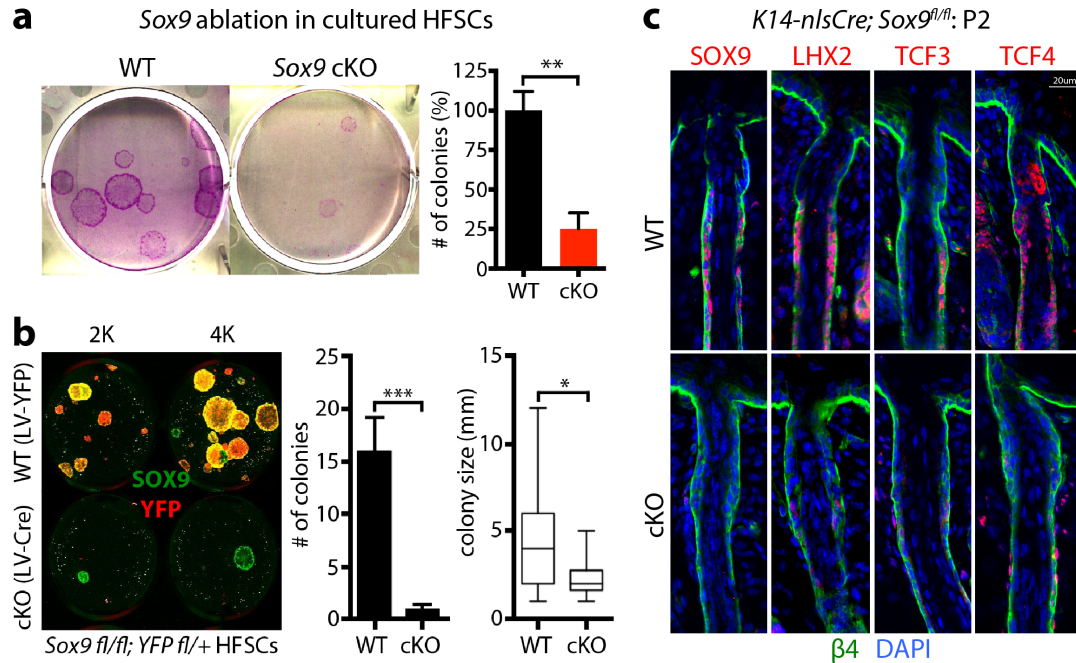


Figure 2-12. SOX9 is essential for HFSC specification and maintenance. **a**, Colony formation assays on WT and *Sox9*-cKO HFSCs. Following *Krt15-CrePGR* ablation *in vivo*, 10K *Sox9*-cKO HFSCs were seeded. **b**, *Sox9^{fl/fl} Rosa26YFP^{fl/+}* HFSCs were seeded at 2K and 4K and transduced with lentiviral-Cre to achieve *Sox9* ablation *in vitro*. All yellow and green colonies were not effectively targeted and are still SOX9+. All red colonies (SOX9-negative) aborted, as revealed by quantifications of colony numbers and sizes shown at right. **c**, HFSC-specification fails in *Sox9*-cKO mice. Note: *Sox9* cKO mice were engineered by Dr. Meelis Kadaja, and I analyzed these tissue blocks.

SOX9-transduced epidermal keratinocytes *in vitro* (Fig. 2-13). Further consistent with a special importance for SOX9, HFSC SE genes *Bnc2* and *Gas1* showed appreciable upregulation in response to SOX9 overexpression *in vitro* (Fig. 2-13). These results highlight an environmental sensitivity of SEs to levels of this key HFSC master regulator.

If SOX9 is a master regulator whose levels dictate whether super-enhancers will be epigenetically active or silenced in the epidermal lineage, then inducing SOX9 in the epidermis *in vivo* should activate genes such as *Tcf7l1* and *Lhx2* whose super-enhancers

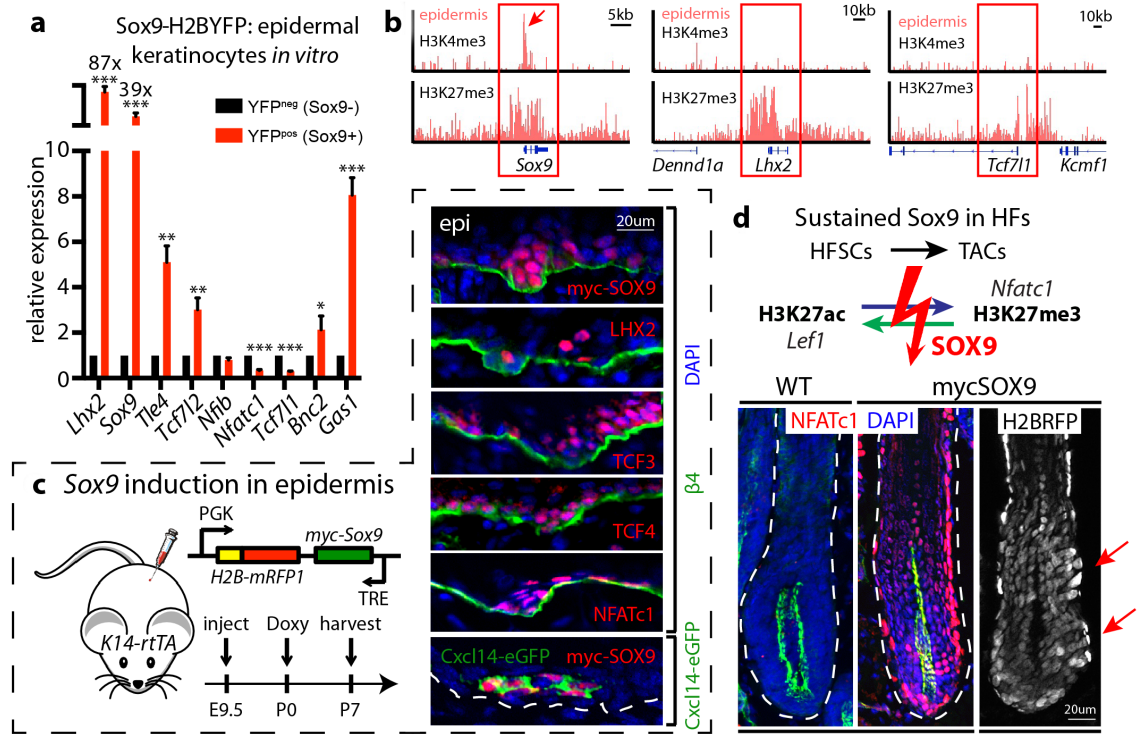


Figure 2-13. SOX9 is a master regulator governing HFSC fate. **a**, qRT-PCR demonstrates that *Sox9* overexpression in cultured epidermal keratinocytes robustly induces transcripts for HFSC-TFs (*Lhx2*, *Tle4*, *Tcf7l2*), and other SE-associated HFSC genes (*Bnc2*, *Gas1*). **b**, HFSC-TF genes *Lhx2* and *Tcf7l1* are PcG-repressed in epidermis, while *Sox9* is poised. **c**, Forced *in vivo* expression of *Sox9* in epidermal progenitors activates HFSC-TF genes. Note induction of HFSC super-enhancer regulated *Cxcl14-SE-eGFP*. **d**, Sustained SOX9 during HF regeneration. Note prevention of swap in H3K27 modifications of key SEs upon TAC fate commitment. NFATc1 atypically persists in lower ORS and TACs, and minibulge-like structures occur along ORS (arrows).

are polycomb-silenced (Fig. 2-13) (Lien et al., 2011). To test this possibility, I transduced a doxycycline-inducible lentiviral SOX9 expression vector into *K14-rtTA* embryos and activated its expression in the epidermis of adult mice. Remarkably, epidermal SOX9 at levels comparable to that in the HFSC niche resulted in activation of *Lhx2*, *Tcf7l1*, *Tcf7l2* and *Nfatc1* (Fig. 2-13). Although the full details underlying this reprogramming event are

beyond the scope of the present study, SOX9 levels clearly mattered, and prior studies showing SOX9 co-immunoprecipitating with Ep300 and CBP histone acetylases suggest direct participation in chromatin activation (Fig. 2-13).

As strikingly, when SOX9 levels were sustained in the hair lineage, NFATc1, LHX2 and TCF3/4 persist and minibulge-like structures appeared along the outer root sheath. Moreover, when SOX9 levels were sustained, HFSC transcription factors were expressed in TACs, while surprisingly, TAC transcription factors such as LEF1 were markedly repressed in TACs (Fig. 2-14). Together these data suggest that when SOX9 levels remain high, the signaling cues that normally drive the HFSC→TAC transition are overridden, preventing PcG-silencing of HFSC transcription factor super-enhancers and H3K27ac-activation of super-enhancers governing TAC transcription factors.

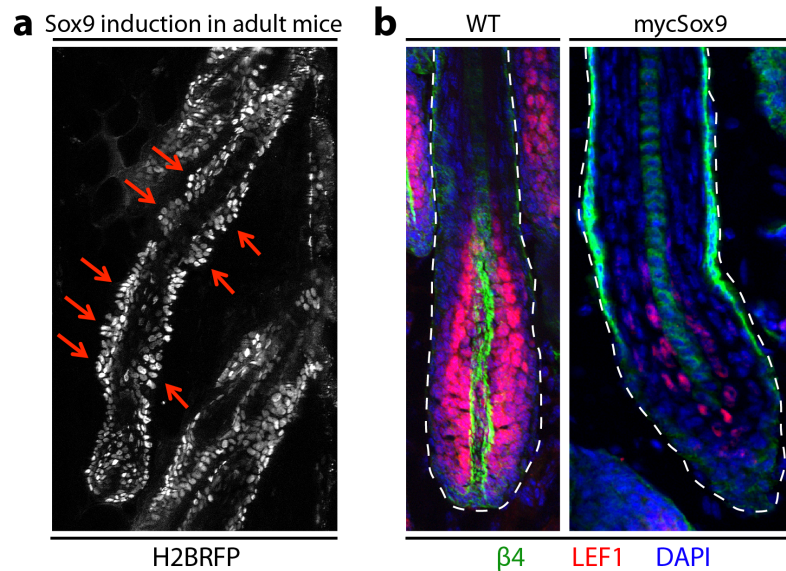


Figure 2-14. Sustained *Sox9* expression in committed progenitors perturbs lineage progression. **a**, Sustained SOX9 in adult mice (Doxycycline for 3 weeks in adult mice, starting at P21) leads to *de novo* formation of minibulge-like structures along the ORS. **b**, Immunofluorescence showing that *Lef1* (normally H3K27me3 repressed in HFSCs, but H3K27ac super-enhancer induced in TACs) remains repressed in mycSOX9+ HFSCs.

Discussion

In summary, by profiling skin stem cells in their native niche, I discovered that paradigms established for embryonic stem cell super-enhancers *in vitro* (Whyte et al., 2013) hold for adult stem cell super-enhancers *in vivo*. Importantly, my studies confirm the prior notion that super-enhancers – long domains of accessible chromatin highly enriched in cell-type specific transcription factors – drive high levels of cell identity genes *in vivo*. Although a substantial number of housekeeping genes, driven by typical enhancers, are also expressed at high levels, their expression is intended to be stably maintained in different cell lineages, which doesn't require as elaborate regulatory networks as conferred by super-enhancers.

Moreover, I have unearthed many new insights regarding super-enhancers that drive auto-regulation of master regulators that specify cellular state, whether it be the establishment of stem cells during embryogenesis, their maintenance in their native niche or their lineage determination. As HFSCs transition from an undifferentiated to committed fate, most of these HFSC master regulators are suppressed, which results in the decommissioning of the majority of super-enhancers. Accordingly, genes controlled by super-enhancers, but not typical enhancers, are dramatically down-regulated during lineage progression, while novel super-enhancers emerge to drive TAC-specific genes. In this respect, the mutually exclusive H3K27 modifications of super-enhancers (H3K27ac) and PcG-silencing (H3K27me3) that provide a powerful two-way switch for lineage commitment of adult stem cells are of additional relevance. Thus, the dynamics and exquisite specificity of super-enhancers appear to be instrumental to facilitate cell state transitions and fate switches.

Most importantly, however, I discovered a hitherto unappreciated complexity in the organization, constituency and dynamics of super-enhancers that endows them with the ability to shift allegiance from one cohort of master regulators to another when stem cells depart their niche and become exposed to new environments, without losing their stemness. Such features differ from lineage progression but are essential for tissue stem cells to repair wounds.

I show that in skin, this is achieved through SOX9 levels, which when high, dictates the transcriptional landscape of HFSCs, but when low, facilitates the plasticity that is necessary to allow HFSCs to survive outside the confines of the niche until the cells reach and adapt to their new microenvironment. This plasticity is exhibited not only in culture, but also when HFSCs participate in wound-repair or embark upon their hair lineage. *In vitro*, *Sox9* expression remains low and plasticity persists; *in vivo*, *Sox9* is silenced both in wound-reepithelialized epidermis and in transit-amplifying cells as they commit to make hair. By coupling SOX9, which senses changes in the microenvironment of HFSCs, to chromatin platforms that are optimized for sensing TF concentration, super-enhancers orchestrate the chromatin dynamics required for skin stem cells to pursue distinct lineages and repair wounds.

In summary, the ability of stem cells to remodel their super-enhancers and survive with only a streamlined subset of niche master regulators begins to explain the emerging plasticity of adult stem cells as well as the ability of their neighboring progenitors to regain stem cell behavior when returned to the niche microenvironment. As future studies are conducted, the complex mechanisms underlying the fascinating dynamics of super-enhancers in the context of stem cell biology will continue to unfold.

Materials and Methods

Mouse lines

Female CD1 mice (8 weeks old, Charles River) were used for the purification of HFSCs. Female CD-1 mice transgenic for *Krt14-H2B-GFP* (30-32 days old) (Tumbar et al., 2004) were used for the purification of TACs. *Krt15-CrePGR; Sox9^{fl/fl}; R26YFP^{fl/+}* mice have been described (Kadaja et al., 2014). *Krt19-CreER* mice have been described (Means et al., 2008). CreER was activated by intraperitoneal injection of mice with 20mg ml⁻¹ tamoxifen (Sigma) in corn oil (Sigma) to specifically label HFSCs. For the generation of *K14-H2B-iRFP* mice, iRFP was first amplified from pShuttle-CMV-iRFP (Addgene plasmid 31856) and fused with H2B, before the H2B-iRFP construct was assembled with the *Krt14* promoter, β -globin intron and poly(A) sequences (Vasioukhin et al., 1999). Transgenic mice were generated with standard pronuclear injections. For lentiviral injections, transduced mice were confirmed by genotyping with RFP primers: forward 5'-ATCCTGTCCCCTCAGTTCCAGTAC-3', reverse 5'-TCCACGATGGTGTAGTCCTCGTTG-3. For *TRE-mycSox9* transduced mice, positive mice were fed with doxycycline-containing chow, starting either at P0 (newborn) or at P21 (adult). No formal randomization was performed, and studies were not blinded. Mice were maintained in the Association for Assessment and Accreditation of Laboratory Animal Care-accredited animal facility of The Rockefeller University (RU), and procedures were performed with Institutional Animal Care and Use Committee (IACUC)-approved protocols.

Flow Cytometry

Preparation of adult mice back skins for isolation of HFSCs and TACs were done as previously described (Nowak et al., 2009). Briefly, for telogen skin, subcutaneous fat was removed with a scalpel, and skins were placed dermis side down on 0.25% Trypsin-EDTA (Gibco) at 37°C for 35 min. Single-cell suspensions were obtained by scraping the skin gently. Anagen skin was treated with collagenase at 37°C for 30 minutes to dissociate dermal cells and then incubated with 0.25% Trypsin-EDTA (Gibco) at 37°C for 15 minutes to detach and generate single cell suspensions of the epidermal and HF cells. Cells were then washed with PBS containing 5% of fetal bovine serum (FBS), then filtered through 70µm and 40µm cell strainers (VWR). Cell suspensions were incubated with the appropriate antibodies for 30 min on ice. The following antibodies were used for FACS: α6-PE (1:100, eBiosciences), CD34-eFluoro660 (1:100, eBiosciences) and Sca-1-PerCP-Cy5.5 (1:1000, eBiosciences). 4'6'-diamidino-2-phenylindole (DAPI) was used to exclude dead cells. Cell isolations were performed on FACS Aria sorters running FACSDiva software (BD Biosciences).

ChIP-seq

Immunoprecipitations were performed on FACS-sorted populations from female mice or on cultured HFSCs (Lien et al., 2011). For each ChIP-seq run, 7×10^6 to 2×10^7 cells were used. Antibodies used for ChIP-seq were anti-H3K27ac (Abcam, ab4729), anti-H3K4me1 (Abcam, ab8895), anti-Crsp1/Trap220 (Med1, Bethyl Laboratories, A300-793A) and anti-H3K27me3 (Millipore, 07-449). Briefly, cells were cross-linked in 1% (wt/vol) formaldehyde solution (50mM HEPES-KOH, pH7.5, 100mM NaCl, 1mM

EDTA, 0.5mM EGTA, 11% formaldehyde), resuspended (first in Lysis buffer 1: 50mM HEPES-KOH, pH7.5, 140mM NaCl, 1mM EDTA, 10% glycerol, 0.5% NP-40, 0.25% Triton X-100, 1x Protease Inhibitor cocktail; then in Lysis buffer 2: 10mM Tris-HCl, pH8.0, 200mM NaCl, 1mM EDTA, 0.5mM EGTA, 1x Protease Inhibitor cocktail), and lysed (Lysis buffer 3: 10mM Tris-HCl, pH8.0, 100mM NaCl, 1mM EDTA, 0.5mM EGTA, 0.1% Na-Deoxycholate, 0.5% N-lauroylsarcosine, 1x Protease Inhibitor cocktail). To solubilize and shear cross-linked DNAs, lysates were subjected to a Bioruptor Sonicator (Diagenode, UCD-200) according to a 30x regimen of 30s sonication followed by 60s rest. The resulting whole-cell extract was incubated overnight at 4°C with 10 µL of Dynabeads Protein G magnetic beads (Life Technologies) which had been pre-incubated with 5µg of the appropriate Ab in PBS (or according to manufacturer's instructions). After ChIP, samples were washed (Low salt wash buffer: 20mM Tris-HCl, pH8.0, 150mM NaCl, 2mM EDTA, 0.1% SDS, 1% Triton X-100; High salt wash buffer: 20mM Tris-HCl, pH8.0, 500mM NaCl, 2mM EDTA, 0.1% SDS, 1% Triton X-100; LiCl wash buffer: 10mM Tris-HCl, pH8.0, 250mM LiCl, 1mM EDTA, 1% Na-Deoxycholate, 1% NP-40; TE Buffer: 10mM Tris-HCl, pH8.0, 1mM EDTA), and bound complexes were eluted and reverse-cross-linked (Elution Buffer: 50mM Tris-HCl, pH8.0, 10mM EDTA, 1% SDS, reverse cross-link at 65°C for 12h). ChIP DNA was prepared for sequencing by repairing sheared DNA and adding Adaptor Oligo Mix (Illumina) in the ligation step. A subsequent PCR step with 25 amplification cycles added the additional Solexa linker sequence to the fragments to prepare them for annealing to the Genome Analyzer flow cell. After amplification, a range of fragment sizes between 150–300 bp was selected and the DNA was gel-purified (Qiagen Gel Extraction Kit, elute in

Nuclease-free H₂O) and diluted to 10 nM for loading on the flow cell. Sequencing was performed on the Illumina HiSeq 2500 Sequencer following manufacturer protocols. ChIP-seq reads were aligned to the mouse genome (mm9, build 37) using Bowtie aligner (Langmead et al., 2009). ChIP-Seq signal tracks were presented by Integrative Genomics Viewer (IGV) software.

Bioinformatics analysis

H3K27ac peaks were called by the program MACS (Zhang et al., 2008) (v 1.4.2, default parameters) from the ChIP-seq data with the input as controls. The peaks were associated to genes using the mouse RefSeq annotations; those located within 2kb of transcription start sites were called as “promoter” peaks and the rest were “enhancer” peaks. The H3K27ac enhancer peaks were used for the identification of super-enhancers, using the algorithm described previously, wherein enhancer peaks were stitched together if they are located within 12.5kb of each other and if they don’t have multiple active promoters in between. Enhancers were then ranked according to increasing H3K27ac signal intensity (Whyte et al., 2013). Enhancer-gene assignments were performed using the following criteria to make gene assignments: (1) proximity of genes to the SE of stem cells; (2) high transcriptional activity in stem cells (by RNA-seq and by ChIP-seq for presence of H3K4me3/H3K79me2 marks and no H3K27me3 marks in the promoter/typical enhancer and/or gene body; (3) correlation between loss of the SE (or shift in its epicenter peaks), loss of gene transcription and loss of H3K79me2 mark \pm H3K27me3 mark in proliferative short-lived progenitors; (4) correlation between loss of the SE (or shift in its epicenter), loss of gene transcription and loss of H3K79me2 mark \pm

H3K27me3 mark in proliferative cultured stem cells. The overlap of super-enhancers with ChIP-seq peaks for MED1 and other TFs was defined by ≥ 1 base overlap. For TF enrichment analysis at super-enhancers, H3K27ac peaks not located at super-enhancers (i.e., typical enhancers) were randomly picked, extended to match the sizes of super-enhancers and used as background controls. GO function enrichment analyses were carried out by the software GREAT (McLean et al., 2010) using the list of super-enhancer coordinates and the default setting. For motif analysis of enhancers located in superenhancers, 1-kb sequences under the H3K27ac peaks were searched for enriched motifs using the software HOMER (v4.6) with the default setting (PMID 20513432). Epicenters were defined as 1kb-regions flanking either side of the H3K27ac peaks. 1-kb was chosen based on our analysis of the distances of H3K27ac peaks to their nearest transcription factor ChIP-seq peaks in HFSCs *in vivo*, which showed an enrichment of TF binding within 1-kb regions of H3K27ac peaks. Overlapping epicenters were merged during this analysis. To analyze epicenter shifting, for each of the overlapping super-enhancers between HFSCs *in vivo* and *in vitro*, we determined the number of epicenters that were not overlapping in the two samples and considered them as shifting epicenters. To generate the heatmap, the program seqMiner (Ye et al., 2011) was used to calculate ChIP-seq read densities, which were the maximal numbers of overlapping ChIP-seq reads in 50-bp bins from -5 kb to +5 kb of the H3K27ac peak summits. The density matrix was clustered based on the H3K27ac ChIP-signal and then used to generate a heatmap.

Antibodies

The following antibodies and dilutions were used: SOX9 (rabbit, 1:1000, Millipore), NFIB (rabbit, 1:1000, Active Motif), LHX2 (rabbit, 1:2000, Fuchs lab), K6 (guinea pig, 1:5000, Fuchs Lab), K24 (rabbit, 1:5000, Fuchs lab), CD34 (rat, 1:100, BD-Pharmingen), LEF1 (rabbit, 1:100, Fuchs lab), NFATc1 (mouse, 1:100, Santa Cruz), TCF3 (guinea pig, 1:200; Fuchs laboratory), TCF4 (rabbit, 1:300; Cell Signaling Technology), FHL2 (rabbit, 1:100, Abcam), PRRG4 (rabbit, 1:100, Abcam), CUX1 (rabbit, 1:200, Santa Cruz), β 4-Integrin (rat, 1:100, BD-Pharmingen), GFP (chicken, 1:2000, Abcam), RFP (rabbit, 1:5000, MBL; or guinea pig, 1:3000, Fuchs lab). Secondary Abs coupled to Alexa488, RRX, or Alexa647 were from Life Technologies. Nuclei were stained using 4'6'-diamidino-2-phenylindole (DAPI).

Histology, Immunofluorescence and Imaging

Back skins from mice were embedded in OCT (Tissue Tek), frozen, cryosectioned (10-20 μ m) and fixed for 10 min in 4% paraformaldehyde (PFA) in phosphate buffered saline (PBS). For lentivirally transduced mice, head and backskins were pre-fixed in 4% PFA for 4h at 4 degrees, followed by washes in PBS and incubation in 30% sucrose, before embedding in OCT. Sections were blocked for 1hr in gelatin block (5% normal donkey serum, 1% BSA, 2% fish gelatin, 0.3% Triton X-100 in PBS). Primary antibodies were diluted in blocking buffer and incubated at 4°C overnight (O/N). MOMBasic kit (Vector Laboratories) was used for blocking when primary antibodies were generated from mouse. After washing with PBS 3x for 5min each, secondary antibodies, were added for 1hr at room temperature (RT). Slides were washed with PBS,

counterstained with 4'6'-diamidino-2-phenylindole (DAPI) and mounted in Prolong Gold (Invitrogen). Images were acquired with an Axio Observer.Z1 epifluorescence microscope equipped with a Hamamatsu ORCA-ER camera (Hamamatsu Photonics), and with an ApoTome.2 (Carl Zeiss) slider that reduces the light scatter in the fluorescent samples, using 20x objective, controlled by Zen software (Carl Zeiss). Z stacks were projected and RGB images were assembled using ImageJ. Panels were labeled in Adobe Illustrator CS5.

Lentiviral expression constructs, viral production and *in utero* injections

Lentiviral super-enhancer reporters were generated by PCR amplification of selected enhancer regions from BAC clones (CHORI), followed by insertion into KpnI and BsaBI restriction sites of the Rbpj-EGFP construct (Williams et al., 2011). To generate the *Sox9* expression construct, *Sox9* cDNA was PCR amplified, and inserted into the *LV-TRE-PGK-H2BmRFP1* construct (Chang et al., 2013). Production of VSV-G pseudotyped lentivirus was performed by calcium phosphate transfection of 293FT cells (Invitrogen) with enhancer reporter plasmids and helper plasmids pMD2.G and pPAX2 (Addgene plasmids 12259 and 12260). Viral supernatant was collected 46 h after transfection and filtered through a 0.45- μ m filter. For *in utero* lentiviral transduction, viral supernatant was concentrated by ultracentrifugation. Final viral particles were resuspended in viral resuspension buffer (20 mM Tris pH 8.0, 250 mM NaCl, 10 mM MgCl₂, 5% sorbitol) and 1 μ l of viral suspension was injected in utero into E9.5 embryos.

Partial Thickness Wound (Dermabrasion)

Animals were anesthetized with Ketamine/Xylazine and administered Buprenorphine analgesia. Skin was shaved and remaining hair cleared with hair removal cream. Skin was gently stretched between two fingers and epidermis removed using a small rotary drill (Dremel) with a polishing wheel attachment (model 520), to create a partial-thickness wound.

Cell Culture

Primary HFSCs were isolated from P52-60 *K14-H2B-iRFP* mice and plated onto mitomycin C-treated dermal fibroblasts in E-media supplemented with 15% (vol/vol) serum and 0.3 mM calcium (Nowak et al., 2009). For colony formation assays, equal numbers of *Sox9*-deficient live cells were plated. After 14 days in culture, cells were fixed and stained with 1% (wt/vol) Rhodamine B (Sigma). Colony diameter was measured from scanned images of plates using Image J and colony numbers were counted. For viral infections, HFSCs were spun with lentivirus for 30 min at 1100g in the presence of polybrene (100 µg/ml) (Beronja et al., 2010). For *Sox9* over-expression studies, the *PGK-Sox9-IRES-H2BYFP* construct was transfected into cultured HFSCs or epidermal keratinocytes. 72h later, YFP+ and YFP- cells were purified by FACS.

RNA extraction and qRT-PCR

FACS-isolated cells were sorted directly into Trizol^{LS} (Invitrogen). Total RNA was purified using the Direct-zol RNA MiniPrep kit (Zymo Research) per manufacturer's instructions. DNase treatment was performed to remove genomic DNA (RNase-Free

DNase Set, Qiagen) Equal amounts of RNA were reverse-transcribed using Oligo-dT primers (Superscript III, Life Technologies). qRT-PCR was performed on an Applied Biosystems 7900HT Fast Real-Time PCR system. cDNAs were normalized to equal amounts using primers against *Ppib2*. Primers were designed using Primer 3 and amplified products encompassed exon/intron boundaries.

The following primer sequences were used:

Sox9 forward 5'-AGAAAGACCACCCCGATTACAAGT-3',

Sox9 reverse 5'-CGGCGGACCCTGAGATTG-3';

Lhx2 forward 5'-GCCCCGGGCAAGTTCAG-3',

Lhx2 reverse 5'-GGGGGTGGCGAGTCATTAGA-3';

Nfib forward 5'-ATGACCCATCCAGTCCTCAA-3',

Nfib reverse 5'-TTGAAGGAAAGGCTCTCCAA-3';

Tcf7l1 forward 5'-TGGTCAACGAATCGGAGAAT-3',

Tcf7l1 reverse 5'-TCACTTCGGCGAAATAGTCG-3';

Tcf7l2 forward 5'-CTCCACAGCTCAAAGCATCA-3',

Tcf7l2 reverse 5'-CACCACCTTCGCTCTCATCT-3';

Nfatc1 forward 5'-AACGCCCTGACCACCGATAGCACT-3',

Nfatc1 reverse 5'-CCCGGCTGCCTTCCGTCTCATA-3';

Tle4 forward 5'-GGTCAGTCTCACCTCCCAAT-3',

Tle4 reverse 5'-GAAACTGGATGATGGGGATA-3';

Ppib2 forward 5'-GTGAGCGCTTCCCAGATGAGA-3',

Ppib2 reverse 5'-TGCCGGAGTCGACAATGATG-3';

Statistics

For all measurements, 3 biological replicates and 2 or more technical replicates were used. Experiments were independently replicated twice, and representative data are shown. To determine the significance between two groups, comparisons were made using unpaired two-tailed Student's *t* test in Prism6 (GraphPad software). For all statistical tests, the 0.05 level of confidence was accepted for statistical significance.

Chapter 3:
The role of Nuclear Factor I transcription factors NFIB and NFIX
in the maintenance of skin appendages

Introduction

The nuclear factor I (NFI) gene family of transcription factors encodes site-specific DNA-binding proteins (Gronostajski et al., 1985; Hennighausen et al., 1985; Leegwater et al., 1985; Nowock et al., 1985; Roulet et al., 2000). Initially identified as host proteins essential for adenoviral DNA replication (Nagata et al., 1982), NFI proteins were later found to function in gene regulation, playing a dual role as transcriptional activators and repressors (Jones et al., 1987). In vertebrates, the NFI gene family comprises four members including *Nfia*, *Nfib*, *Nfic* and *Nfix*. Common to all members is a highly conserved N-terminal DNA-binding and dimerization domain, as well as a C-terminal transcription modulation domain showing high variability due to extensive alternative splicing (Meisterernst et al., 1989; Mermoud et al., 1989). NFI proteins can form either homo- or heterodimers, upon which they recognize the palindromic consensus binding sequence 5'-TGGCA-(N_{3,5})-TGCCA-3' (Kruse and Sippel, 1994; Meisterernst et al., 1988).

Members of the NFI family are expressed in unique but overlapping patterns during mouse development and in adult tissues. Genetic loss-of-function studies have revealed essential functions for individual family members during mouse development. Disruption of the *Nfia* gene causes perinatal lethality due to defects in brain development (das Neves et al., 1999). Similarly, loss of *Nfib* results perinatal lethality owing to its critical role in lung and brain formation (Gründer et al., 2002; Steele-Perkins et al., 2005). *Nfic*-deficient mice display abnormal tooth formation, resulting in severe runting and premature death of mice raised on standard laboratory chow (Steele-Perkins et al., 2003). Finally, ablation of *Nfix* yields complex phenotypes including brain malformation,

compromised bone ossification and developmental defects in skeletal muscle. Consequently, *Nfix*-deficient animals succumb within the first postnatal month, likely due to nutrient deprivation (Campbell et al., 2008; Driller et al., 2007; Messina et al., 2010).

In the skin, prior studies had revealed that NFIB is involved in multiple processes of epidermal development (Chiung-Ying Chang, *unpublished*). During embryogenesis, *Nfib*-null animals show delayed formation of the skin barrier and impaired hair follicle induction. Conditional *Nfib*-knockout mice, driven by skin-epithelium specific K14-Cre, similarly showed retardation of hair follicle growth and a diminished population of transit-amplifying cells (Chiung-Ying Chang, *unpublished*). Tracing the origins of impaired hair follicle development, it was found that the HFSC compartment seemed defective. Despite proper specification of HFSCs, evidenced by co-expression of HFSC transcription factors SOX9, LHX2 and NFATc1 during early postnatal development, their maturation and maintenance appeared dysfunctional. SOX9 expression waned shortly after birth, suggesting HFSC function might be perturbed without NFIB. Indeed, hair follicle growth was severely retarded, and follicles precociously entered the destruction phase of the hair cycle (catagen). When challenged upon wounding, *Nfib*-deficient HFSCs failed to participate in the wound healing process, and hair follicles degenerated instead (Chiung-Ying Chang, *unpublished*).

Despite these striking phenotypes in embryonic skin, NFIB is not required for maintaining HFSC function in adult mice (Chang et al., 2013). Unexpectedly, ablation of *Nfib* in mature HFSCs using inducible Cre recombinase, driven either by *K15-CrePGR* or *Sox9-CreER*, did not yield any phenotypic consequences to hair growth or hair follicle maintenance. One possibility to explain the absence of phenotype in adult *Nfib*-deficient

HFSCs is genetic redundancy. Indeed, adult HFSCs characteristically express both *Nfib* and *Nfix* at high levels, where both genes are regulated by super-enhancers (Adam et al., 2015). Given that all NFI-factors recognize a common consensus binding sequence, it is feasible that NFIX can functionally compensate for the loss of NFIB in adult HFSCs.

Results

Loss of *Nfix* does not yield overt phenotypes in hair follicles

To investigate a potential role for NFIX in HFSCs, I performed immunofluorescence labeling with anti-NFIX antibodies to determine its expression pattern throughout development (Fig. 3-1). Interestingly, NFIX was not expressed in skin epithelium during embryonic development, but became robustly active in the outer root sheath of developing hair follicles at P6. Thereafter, NFIX was prominently expressed in basal progenitors of the epidermis, hair follicles as well as emerging TACs. The antibody was validated to be specific for NFIX, as evidenced by lack of signal in *Nfix*-deficient mice (Chiung-Ying Chang, *unpublished*; and see below).

Given the robust expression of NFIX in adult skin, I performed genetic loss-of-function studies to investigate its role in maintenance and growth of hair follicles. To do so, I generated *Nfix* conditional knockout mice using *Sox9-CreER* (Soeda et al., 2010) as driver for inducible, hair follicle-specific gene ablation (*Nfix* cKO mice) (Fig. 3-2). Thus, the activity of the *Sox9-CreER* recombinase can be spatially (entire hair follicles) and temporally controlled and is dependent on chemical application of Tamoxifen (TAM). To efficiently ablate *Nfix* in adult hair follicles, I treated *Sox9-CreER; Nfix^{fl/fl}; YFP^{fl/+}* and control littermate mice with TAM starting in second telogen (P60-P65) and monitored

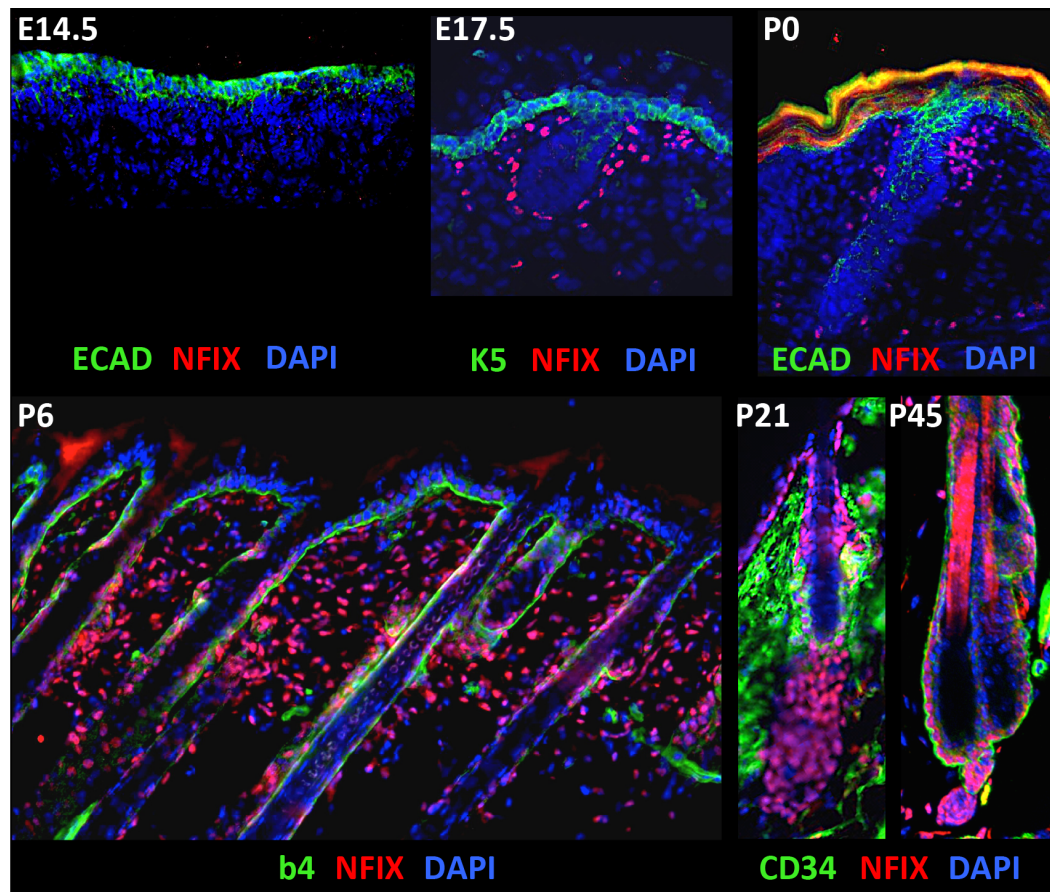


Figure 3-1. NFIX expression pattern in skin during development. NFIX is not expressed in epithelium during embryonic development, but becomes active in ORS around P6. Note expression of NFIX in dermal cells surrounding hair follicles. In adult mice, NFIX is broadly expressed in progenitors of epidermis, HF's and emerging TACs.

hair growth and cycling, as well as follicle morphology and molecular markers in response to loss of *Nfix* (Fig. 3-2). Anti-NFIX immunostaining demonstrated that *Nfix* was efficiently targeted in hair follicles, while epidermal progenitors retained its expression, consistent with *Sox9-CreER* only being active in hair follicles. In contrast, NFIB was still robustly expressed in progenitors of both the epidermis and hair follicles. I then took multiple skin biopsies from the same mouse, to monitor the behavior of hair follicles over time.

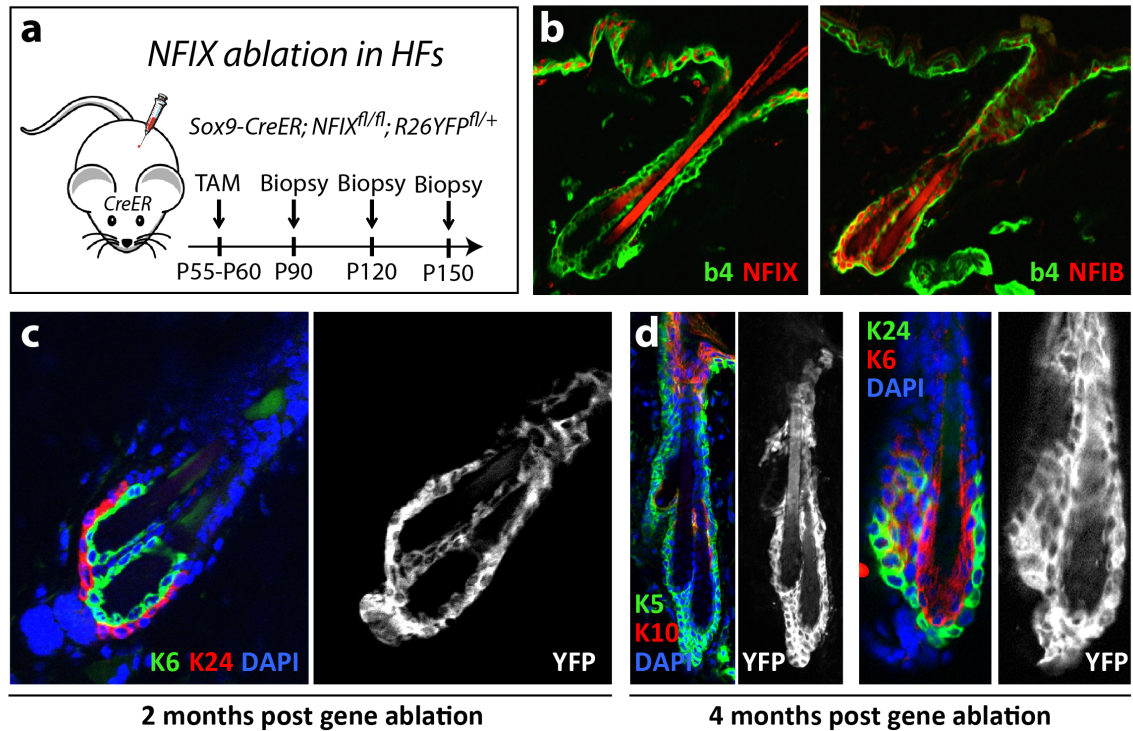


Figure 3-2. Ablation of *Nfix* in adult HFSCs does not perturb HF morphology or function. **a**, Gene targeting strategy: *Sox9-CreER* is only active in hair follicle progenitors. Multiple biopsies were taken post-treatment to monitor phenotype over time. **b**, Immunofluorescence showing efficient targeting of *Nfix* in HFcs but not in epidermal progenitors. In contrast, NFIB remains robustly active. **c**, Loss of NFIX does not affect HFSCs (K24+) or HF morphology 2 months post-TAM. **d**, Longitudinal study showing no gross alterations in bulge architecture at 4 months after gene ablation.

However, despite efficient targeting of telogen phase HFSCs in >90% of follicles, the hair coat of *Nfix* cKO mice seemed unaffected, and no significant alterations were detected in HF morphology or cycling over the course of the following 4 months post gene ablation. *Nfix* cKO mice regenerated their hair coat, and K24+ HFSCs were maintained over the course of the experiment (Fig. 3-2). Thus, similar to *Sox9-CreER*; *Nfib* cKO mice, the loss of *Nfix* appeared to have no overt functional consequence to epithelial cells in the hair follicle of adult mice. Collectively, these results suggested the

tantalizing hypothesis that genetic redundancy in NFI-family members might exist for the robust maintenance of adult HFSCs. In support of this notion, the curious expression pattern of NFIX might explain the disparate effects of *Nfib* loss at different times during development: During embryogenesis, *Nfix* is not expressed, hence the dramatic defects on skin epithelium in the absence of *Nfib*. In contrast, NFIX becomes active shortly after birth and maintains its robust expression in HFSCs. Thus, it is feasible that adult mice show genetic redundancy for functional compensation, with both *Nfib* and *Nfix* being highly expressed and driven by super-enhancers in HFSCs. If this is indeed the case, the combined loss of *Nfib* and *Nfix* will be required to reveal the function of NFI family members in adult hair follicles.

NFIB and NFIX function redundantly in murine hair follicles

To test this intriguing hypothesis, I generated *Sox9-CreER; Nfib^{fl/fl}; Nfix^{fl/fl}; YFP^{fl/+}* mice (NFI-dKO). Similar to the strategy outlined above, I administered TAM to NFI-dKO mice in second telogen to induce ablation of both *Nfib* and *Nfix* during the resting phase of the hair cycle (Fig. 3-3). To verify efficient gene targeting, I used immunofluorescence analysis to demonstrate that NFIB and NFIX were absent in YFP+ follicles of dKO mice, whereas control follicles showed robust nuclear expression of both transcription factors. Indeed, the combined loss of NFI family members induced strong phenotypes in adult hair follicles: The most striking defects observed were dramatic alterations in hair follicle morphology at 1 month after gene ablation (Fig. 3-3): Hair follicles had changed their stereotypical structure and became distorted. In many cases,

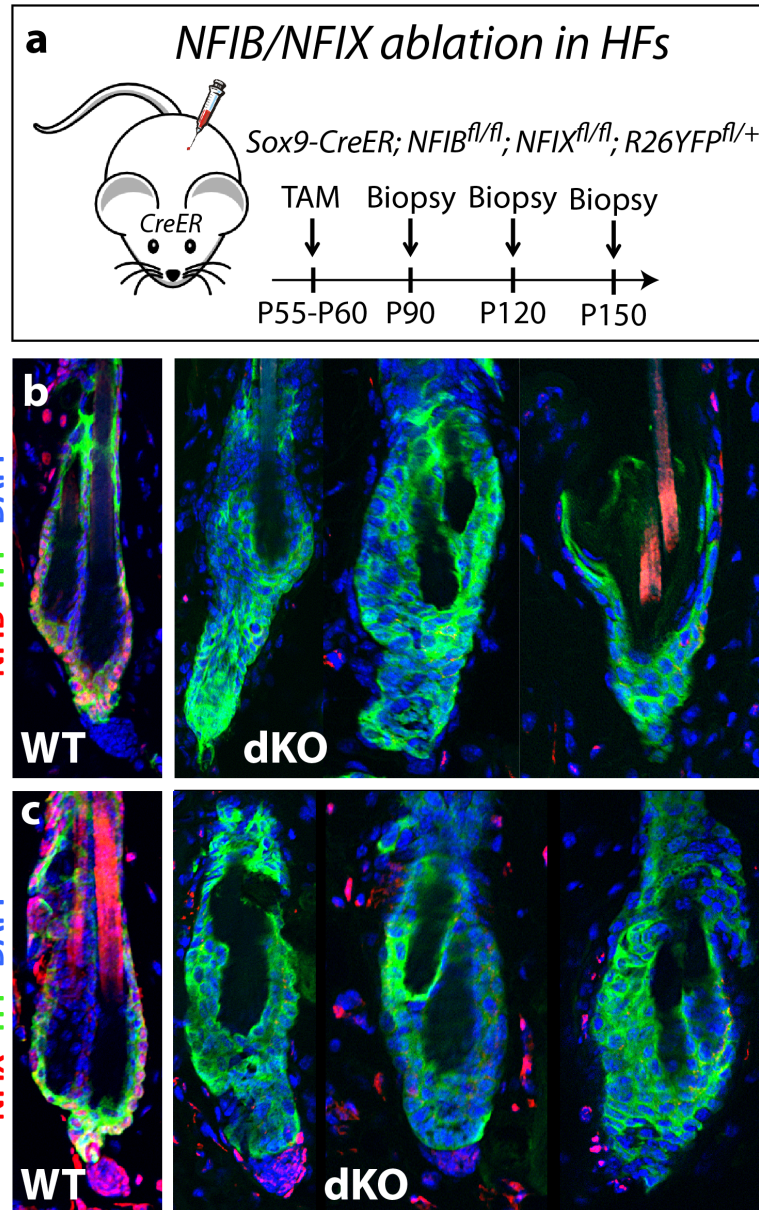


Figure 3-3. NFI-dKO mice show dramatic alterations in hair follicle morphology. **a**, Gene targeting strategy: *Sox9-CreER* is only active in hair follicle progenitors. Multiple biopsies were taken post-treatment to monitor phenotype over time. **b-c**, Immunofluorescence showing efficient targeting of *Nfib* and *Nfix* in YFP+ HFs of dKO mice. Note morphological changes in dKO follicles at 1 month after TAM treatment.

the two bulges, typically seen in second telogen, seemed to collapse and had merged into one. This was frequently associated with the loss of hair, which is typically anchored by the bulge. Furthermore the hair germ, a primed stem cell population at the base of the follicle, appeared enlarged and elongated in some dKO follicles.

To obtain more insights into the phenotypic changes, I performed immunofluorescence analyses. Studies on *Nfib*-deficient embryos had revealed defects in epidermal differentiation (Chiung-Ying Chang, *unpublished*). Thus, I probed for differentiation markers in hair follicles (Fig. 3-4). Unexpectedly, I discovered that in the absence of NFI transcription factors, hair follicles experienced the ectopic induction of epidermal differentiation markers. Keratin 10 (K10) is typically present in the suprabasal (spinous) layer of the epidermis, representing an early differentiation marker. In normal hair follicles, K10 is similarly expressed in suprabasal cells, which likely helps to provide a barrier to the hair channel. In dKO mice, however, K10 expression was drastically increased in the hair channel, along with dead, keratinized material accumulating in the orifice close to the skin surface (Fig. 3-4). Frequently, the inner bulge layer, adjacent to HFSCs, became entirely K10+ as well. This phenomenon was not limited to ectopic K10. Immunofluorescence staining with anti-FILAGGRIN antibodies, a marker for late epidermal differentiation, revealed similarly dramatic changes, with FILAGGRIN accumulating and extending deep into the hair channel (Fig. 3-4). Finally, ectopic epidermal differentiation was also observed during the regenerative phase of the hair cycle: During anagen, ectopic K10 was also induced in the inner root sheath (IRS) lineages, where NFIB and NFIX are specifically expressed. Collectively, these changes suggested that a program of terminal epidermal differentiation was readily induced in

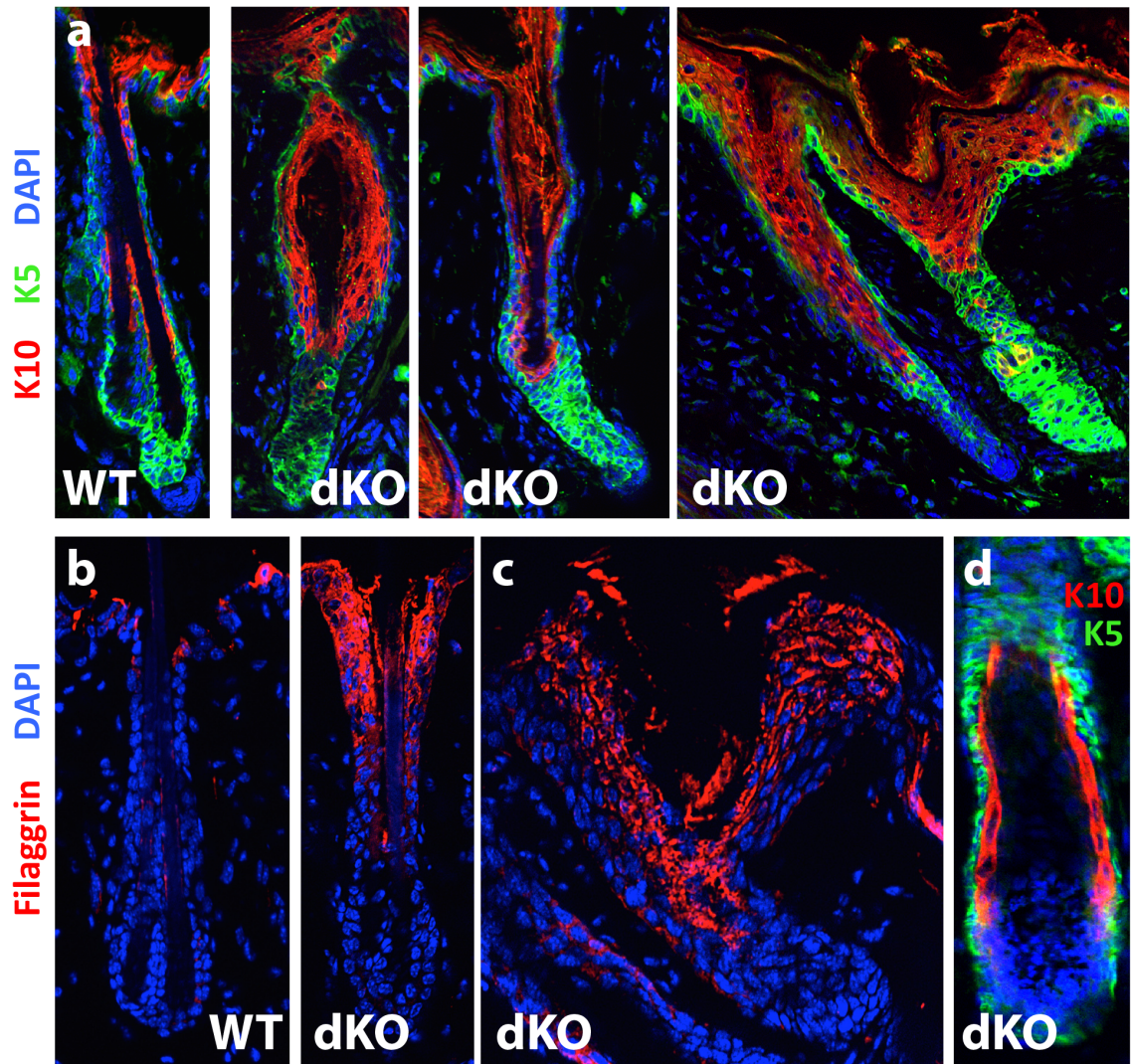


Figure 3-4. Ectopic epidermal differentiation in NFI-deficient hair follicles. **a**, The epidermal differentiation marker K10 is ectopically induced in NFI-dKO hair follicles. **b-c**, Terminal differentiation marker FILAGGRIN, typically restricted to the stratum granulosum in the epidermis, is ectopically active in dKO hair follicles at 2 weeks after treatment (**b**), and becomes progressively worse over time (**c**, 2 months after TAM). **d**, Abnormal induction of K10 in the inner root sheath (IRS) of anagen follicles.

dKO mice, and provided first hints towards a function of these transcription factors. The data suggest that NFI-TFs maintain the undifferentiated fate of hair follicle progenitors.

Given the induction of terminal differentiation markers, I wondered to what extent functional K24+ HFSCs might remain in NFI-dKO mice. K24+ cells were scattered and appeared outside of the normal bulge niche (Fig. 3-5). However, whether these are HFSCs that have migrated upwards, or represent ectopic induction of K24 in other follicular cells awaits further investigation. Nonetheless, a clear ‘bulge niche’, with an organized array of K24+ HFSCs was no longer observed in dKO mice (Fig. 3-5).

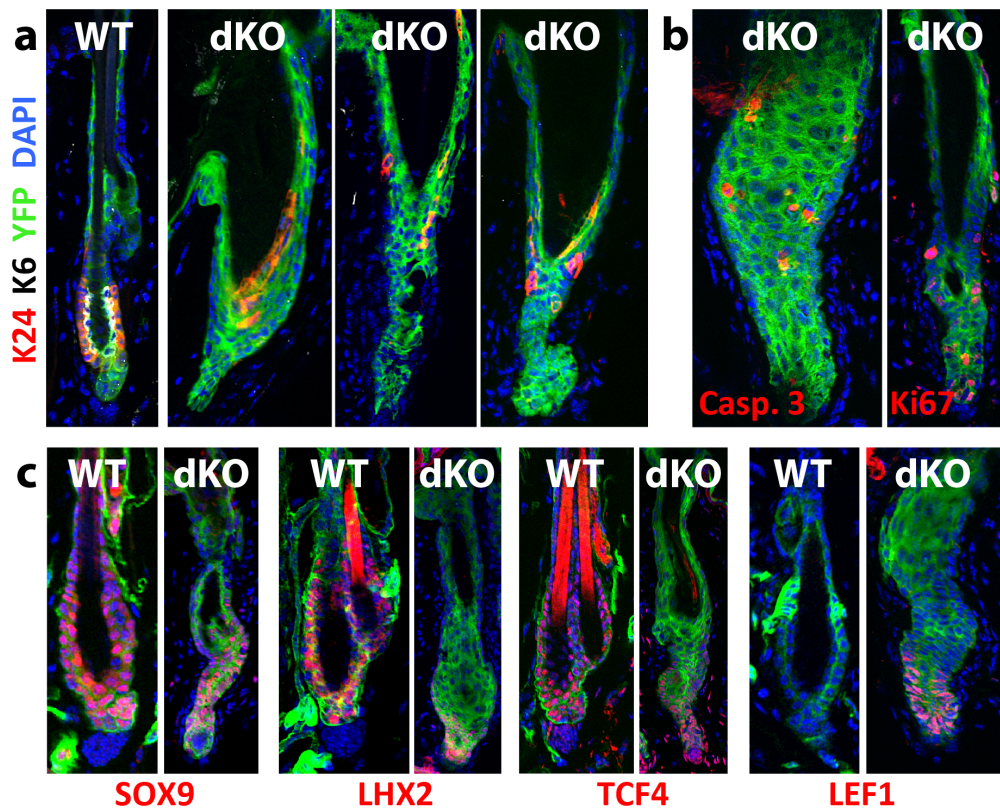


Figure 3-5. Morphological and molecular changes in the NFI-dKO HFSC niche. a, Loss of an organized array of K24+ bulge cells in dKO mice. **b,** Cellular turnover in dKO follicles. Both apoptosis (active Caspase 3) and proliferation (Ki67) are observed. **c,** HFSC-TFs are suppressed in the bulge niche, but remain active at the base of the follicle. Note ectopic induction of LEF1, a marker for HF fate commitment.

Immunofluorescence to probe for typifying HFSC markers corroborated that functional HFSCs were lost. HFSC master regulators SOX9, LHX2, and TCF4 were all suppressed in the former bulge region, but remained active in the elongated structures at the base of the follicles, which likely represent hair germ cells. Curiously, these cells also displayed nuclear LEF1, a marker for fate commitment in the hair follicle (Fig. 3-5). Furthermore, both markers for apoptosis (active Caspase 3) and proliferation (Ki67) were observed in dKO follicles. Combined with differentiation markers, these data suggest that the dKO bulge niche is drastically altered, and typical features of HFSCs were no longer detected. Accordingly, dKO mice did not regenerate their hair coat.

NFI-TFs maintain the function of multiple skin appendages

I then wondered whether the function of NFI transcription factors was restricted to the hair follicle, or is a more general feature for multiple skin appendages. Immunostaining for sebaceous gland markers provided insights: ADIPOPHILIN is a lipid-droplet associated protein and typifies mature sebocytes. Whereas WT follicles displayed robust ADIPOPHILIN staining above the bulge region, sebaceous glands seemed to gradually disappear over time in the dKO mice (Fig. 3-6). Although the fate of sebocytes and their progenitors remains to be determined, one attractive hypothesis is that these cells, too, adopt epidermal differentiation markers and are thus lost.

Furthermore, NFI factors are also active in sweat glands, as is the *Sox9* promoter driving CreER. I worked with Catherine Lu in the lab to investigate the functional consequence of NFI ablation in mature sweat glands and ducts. WT sweat ducts appeared

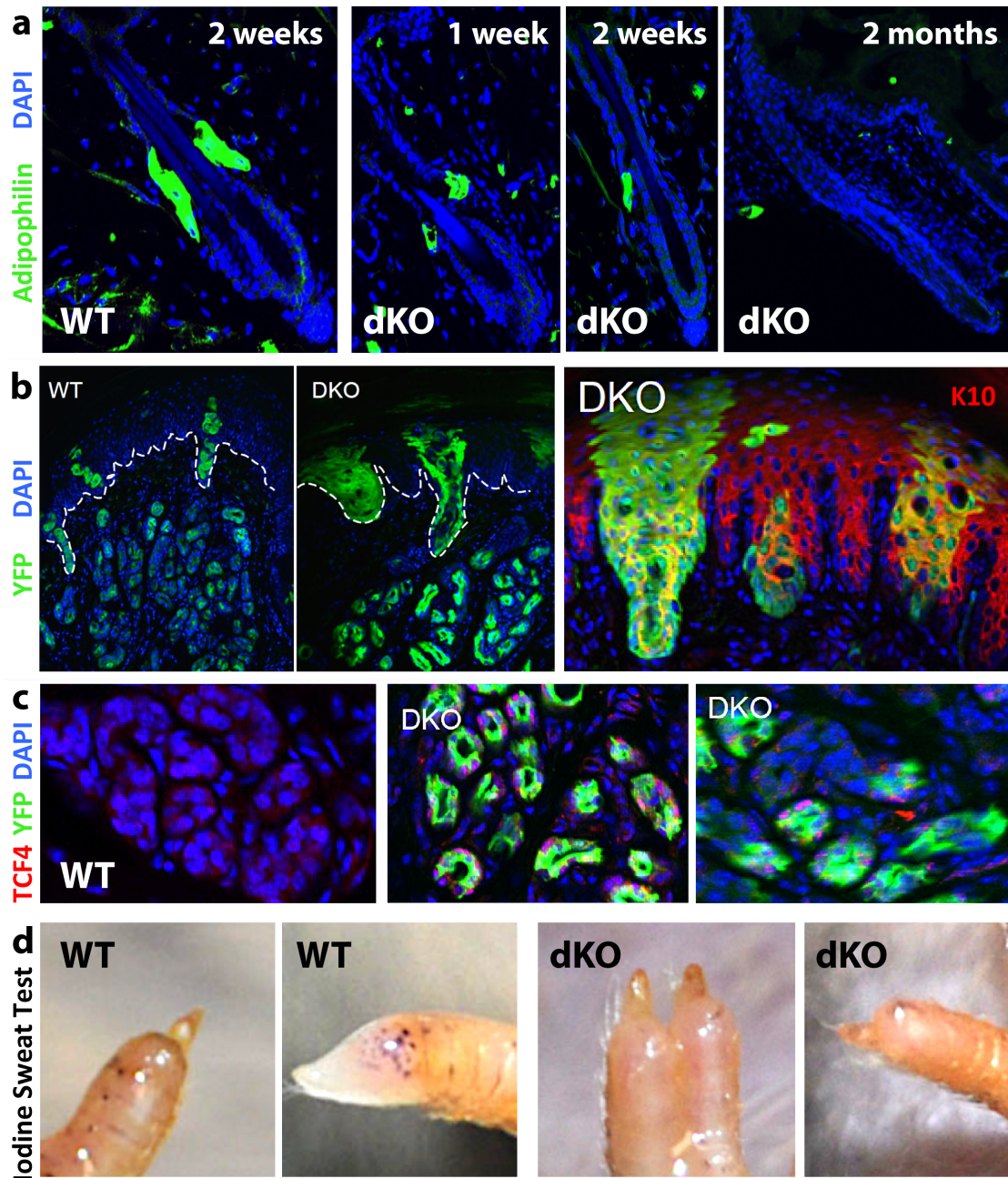


Figure 3-6. Loss of NFI-TFs affects multiple skin appendages. **a**, Temporal loss of sebaceous glands in dKO mice. Time indicated refers to time after gene ablation **b**, Enlargement of sweat ducts in dKO mice. **c**, Ectopic induction of WNT effector TCF4 in YFP+ (dKO) sweat glands. **d**, Iodine sweat test reveals functional impairment of dKO sweat glands. Note brown spots on fingertips of WT, but not dKO mice. *Note:* Sweat gland analyses were performed by Dr. Catherine Lu (postdoctoral fellow, Fuchs lab).

narrow and had a coiled structure (Fig. 3-6). In contrast, dKO sweat ducts seemed enlarged and adopted an abnormal morphology, reminiscent of sweat ducts undergoing wound repair (Lu et al., 2012). Even more intriguing were the effects observed in the sweat glands. While mature sweat glands in WT mice represent a WNT-repressed environment, NFI-dKO glands displayed ectopic induction of WNT-effector TCF4. This appeared to be a cell-autonomous or paracrine effect, as YFP^{neg} glands did not show this phenomenon (Fig. 3-6). To test the functional consequence of these alterations, Catherine Lu performed iodine/starch-based sweat tests on paw pads of the animals. This procedure detects sweat, reflective of a functional gland (Lu et al., 2012). WT mice scored positive for the test, indicated by the black dots appearing on the animal's fingertips. In contrast, the test was negative in NFI-deficient animals, suggesting these mice did not sweat (Fig. 3-6). The alterations in WNT signaling, the aberrant structure of the sweat ducts, and our failure to detect sweat collectively suggested that in the absence of NFI factors, sweat glands were functionally impaired. In summary, my analyses on dKO mice revealed that NFIB and NFIX act redundantly to maintain the function of multiple skin appendages.

Molecular insights into HFSC behavior upon loss of *Nfib* and *Nfix*

The striking phenotype of NFI-dKO hair follicles suggested equally dramatic changes on the level of gene expression and chromatin landscapes. To test this hypothesis and gain insights into the molecular changes of NFI-dKO follicles, I FACS-purified HFSCs from WT and dKO mice and subjected them to RNA-sequencing. One major challenge in devising an ideal experimental strategy for the purification of HFSCs was the strong phenotype in the dKO mice: Epidermal differentiation markers turned on

rapidly (within 1-2 weeks post TAM), molecular markers of stem cells disappeared over time (within 3-4 weeks post TAM), and morphological alterations appeared to even precede the molecular changes. I determined the 2 weeks time point (following gene ablation) as being optimal, as molecular changes had initiated, but dKO HFSCs still expressed CD34 and other known stemness markers. RNA-sequencing revealed 1307 genes as significantly changed between WT and dKO HFSCs (Figure 3-7, Table 3-1).

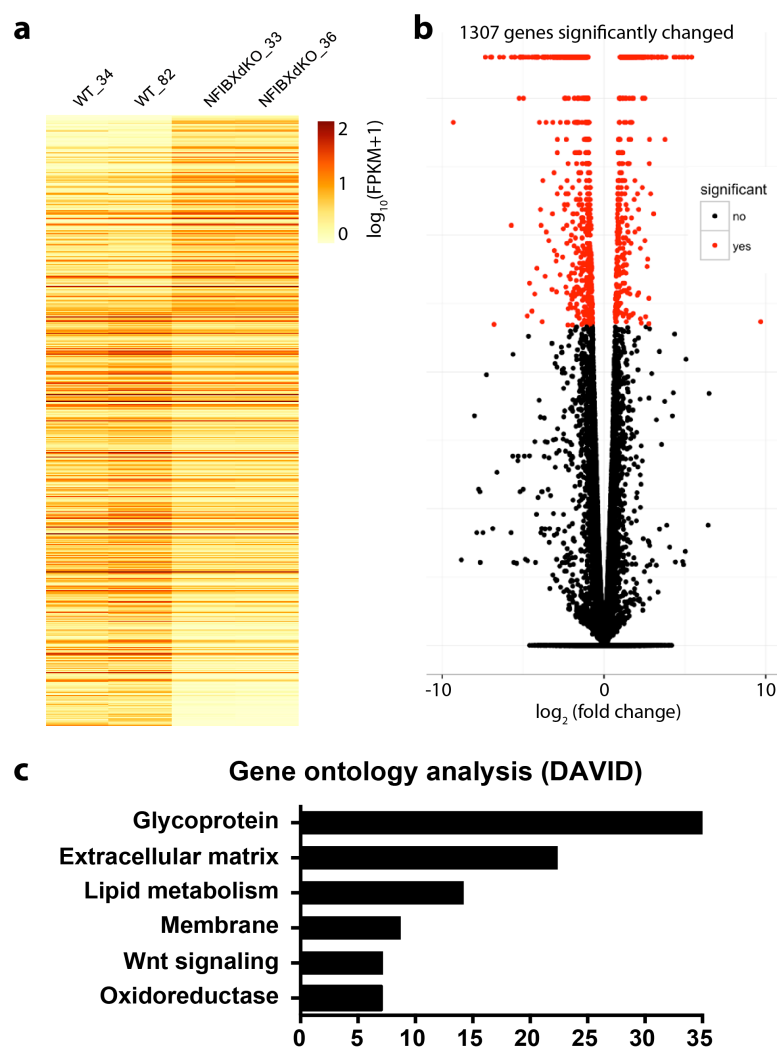


Figure 3-7. RNA-seq analysis on NFI-dKO HFSCs. **a**, Heatmap showing relative expression levels between WT and dKO (n=2). **b**, Volcano plot showing significantly changed genes. **c**, Gene ontology analysis on significantly changed genes (DAVID).

Table 3-1. Selected list of differentially expressed genes (WT vs. NFI-dKO)

Pathway	Gene	Δ dKO/ WT	Pathway	Gene	Δ dKO/ WT	Pathway	Gene	Δ dKO/ WT
HFSC Identity	<i>Krt24</i> *	-16.46x	WNT	<i>Wnt16</i>	+7.50x	ECM, Adhesion	<i>Myoc</i> *	-638x
	<i>Lgr5</i> *	-3.31x		<i>Wnt6</i>	+5.38x		<i>Ltbp2</i>	-35x
	<i>Lhx2</i> *	-3.06x		<i>Tnfrsf11b</i> ^Δ	+5.17x		<i>Adamts14</i> *	-8.08x
	<i>Krt14</i> *	-2.28x		<i>Wnt3a</i>	+4.54x		<i>Ecm1</i>	-7.86x
	<i>Krt15</i> *	-1.75x		<i>Apcdd1</i> * ^Δ	+3.87x		<i>Col8a2</i> *	-6.26x
	<i>Tcf7l1</i> *	-1.75x		<i>Wnt5a</i>	+3.53x		<i>Prickle2</i> *	-2.57x
	<i>Sox9</i> *	-1.53x		<i>Wif1</i>	+3.37x		<i>Tnc</i> *	+3.21x
	<i>Cd34</i> *	-1.29x		<i>Wnt3</i>	+3.30x		<i>Sdk1</i> *	+3.47x
	<i>Krt10</i> *	+1.32x		<i>Wnt7b</i>	+2.66x		<i>Ncam1</i> *	+11.85x
	<i>Krt1</i>	+1.78x		<i>Wls</i>	+2.36x		<i>Gpnmb</i>	+12.40x
	<i>Krt17</i> *	+3.32x		<i>Axin2</i> ^Δ	+2.29x		<i>Itga8</i>	+35.86x

* direct NFIB targets

^Δ Wnt target genes

Gene ontology (GO) analysis revealed that categories including “Glycoprotein”, “Extracellular Matrix” and “Membrane” were highly represented, suggesting a function for NFI proteins in regulating cellular behavior with its microenvironment (Fig. 3-7). This is also reflected in Table 3-1, showing dramatic changes for genes related to ECM and cell adhesion. Equally interesting was WNT signaling, which was enriched in the GO terms. Closer inspection of differentially expressed genes revealed that a number of WNT ligands, as well as the *Wls* gene, essential for secretion of WNTs, were prominently induced in dKO follicles. The upregulation of WNT target genes *Axin2*, *Apcdd1* and *Tnfrsf11b* provided further insights into potential autocrine signaling, illustrating that dKO HFSCs also actively respond to WNT ligands (Table 3-1).

As indicated above, HFSCs are gradually lost over time in dKO mice. This was already reflected on the gene expression level. HFSC identity genes, often driven by super-enhancers, were decreased, with typifying HFSC keratin K24 almost entirely

suppressed. Conversely, keratins characteristic of epidermal differentiation (K1, K10) trended upwards, reflective of the transition stage of dKO HFSCs to become committed.

To test the impact of NFI-loss of chromatin landscapes, WT, *Nfix* cKO and NFI-dKO HFSCs were purified 2 weeks after TAM and subjected to ATAC-seq, which provides information about accessible chromatin (Buenrostro et al., 2013) (Fig. 3-8).

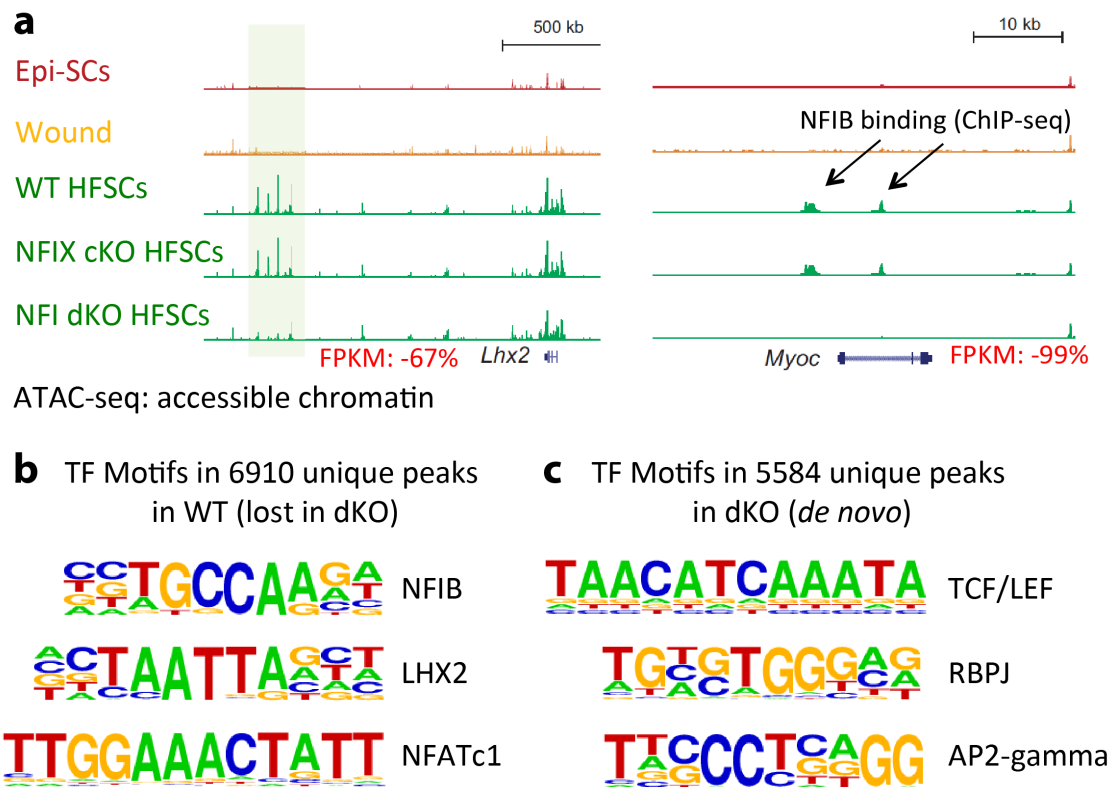


Figure 3-8. Changes in chromatin accessibility in NFI-dKO HFSCs. **a**, ATAC-seq gene tracks showing specific loss of accessible chromatin in dKO HFSCs at the super-enhancer regulating *Lhx2* (green shade), or typical enhancer for *Myoc*. Note corresponding suppression of gene expression. **b**, Motif analysis on ATAC-seq peaks unique to WT (lost in dKO). Note enrichment for known HFSC master TFs, including NFIB. **c**, Motif analysis on ATAC-seq peaks unique to dKO (*de novo*). Note enrichment for TFs driving epidermal differentiation, including RBPJ and AP2-gamma. Note: Dr. Yejing Ge, postdoctoral fellow (Fuchs lab) assisted with ATAC-seq procedures.

The loss of HFSC identity based on gene expression was paralleled on the chromatin level. NFI-dKO HFSCs showed specific loss of accessible chromatin at the super-enhancer region driving master TF *Lhx2*, corresponding to a 67% reduction in *Lhx2* expression (Figure 3-8). The promoter region of *Lhx2* seemed unaffected. In contrast, *Nfix* single cKO mice did not show these alterations, and behaved like WT HFSCs, consistent with the absence of phenotypic changes in these mice. The effect of NFI transcription factor loss was not limited to super-enhancers: The *Myoc* gene, encoding for the secreted glycoprotein MYOCILIN, was entirely suppressed. This was readily explained by the loss of open chromatin at the *Myoc* promoter and enhancer, both of which were physically bound by NFIB (ChIP-seq) (Figure 3-8).

Probing deeper for changes in chromatin accessibility and the driving forces behind it, I performed motif analysis to identify global changes in putative TF binding (Fig. 3-8). In WT HFSCs, the ATAC-peaks (open chromatin) that were uniquely active contained TF binding motifs for known HFSC TFs, including NFIB, LHX2 and NFATc1, indicative of the homeostatic regulatory programs that maintain HFSC identity (Adam et al., 2015). Many of these peaks were lost in dKO HFSCs. Instead, thousands of chromatin regions became uniquely active in dKO HFSCs, which now harbored binding sites for TCF/LEF, RBPJ and AP2-gamma TFs (Fig. 3-8). This was particularly intriguing, given the established role and cooperation of NOTCH/RBPJ and AP2-gamma in driving epidermal differentiation (Blanpain et al., 2006; Moriyama et al., 2008; Wang et al., 2008). This rewiring of regulatory circuitries in NFI-deficient HFSCs might provide the mechanistic basis for the ectopic epidermal differentiation (K10, FILAGGRIN) that was readily observed in the dKO mice.

To investigate whether signs of active NOTCH signaling were indeed detected in dKO mice, I performed immunofluorescence analyses using anti-HES1 antibodies. HES1 is a canonical downstream target of NOTCH/RBPJ, and has well-established roles during epidermal differentiation (Blanpain et al., 2006; Moriyama et al., 2008). At the timepoint when RNA- and ATAC-sequencing were performed, HES1 was silent in both WT and dKO HFSCs. However, at later stages, HES1 was robustly active in dKO follicles, consistent with the RBPJ motif being highly enriched in dKO chromatin. To further corroborate the notion that dKO follicles adopt an epidermal fate, I stained for GATA3, a transcription factor prominently expressed in the epidermis, where it is regulated by a super-enhancer. Similarly to HES1, GATA3 expression was not detected at the early stages, but became induced and persisted at 2 months after gene ablation.

Collectively, these data suggest that in the absence of *Nfib* and *Nfix*, HFSCs rewire their transcriptional circuitries to adopt an epidermal fate. This process appeared to be driven by NOTCH signaling, but awaits further investigation.

Discussion

In this chapter, I have explored the functional role of NFI transcription factors NFIB and NFIX in hair follicle stem cells. I first became interested in NFI transcription factors due to their intricate regulation: Both *Nfib* and *Nfix* are regulated by super-enhancers in HFSCs, where they are expressed at high levels. Moreover, given prior work showing the absence of phenotypic changes in skin epithelium of adult mice in *Nfib*-deficient mice, I hypothesized that genetic redundancy may have evolved as safeguard to protect against the loss of one of these potentially critical transcription factors.

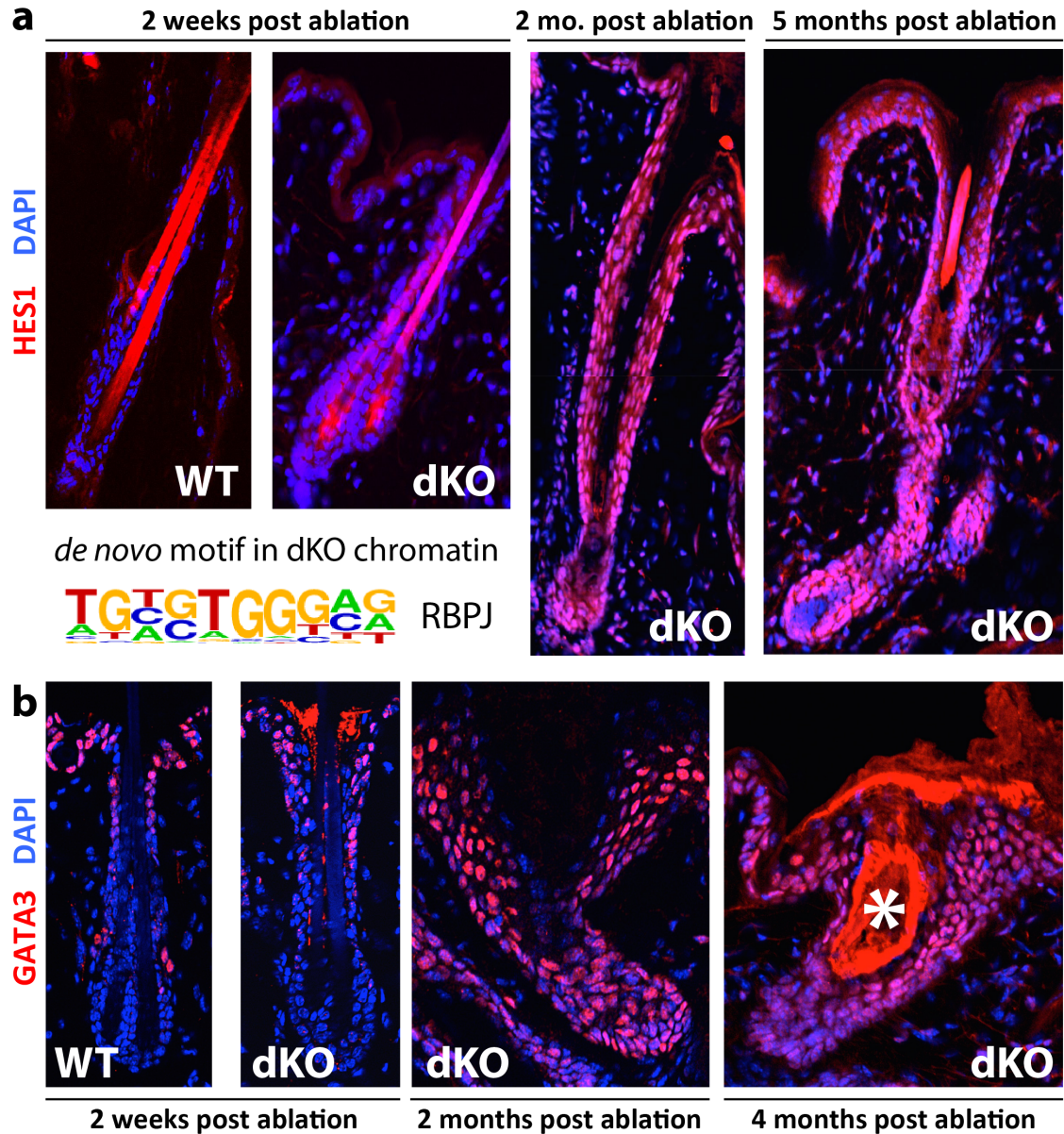


Figure 3-9. Activation of epidermal transcriptional regulators in NFI-dKO hair follicles. **a**, Immunofluorescence analysis using anti-HES1 antibodies. Note absence of HES1 in WT and dKO HF's at 2 weeks post gene ablation, but robust induction of HES1 in dKO follicles at later stages. **b**, Epidermal transcription factor GATA3 is ectopically expressed in dKO follicles. Asterisk marks a keratin pearl accumulating at later stages.

Several interesting aspects emerged from this work. First, studies on *Nfix* single cKO mice indeed confirmed that genetic redundancy protects hair follicles from perturbations. Neither the individual loss of *Nfib* or *Nfix* appeared to cause phenotypic changes in adult skin epithelium. In sharp contrast, the combined loss of NFI factors led to rapid and robust alterations in hair follicle architecture and function.

The most striking changes were related to the ectopic induction of terminal epidermal differentiation markers in hair follicles. In WT mice, KERATIN 10 (K10) and FILAGGRIN are typically restricted to suprabasal cells, mainly in the epidermal layers, but also in the hair channel to provide barrier function. However, in the absence of NFI-transcription factors, K10 and FILAGGRIN were dramatically increased. Expression was upregulated first in the hair channel, but rapidly continued to move down and was eventually seen in the bulge region, including in HFSCs. Furthermore, in anagen hair follicles, epidermal differentiation markers were turned on in the IRS layers, which also contribute to the hair channel. As a consequence, the hair channel became blocked by accumulating, dead keratin material, preventing new hair to penetrate through the orifice.

These defects were complemented by severe changes in the HFSC compartment. dKO HFSCs were rapidly lost, and appeared to suppress HFSC identity markers, including typifying HFSC TFs SOX9, LHX2 and TCF4 as well as the characteristic structural proteins K24 and CD34.

As importantly, striking defects were also observed in sebaceous and sweat glands. Mature sebocytes disappeared gradually over time, as indicated by the loss of lipid-droplet associated protein ADIPOPHILIN. The phenotype in sweat glands mirrored the effect seen on hair follicles in two regards. First, as seen in the hair channel, the sweat

duct seemed enlarged and displayed aberrant morphology, reminiscent of ducts participating in wound repair (Lu et al., 2012). Second, dKO sweat glands displayed ectopic activation of WNT-effector TCF4. This was curious, as WT sweat glands were found to be in a WNT-silenced environment. dKO HFSCs also displayed ectopic WNT activation, suggesting common properties of NFI-TFs across multiple skin appendages. Most importantly, however, the function of sweat glands was perturbed. Iodine/starch sweat tests revealed that NFI-dKO mice did not produce sweat, just as they were incapable of growing hair.

Probing for mechanism, the combination of RNA-seq and ATAC-seq offered unique insights into the shifts in transcriptional and chromatin landscapes that had occurred. In dKO HFSCs, chromatin regions that harbor TF binding sites to maintain homeostatic HFSCs programs were closed, while new regions were readily made accessible. As such, novel binding sites for NOTCH-effector RBPJ and AP2-gamma emerged, at the expense of key HFSC super-enhancers, which appeared to be decommissioned. The rewiring of chromatin to open up sites for NOTCH and AP2 was particularly intriguing, given the well-documented roles of these pathways in governing epidermal differentiation. Thus, the collective data suggest a mechanism in which the loss of NFI-TFs destabilizes the homeostatic gene regulatory program that maintains HFSCs, and simultaneously directs them towards differentiation. The outcome is organ degeneration, whether it be hair follicles, sebaceous glands or sweat glands. Further studies targeting the NOTCH pathway will be underway to strengthen the connection between chromatin changes and the observed phenotype.

Finally, it is noteworthy that the changes in extracellular matrix (ECM) components and cellular adhesion were equally striking, although they have remained unexplored thus far. ECM restructuring is particularly interesting, since the morphological changes in dKO follicles precede the molecular alterations. In fact, hair follicle distortions or cellular rearrangements can be observed as early as one week following gene ablation. Sweat ducts also displayed aberrant structures, again pointing to commonalities between multiple skin appendages. Thus, it is feasible that defects in cell adhesion, or impaired growth factor signaling typically associated with intact ECM, might be the most upstream event that kicks off the cascade of changes, ultimately resulting in terminal differentiation and follicular degeneration. While certainly intriguing, more studies will be required to pinpoint the series of events leading to demise of skin appendages in dKO mice.

In summary, my results illustrate the importance of NFI transcription factors NFIB and NFIX in the maintenance of multiple skin appendages. Further exploration of the underlying cause, and characterization of the roles of altered signaling pathways will shed light into the mechanisms by which progenitor status in the skin is maintained throughout the lifetime of an animal.

Materials and Methods

Mouse lines

Sox9-CreERT2, *Nfib^{fl/fl}* and *Nfix^{fl/fl}* mice have been described (Campbell et al., 2008, Soeda et al., 2010, Hsu et al., 2011b), and were bred to generate *Sox9-CreERT2*; *Nfib^{fl/fl}*; *Nfix^{fl/fl}*; *R26YFP^{fl/+}* mice. CreER was activated in second telogen (P60-P65) by intraperitoneal injection of mice with 20mg ml⁻¹ tamoxifen (Sigma Cat#T5648) in corn oil (Sigma), resulting in gene ablation and simultaneous labeling of hair follicles with YFP. Mice were maintained in the Association for Assessment and Accreditation of Laboratory Animal Care-accredited animal facility of The Rockefeller University (RU), and procedures were performed with Institutional Animal Care and Use Committee (IACUC)-approved protocols.

Flow Cytometry

Preparation of adult mice back skins for isolation of HFSCs were done as previously described (Nowak et al., 2009). Briefly, for telogen skin, subcutaneous fat was removed with a scalpel, and skins were placed dermis side down on 0.25% Trypsin-EDTA (Gibco) at 37°C for 35 min. Single-cell suspensions were obtained by scraping the skin gently. Anagen skin was treated with collagenase at 37°C for 30 minutes to dissociate dermal cells and then incubated with 0.25% Trypsin-EDTA (Gibco) at 37°C for 15 minutes to detach and generate single cell suspensions of the epidermal and HF cells. Cells were then washed with PBS containing 5% of fetal bovine serum (FBS), then filtered through 70µm and 40µm cell strainers (VWR). Cell suspensions were incubated with the appropriate antibodies for 30 min on ice. The following antibodies were used for

FACS: α 6-PE (1:100, eBiosciences), CD34-eFluoro660 (1:100, eBiosciences) and Sca-1-PerCP-Cy5.5 (1:1000, eBiosciences). YFP fluorescence (*Rosa26-YFP^{fl/+}* alleles) was also used as positive selection marker. 4'6'-diamidino-2-phenylindole (DAPI) was used to exclude dead cells. Cell isolations were performed on FACS Aria sorters running FACSDiva software (BD Biosciences).

RNA extraction, RNA-sequencing and data processing

FACS-isolated cells were sorted directly into Trizol^{LS} (Invitrogen). Total RNA was purified using the Direct-zol RNA MiniPrep kit (Zymo Research) per manufacturer's instructions. DNase treatment was performed to remove genomic DNA (RNase-Free DNase Set, Qiagen). Equal amounts of RNA were reverse-transcribed using Oligo-dT primers (Superscript III, Life Technologies). Quality of RNA samples was determined using an Agilent 2100 Bioanalyzer, and all samples for sequencing had RNA integrity (RIN) numbers >9. cDNA library construction using the Illumina TrueSeq mRNA sample preparation kit was performed by the Weill Cornell Medical College Genomic Core facility (New York, NY), and cDNA libraries were sequenced on an Illumina HiSeq 2000 instrument.

Sequencing reads from bulk RNA-seq were aligned to the mouse reference genome (Version mm10 from UCSC) using Bowtie2 (version 2.2.9) (Langmead and Salzberg, 2012) with default parameters. The expression values of each gene were quantified as transcript per million (TPM) using RSEM (v1.2.30) (Li and Dewey, 2011). Differential gene expression analyses were performed on normalized raw counts using DEseq package (Anders and Huber, 2010) in R software. Genes with fold change >2 and

FDR < 0.1 were considered to be differentially expressed. A list of selected genes was presented by a heatmap with z-scores normalized expression value.

ATAC-seq

ATAC-seq libraries were prepared from freshly FACS-sorted HFSCs. Library preparation and analysis was performed as described (Buenrostro et al., 2013). Briefly, FACS-sorted cells were pelleted and incubated with cold lysis buffer (10 mM Tris-HCl, pH 7.4, 10 mM NaCl, 3 mM MgCl₂, 0.1% IGEPAL CA-630). After removing lysis buffer by centrifugation, tagmentation reaction was performed by an Illumina DNA Sample Preparation Kit according to manufacturer's instructions. After PCR amplification, the samples were sequenced on Illumina HiSeq 2000 using a 50bp paired-end-reads setting. 50-bp paired-end reads were aligned to mm10 using bowtie with the parameters -X 2000 and -m 1. Duplicates were removed using Picard. ATAC-seq signal tracks were presented by Integrative Genomics Viewer (IGV) software (Robinson et al., 2011).

Antibodies

The following antibodies and dilutions were used: NFIB (rabbit, 1:1000, Active Motif), NFIX (rabbit, 1:1000, Thermo Fisher), SOX9 (rabbit, 1:1000, Millipore), LHX2 (rabbit, 1:2000, Fuchs lab), K6 (guinea pig, 1:5000, Fuchs Lab), K24 (rabbit, 1:5000, Fuchs lab), CD34 (rat, 1:100, BD-Pharmingen), LEF1 (rabbit, 1:100, Fuchs lab), TCF4 (rabbit, 1:300; Cell Signaling Technology), GATA3 (rat, 1:200, Ebioscience), HES1 (rabbit, 1:1000, Fuchs lab), P-CADHERIN (rat, 1:100, Fuchs lab), β 4-Integrin (rat,

1:100, BD-Pharmingen), GFP (chicken, 1:2000, Abcam). Secondary Abs coupled to Alexa488, RRX, or Alexa647 were from Life Technologies. Nuclei were stained using 4'6'-diamidino-2-phenylindole (DAPI).

Histology, Immunofluorescence and Imaging

For immunofluorescence analysis, mouse backskins were dissected and either embedded directly in OCT (Tissue Tek), or fixed with 4% paraformaldehyde (PFA) in PBS for 1 hours at 4°C to preserve the cytoplasmic fluorescent signal and then incubated with 30% sucrose for overnight followed by embedding in OCT. Frozen tissue blocks were sectioned at 12 µm on a cryostat (Leica), and mounted on SuperFrost Plus slides (Fisher). Non-prefixed tissue sections were incubated with 4% PFA (Paraformaldehyde) for 10 minutes and rinsed 5 times with PBS. The tissue sections were blocked for 1 hour at room temperature in blocking solution (5% normal donkey serum, 0.5% bovine serum albumin, 2.5% fish gelatin and 0.3% Triton X-100 in PBS). Sections were incubated with primary antibodies diluted in blocking solution at 4°C overnight. Sections were then washed three times with PBS and incubated with secondary antibodies in blocking solution at room temperature for 1 hour. Finally, sections were washed three times with PBS and mounted with ProLong Gold Antifade Mountant (Thermo Fisher Scientific).

Images were acquired with an Axio Observer.Z1 epifluorescence microscope equipped with a Hamamatsu ORCA-ER camera (Hamamatsu Photonics), and with an ApoTome.2 (Carl Zeiss) slider that reduces the light scatter in the fluorescent samples, using 20X objective, controlled by Zen software (Carl Zeiss). Images were processed using ImageJ and Adobe Photoshop CS5.

Sweat Tests

An iodine-starch method was used as described in (Lu et al., 2012). Briefly, an iodine/alcohol solution (2%) was applied to the palmar surface of a mouse. After the alcohol evaporated, a suspension of 1 g starch/ml castor oil was applied. Fine black dots appeared within 2 min on paw pads and at the toe tips of actively sweating mice.

Statistics

Statistical and graphical data analyses were performed using Microsoft Excel and Prism 6 (Graphpad) software. All experiments shown were replicated at least twice, and representative data are shown. For all measurements, three biological replicates and two or more technical replicates were used. To determine the significance between two groups, comparisons were made using unpaired two-tailed Student's t-test. For all statistical tests, the 0.05 level of confidence was accepted for statistical significance.

Chapter 4:
Summary and Future Directions

Stem cells reside in specialized niches, which dictate their activity and ensure their long-term maintenance. Changes in this microenvironment allow stem cells to exit the niche and build or repair tissue, yet pose a dilemma for these cells: how can they survive outside their niche, and what defines the point of reversibility versus commitment to differentiation? Using hair follicle stem cells, I've tackled these fascinating problems during my graduate work. Inspired by the idea that stem cells acquire greater fate flexibility after injury or transplantation, I posited that stem cells make lineage choices by integrating microenvironmental changes with transcriptional circuitries determining cell identity. To test this hypothesis, I explored how chromatin landscapes change during lineage selection in homeostasis, wound repair and upon culturing the cells.

Dynamic super-enhancer remodeling facilitates lineage progression

To first understand how adult stem cells maintain their unique identities, I employed a chromatin-based approach. *In vivo* ChIP-seq on HFSCs revealed that a cohort of 8 key transcription factors (TFs) binds concomitantly within large open (H3K27ac) chromatin domains, known as super-enhancers. Despite controlling a mere fraction of active genes, super-enhancers serve as platforms for HFSC transcription factors to regulate ~400 critical 'stemness' genes, and hence govern HFSC identity. Accordingly, when stem cells commit to differentiation, extensive chromatin remodeling must occur to overcome the potent HFSC super-enhancer network. My comparative profiling of HFSCs and their committed progeny showed that once triggered by external signals, new fate is acquired by decommissioning old and establishing new super-enhancers, an auto-regulatory process that involves epigenetic silencing of one transcription factor cohort

while super-enhancer activating another. Thus, committed cells establish barriers to cellular plasticity by coupling bidirectional chromatin switches with TFs governing alternate fates. Once committed, proliferative HFSC progeny divide asymmetrically to fuel production of differentiating cells, ultimately giving rise to the mature hair.

My studies in adult stem cells have uncovered a hitherto unappreciated complexity in organization, constituency and dynamics of super-enhancers. I found that within super-enhancers, smaller segments or ‘epicenters’ exist where the concentration of binding sites for stemness transcription factors is particularly high (Figure 4-1) (Adam et al., 2015). As such, epicenters are cell-stage specific and serve as highly accurate chromatin sensors that respond to local changes in the microenvironment. Moreover, epicenters cloned from super-enhancers are sufficient to target proper developmental-specific behavior of an eGFP reporter (Figure 4-1) (Adam et al., 2015), underscoring the functional relevance of these chromatin domains in lineage-specific gene expression. Thus, epicenters harbor all the information necessary to express genes in the right place and time during development. This discovery should yield powerful genetic tools to drive expression with unprecedented precision.

Stem cell behavior and plasticity depends on their microenvironment

Dynamic chromatin remodeling need not always be associated with fate change. When outside their native niche, stem cells can maintain their identity and yet must dramatically change their chromatin landscape to adapt and survive. In culture, hair follicle stem cells extensively remodel super-enhancers and suppress master identity genes, including hair follicle stem cell-specific transcription factors. However, upon

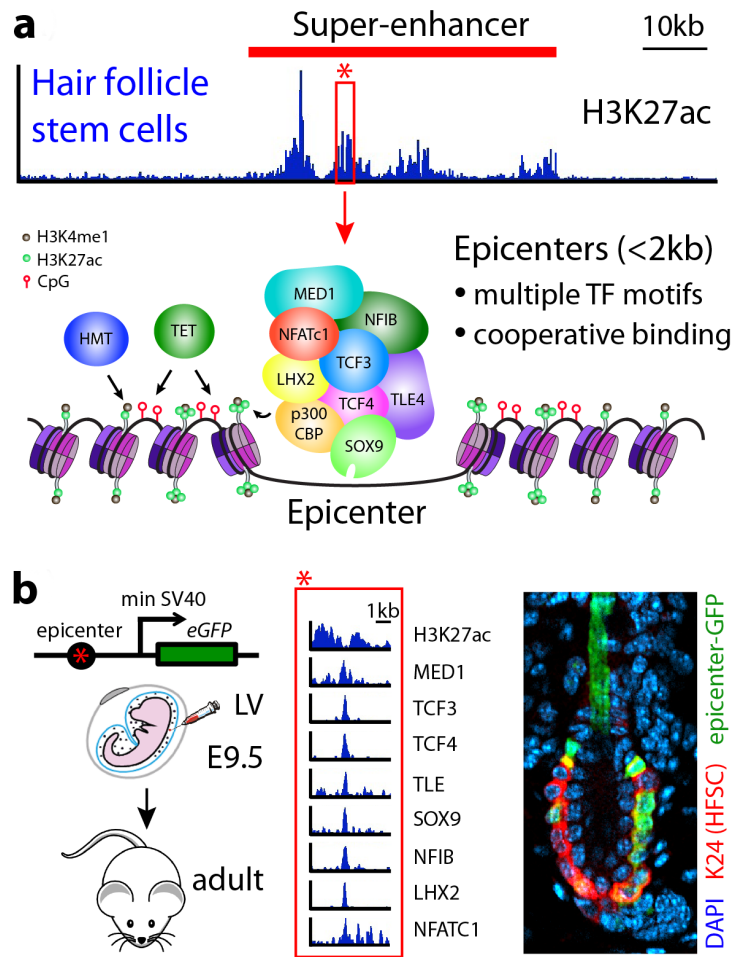


Figure 4-1. Super-enhancer epicenters represent accurate chromatin sensors. a, HFSC super-enhancers consist of clusters of active enhancers with exceptionally high density of H3K27ac and transcriptional activators. Red box highlights one of the hair follicle stem cell super-enhancer epicenters, densely bound by multiple cell-stage specific TFs and co-activators. In HFSCs, SOX9 acts as master regulator, which recruits other TFs, Mediator (MED1) and histone acetyltransferases (p300, CBP). Active enhancers are also depleted of 5mC (through TET enzymes) and display high levels of H3K4me1 (through histone methyltransferases, HMTs). **b,** To test whether epicenters faithfully drive reporter gene expression *in vivo*, high-titer lentivirus was injected into the amniotic cavity of E9.5 mouse embryos. The immunofluorescence image marks the nuclei of the skin in blue (DAPI), the HFSCs in red (Keratin 24), and a subset of stem cells that received the viral reporter in green (GFP).

engraftment after passage in culture, these cells reorganize a new niche and regain expression of super-enhancer regulated HFSC transcription factors. Intriguingly, many of the changes arising in cultured hair follicle stem cells are also induced after wounding (Adam et al. 2015). Similar features of plasticity were recently reported for tissue-resident macrophages, which display specific enhancer signatures associated with distinct combinations of transcription factors that are dynamic and responsive to local microenvironments (Gosselin et al., 2014; Lavin et al., 2014). These findings emphasize that cells are highly sensitive of their environment, and provide an explanation for how stem cells can maintain a reversible, yet plastic state when outside their niche. However, chromatin remodeling in tune with the microenvironment poses a dilemma: How can cells retain their unique identities in the face of dramatically altered transcriptional landscapes in different microenvironments? For stem cells, this is particularly relevant, since they not only have to survive outside their niche, but also retain stemness.

In the hair follicle, this is achieved through modulation of SOX9 levels, which acts as master regulator of stem cell plasticity. Although SOX9 is retained at low levels in culture, it is essential: Upon ablation, cultured stem cells are lost, while SOX9 overexpression restores the cohort of hair follicle stem cell factors *in vitro*, similar to what happens upon engraftment and reestablishment of the niche. Forced expression of SOX9 in epidermis, where it is typically absent, activates PcG-repressed super-enhancers of other hair follicle stem cell transcription factor genes. When SOX9 is sustained during stem cell commitment, all HFSC transcription factors remain high and hair differentiation is impaired (Adam et al., 2015). This exemplifies that compared to loss of PcG-repression, sustained SE activation appears more potent in governing lineage switches.

Home sweet home: the impact of niche signals on stem cell plasticity

Following the loss of stem cells in skin or the intestine, early stem cell progeny can readily return to the niche and revert back to being stem cells (Rompolas et al., 2013; van Es et al., 2012; Tian et al., 2011; Yan et al., 2012; Buczacki et al., 2013). By contrast, when niche components are ablated, stem cells cannot respond to tissue-regeneration cues (Rompolas et al., 2012), underscoring the importance of the niche in dictating stem cell behavior (Spradling et al., 2001; Scadden et al., 2014; Hsu et al., 2011a; Hsu et al., 2014). Therefore, epithelial stemness is not only an inherent feature of particular cells, but can be induced by niche signals if the chromatin landscape is permissive and master regulators are retained.

Indeed, intestinal crypts exhibit broadly permissive chromatin, as enhancers for both absorptive and secretory lineages show signs of activation in undifferentiated stem cells and both classes of progenitors (Kim et al., 2014). Even though some enhancers are similarly preset in hematopoietic stem cells, stepwise analysis indicated that the chromatin landscape of hematopoietic stem cells is dynamically reorganized at each point of lineage divergence (Luyten et al., 2014; Lara-Astiaso et al., 2014).

Yet what are the external signals that promote dynamic chromatin rearrangements to induce stem cell lineage commitment? Similarly, what dictates levels of pioneer factors that endow stem cells with features of plasticity? Although evidence for adult stem cells is sparse, studies in cultured embryonic stem cells suggest that super-enhancers are particularly enriched for binding sites of terminal transcription factors of developmental signaling pathways, including WNT, TGF-beta or LIF/STAT3 (Hnisz et al., 2015). Super-enhancers in HFSCs similarly show dramatic enrichment for WNT

effectors TCF3/4 (Adam et al., 2015). As such, it is feasible that super-enhancers provide platforms for signaling pathways to coordinate stem cell behavior with their microenvironment. Thus, if changes in niche signals reach a certain threshold, super-enhancer remodeling may be sufficient to push stem cells beyond the point of no return.

Future Directions

In my graduate work, I tried to illuminate the complexities of chromatin dynamics and illustrate how epigenetic changes impact adult stem cell fate determination and plasticity. Advances in genome technologies have provided means to not only comprehensively analyze the transcriptional profile of stem cells but also to map their epigenetic landscape on a global level and in their native niche. Although only in its infancy, several new concepts have emerged from recent studies: First, stem cell identity is governed by core transcription factor networks in conjunction with defined chromatin states. Once established, these states maintain robust lineage restriction and establish barriers against reversion to previous cellular states. During homeostasis, the niche microenvironment provides signals to reinforce cell fate decisions and maintains stem cells in an undifferentiated state. However, upon niche perturbations, stem cells can enter transitional states of plasticity until they reach their new microenvironment. This is achieved by coupling master transcription factors to chromatin platforms that are exquisitely sensitive to transcription factor concentrations, which in turn are modulated by microenvironmental cues. Although the precise details of epigenetic networks in the regulation of adult stem cells remain to be clarified, modulation of epigenetic pathways should yield further potential for basic research and clinical applications alike.

Beyond implications for stem cells, epigenetic analyses will become increasingly relevant to understand human disease. Genome-wide association studies (GWAS) have identified numerous loci underlying complex disease or traits. The majority of single nucleotide polymorphisms (SNPs) are found in non-coding genomic regions, with disproportionate enrichments in super-enhancers compared to typical enhancers (Maurano et al., 2012; Hnisz et al., 2013). Accordingly, SNPs associated with specific diseases frequently occur in disease-relevant cell types, particularly those SNPs located in super-enhancers. This was well-documented for Alzheimer's Disease, type I Diabetes and Systemic Lupus Erythematosus, but was also observed for many additional diseases including Multiple Sclerosis, Crohn's disease, Vitiligo or Rheumatoid Arthritis (Hnisz et al., 2013). As super-enhancers control the expression of genes that define cellular identity, the enrichment of disease-associated SNPs suggests that altered expression of cell identity genes may often contribute to these diseases. With the newfound knowledge of super-enhancers and their impact on cell fate, GWAS studies can now be revisited to identify changes in transcription factor binding sites, resulting from SNPs. This, in turn, will provide researchers with a better understanding of the causal mechanisms of disease initiation, and help to design better treatments for patients long-term.

Appendix

Table 2-4. Complete list of super-enhancer regulated genes in HFSCs *in vivo*

chr	start	end	enhancerRank	assignment	overlap with TAC SE (1=yes)
chr4	148171224	148291783	1	Casz1	1
chr19	47757295	47800286	2	Col17a1	0
chr13	56408120	56491942	3	Cxcl14	0
chr1	195338483	195409261	4	mir205	1
chr4	123232649	123354875	5	Macf1	1
chr2	37662357	37794439	6	Lhx2	0
chr8	86710451	86728679	7	mir23a	1
chr7	38960608	38986373	8	Plekhf1	0
chr13	63332139	63389378	9	mir23b	1
chr11	100139607	100157841	10	Krt17	1
chr4	81917457	82037987	11	Nfib	0
chr14	8654714	8733152	12	Flnb	0
chr16	23979548	24014760	13	Bcl6	1
chr4	139030453	139082205	14	Iffo2	0
chr15	85486145	85531265	15	Mirlet7c-2, N	1
chrX	166426505	166446954	16	Mid1	1
chr4	40997858	41039906	17	Aqp3	0
chr18	12123798	12185328	18	Cables1	0
chr16	57420437	57506412	19	Filip1l	0
chr11	16669441	16761342	20	Egfr	1
chr4	106628397	106709222	21	Ssbp3	0
chr11	36242047	36303476	22	Odz2	1
chr7	80669450	80706998	23	Chd2	0
chr16	57544368	57580134	24	Filip1l	0
chr2	30555341	30579610	25	mir3089	1
chr1	195213566	195289182	26	mir205	0
chr4	84142330	84194407	27	Bnc2	1
chr7	139914732	139999329	28	Mettl10	1
chr15	101796542	101814795	29	Krt79	1
chr17	27174466	27213275	30	Itpr3	1
chr11	117055751	117097649	31	Sept9	0
chr6	91509771	91557871	32	Lsm3	0
chr11	76067427	76140401	33	Nxn	1
chr7	137751955	137799543	34	Tacc2	1
chr19	5797289	5818202	35	Neat1	0
chr1	95565181	95603910	36	Bok	0
chr2	27542669	27592787	37	Rxra	1
chr12	80588823	80661434	38	Zfp36l1	0
chr2	157235771	157283096	39	Src	0
chr17	46992676	47017773	40	Tbcc	1
chr5	104164023	104208030	41	Aff1	1

chr11	61488460	61522299	42 Fam83g	0
chr15	10115582	10196476	43 Prlr	0
chr16	24729374	24799408	44 Lpp	0
chr19	25373569	25428018	45 Kank1	0
chr3	88311981	88327111	46 Lmna	0
chr11	98938513	98982711	47 Tns4	0
chr4	82177904	82201948	48 Nfib	0
chr11	96191131	96210198	49 Hoxb6	0
chr14	76276320	76303791	50 Tpt1	1
chr7	118828709	118880694	51 Galnt14	0
chr13	49526326	49576778	52 Bcd2	0
chr17	84378080	84437429	53 Zfp36l2	0
chr8	87290029	87318326	54 Nfix	1
chr4	139137371	139156823	55 Iffo2	0
chr12	8782967	8832907	56 Sdc1	1
chr2	167602759	167661435	57 Cebpb	1
chr17	35833781	35868661	58 Ddr1	0
chr13	49439180	49471113	59 Bcd2	0
chr14	120682950	120719031	60 Mbnl2	1
chr14	47960214	48004640	61 Lgals3	1
chr8	63854615	63925245	62 Sh3rf1	0
chr18	80778172	80834705	63 Nfatc1	0
chr2	35513384	35570745	64 Dab2ip	1
chr12	100586568	100632236	65 Foxn3	1
chr2	38194784	38224510	66 Lhx2	0
chr13	40812483	40834504	67 Tfap2a	0
chr4	135690280	135703712	68 Id3	1
chr14	60310830	60387588	69 Shisa2	0
chr11	117784261	117826117	70 Socs3	0
chr7	119255545	119289305	71 Dkk3	0
chr15	96559777	96603272	72 Slc38a2	0
chr15	97701044	97736219	73 Vdr	1
chr15	77630059	77689248	74 Myh9	1
chr16	18455655	18508527	75 Arvcf	0
chr7	123395000	123433148	76 <i>not annotate</i>	0
chr2	79350392	79407410	77 Ssfa2	0
chr13	40991801	41024124	78 Gcnt2	0
chr5	32632375	32653771	79 Fosl2	0
chr13	72761373	72777793	80 Irx2	1
chr1	74334705	74347713	81 Arpc2	1
chr5	113536745	113568384	82 2900026A02	1
chr19	9054909	9074458	83 Ahnak	1

chr15	82986024	83014711	84 Poldip3	0
chr11	113876039	113923566	85 Sdk2	0
chr19	47385209	47410291	86 Sh3pxd2a	1
chr13	103647237	103696840	87 Mast4	1
chr2	164246917	164266118	88 Sdc4	0
chr16	25809481	25862078	89 Trp63	1
chr1	19205844	19232504	90 Tcfap2b	0
chr1	88317857	88346792	91 Ptma	1
chr9	43565540	43598362	92 Pvr1	1
chr4	114208613	114251810	93 Gm12824	0
chr6	50995464	51012122	94 intergenic	0
chr8	129097794	129121010	95 Irf2bp2	1
chr4	82102615	82138198	96 Nfib	1
chr1	93982944	94040567	97 Hdac4	1
chr10	107771766	107828973	98 Pawr	0
chr19	25443982	25487322	99 Kank1	1
chr9	70089856	70129332	100 Myo1e	0
chr15	99871482	99919454	101 Dip2b	0
chr5	22892037	22926078	102 Mll5	1
chr11	98609039	98644811	103 Nr1d1	0
chr8	109131799	109170238	104 Cdh1	1
chr7	74587679	74648520	105 Mef2a	0
chr18	65195338	65215887	106 Nedd4l	0
chr15	101158055	101170040	107 Krt80	1
chr5	50423415	50456573	108 Gpr125	1
chr6	125293650	125306033	109 Tnfrsf1a	1
chr6	129164109	129184470	110 Clec2d	0
chr2	156550796	156576049	111 Dlgap4	1
chr3	116629968	116666268	112 Palmd	0
chr7	29714023	29737629	113 Actn4	1
chr3	75714359	75753740	114 Golim4	0
chr12	81303211	81336540	115 Actn1	0
chr14	22801181	22815019	116 Zfp503	0
chr11	115805355	115832723	117 Itgb4	0
chr8	108701918	108723504	118 Slc7a6	0
chr9	31683034	31714397	119 Barx2	0
chr13	37924910	37974627	120 Rreb1	1
chr2	28372917	28386964	121 Ralgds	0
chr1	135989644	136013255	122 Btg2	0
chr7	80731224	80764627	123 Chd2	1
chr6	92373505	92414852	124 Prickle2	0
chr10	21539982	21576262	125 Sgk1	0

chr18	60882505	60908736	126 <i>not annotate</i>	1
chr10	18570248	18599167	127 Perp	1
chr12	113814657	113835967	128 Inf2	1
chr9	56702281	56726013	129 Cspg4	0
chr9	13355731	13400446	130 Mtmr2	0
chr4	137452484	137489704	131 Ece1	1
chr19	25236195	25266191	132 Kank1	0
chr9	106261775	106281335	133 Dusp7	1
chr5	142888356	142921038	134 Foxk1	0
chr16	85116300	85160768	135 App	0
chr17	13992732	14014081	136 Mllt4	0
chr7	30125395	30149108	137 Sipal13	0
chr10	24150385	24199000	138 Ctgf	0
chr5	115938459	115943147	139 Pxn	1
chr7	89116089	89144285	140 Bnc1	1
chr15	38768726	38811050	141 Fzd6	0
chr4	133160623	133171369	142 Sfn	1
chr3	102925260	102953183	143 Bcas2	0
chr9	101164066	101193472	144 Ppp2r3a	0
chr13	113540908	113567120	145 Ppap2a	0
chr8	86125687	86146402	146 Dnajb1	0
chr15	96660053	96682999	147 Slc38a2	0
chr2	170030530	170073082	148 Zfp217	0
chr14	35161550	35192305	149 Bmpr1a	0
chr3	27087619	27112080	150 Fndc3b	0
chr11	117117159	117147897	151 Sept9	0
chr11	97147592	97173166	152 Npepps	0
chr6	125415526	125437278	153 Cd9	1
chr10	18194313	18228881	154 Nhsl1	0
chr8	89281041	89296698	155 Siah1a	0
chr13	38252127	38263061	156 Dsp	0
chr17	84278519	84302841	157 Zfp36l2	0
chr17	31960150	31981018	158 Sik1	0
chr10	6933350	6970764	159 Ppp1r14c	0
chr15	38369135	38403587	160 Azin1	0
chr14	25598728	25627270	161 Zmiz1	0
chr1	191182766	191213207	162 Kcnk2	0
chr1	138030318	138061695	163 Kif21b	0
chr2	72073171	72094485	164 B230120H23	1
chr5	149798360	149827540	165 <i>not annotate</i>	1
chr2	139554248	139608337	166 lsm1	0
chr8	24576424	24618372	167 Sfrp1	0

chr8	83354539	83395270	168 Gab1	1
chr9	121445318	121484441	169 Trak1	0
chr17	84474355	84515758	170 Zfp36l2	0
chr8	23340255	23385344	171 Thsd1	0
chr9	50675418	50722977	172 Ppp2r1b	1
chr1	181483392	181514644	173 Cnst	0
chr9	71515258	71565120	174 Cgnl1	0
chr5	115449174	115469321	175 Sppl3	1
chr8	96698953	96719695	176 Mt2, Mt1	0
chr6	99469820	99479077	177 Foxp1	1
chr16	95872186	95897846	178 Ets2	0
chr4	57146939	57178161	179 Epb4.1l4b	1
chr17	87749106	87776827	180 Ttc7	1
chr8	125509621	125550686	181 Ankrd11	0
chr15	80898224	80931489	182 Mkl1	0
chr2	145647587	145687699	183 Rin2	1
chr10	18069443	18092837	184 Nhsl1	0
chr7	137156375	137188943	185 Fgfr2	0
chr6	52806618	52844895	186 Tax1bp1	0
chr16	5110549	5136694	187 Ppl	0
chr5	35329475	35349240	188 Rgs12	1
chr13	37637724	37678880	189 Rreb1	0
chr12	109210274	109239362	190 Bcl11b	0
chr4	149942233	149963964	191 Rere	1
chr1	17588535	17617101	192 Pi15	0
chr7	114824966	114856046	193 Ppfibp2	1
chr6	120186819	120227086	194 B4galnt3	0
chr10	12515624	12556930	195 Utrn	0
chr15	80983460	81010414	196 Mkl1	0
chr1	167211069	167246746	197 Tipr1	1
chr13	56514243	56534530	198 Cxcl14	0
chr14	73768670	73791289	199 Itm2b	1
chr2	160777648	160813463	200 Chd6	0
chr2	59505880	59536483	201 Tanc1	1
chr6	52615283	52654042	202 Tax1bp1	0
chr12	74910786	74944796	203 Prkch	0
chr3	89181538	89193208	204 Zbtb7b	1
chr17	71077537	71104984	205 Tgif1	1
chr10	61755775	61784125	206 Hk1	0
chr5	103864934	103896381	207 Ptpn13	1
chr9	102981881	102992462	208 Slco2a1	0
chr13	60122067	60155161	209 Gas1	0

chr16	95481736	95513707	210 Kcnj15	0
chr1	196756310	196773339	211 CD34	0
chr8	129208200	129233574	212 Irf2bp2	0
chr4	114270029	114290621	213 Gm12824	0
chr13	60506146	60530016	214 Gas1	0
chr15	27407286	27437251	215 Ank	0
chr1	184293108	184315870	216 Trp53bp2	0
chr18	65731419	65747323	217 Zfp532	1
chr10	79533407	79540086	218 Sbno2	0
chr2	122152981	122183383	219 Duoxa1	0
chr15	77017269	77045829	220 Rbfox2	0
chr1	94057873	94080285	221 Hdac4	0
chr16	24461647	24498660	222 Lpp	0
chr7	106442607	106468327	223 Serpinh1	0
chr13	63237658	63265365	224 mir23b	1
chr13	3855695	3888784	225 Net1	0
chr5	144857742	144866160	226 Lmtk2	0
chr8	126788758	126813140	227 Galnt2	0
chr2	20458997	20486674	228 Etl4	0
chr11	106518651	106541364	229 Tex2	1
chr18	61782986	61795243	230 Csnk1a1	1
chr7	71042070	71071045	231 Klf13	1
chr12	85514691	85530059	232 Elmsan1	1
chr9	72025310	72046514	233 Tcf12	0
chr17	87701436	87717825	234 Ttc7	0
chr15	102828647	102836666	235 Hoxc8	0
chr10	93506068	93545241	236 Fgd6	0
chr7	119377521	119409915	237 Mical2	1
chr9	43880057	43896434	238 Usp2	0
chr12	5338703	5368108	239 Klhl29	0
chr4	118716192	118750298	240 Slc2a1	0
chr6	90634249	90658536	241 Iqsec1	0
chr7	80536112	80560687	242 Chd2	1
chr6	114823687	114843363	243 Vgll4	1
chr2	26355111	26364705	244 Notch1	1
chr10	31240843	31272090	245 Rnf217	0
chr13	52897620	52920063	246 Auh	0
chr19	25314650	25342946	247 Kank1	0
chr7	109537081	109559814	248 Stim1	0
chr12	5778046	5815446	249 Klhl29	0
chr5	77486374	77515602	250 Hopx	0
chr5	122747820	122776064	251 Pptc7	0

chr15	85441947	85465782	252 Mirlet7c-2, M	1
chr14	75276849	75317048	253 Lrch1	0
chr7	137380980	137402952	254 Fgfr2	1
chr1	39989334	40025728	255 Map4k4	0
chr11	60107194	60132025	256 Tom1l2	0
chr9	13270957	13309126	257 Mtmr2	0
chr5	144806352	144840713	258 Lmtk2	0
chr14	32472319	32495739	259 Btd	0
chr10	76830692	76862550	260 Adarb1	0
chr4	132933351	132964657	261 Slc9a1	0
chr15	88682494	88695399	262 Pim3	0
chr12	81945239	81980463	263 4933426M11	0
chr13	117788827	117817462	264 Parp8	0
chr13	102388966	102425216	265 Pik3r1	0
chr1	92960125	92992779	266 Lrrfip1	1
chr2	152522140	152541984	267 Id1	1
chr1	38348071	38378346	268 Aff3	0
chr3	108556985	108584564	269 Gpsm2	1
chr1	34734159	34757768	270 <i>not annotate</i>	0
chr12	70537460	70564377	271 Arf6	1
chr11	19849927	19890166	272 Spred2	0
chr1	90359418	90403739	273 Arl4c	0
chr9	44286065	44295721	274 Bcl9l	1
chr14	26288991	26309594	275 Zmiz1	1
chr12	120445626	120470934	276 Itgb8	0
chr8	26531387	26552925	277 Fgfr1	0
chr16	24827325	24862034	278 Lpp	0
chr14	121570609	121598693	279 Farp1	0
chr6	134138943	134156882	280 Etv6	0
chr19	21179916	21220131	281 Zfand5	0
chr7	148210397	148234986	282 Pkp3	0
chr8	87259520	87276614	283 Nfix	0
chr11	69678370	69697509	284 Plscr3	0
chr4	123083143	123109920	285 Macf1	0
chr12	56585499	56599816	286 Nfkbia	1
chr1	109471714	109491034	287 Serpinb8	0
chr13	43585993	43599446	288 Ranbp9	0
chr4	105720695	105740882	289 Usp24	0
chr11	69230418	69233948	290 Kdm6b	1
chr4	137020504	137033780	291 Hspg2	1
chr10	126362329	126373144	292 Ctdsp2	0
chr3	51905059	51919339	293 Maml3	0

chr6	122760036	122776463	294 Foxj2	1
chr4	114130892	114150593	295 Gm12824	0
chr4	148431476	148453002	296 Casz1	1
chr3	95470537	95480974	297 Mcl1	1
chr15	80950769	80968715	298 Mkl1	0
chr1	193040236	193049657	299 Atf3	1
chr13	115523696	115547782	300 Fst	0
chr8	93903540	93933488	301 Fto	0
chr5	125605339	125622146	302 Ncor2	0
chr11	70385622	70401240	303 Mink1	0
chr4	81208353	81229113	304 Nfib	0
chr9	76354274	76390215	305 Fam83b	0
chr12	40642984	40670949	306 Arl4a	0
chr10	19934126	19963099	307 Mtap7	0
chr15	37168880	37199146	308 Grhl2	0
chr8	24524679	24546620	309 Sfrp1	0
chr1	158545673	158548772	310 Abl2	0
chr17	56950009	56962874	311 Rfx2	0
chr1	39284923	39309855	312 Npas2	0
chr2	79486811	79506358	313 Ssfa2	0
chr6	118989863	119010112	314 Adipor2	0
chr17	88593364	88615006	315 Fbxo11	0
chr14	26441890	26458570	316 Zmiz1	1
chr18	5002020	5028525	317 Svil	1
chr14	24441867	24460727	318 Dlg5	0
chr8	113450696	113469397	319 St3gal2	0
chr5	144269356	144286312	320 Rac1	0
chr16	24885845	24915542	321 Lpp	0
chr1	73990879	74005507	322 Tns1	0
chr6	52122011	52131451	323 Hoxa7	0
chr13	112680261	112719888	324 Map3k1	0
chr10	67683846	67712866	325 Arid5b	0
chr19	9121968	9154477	326 Ahnak	0
chr18	5401654	5432216	327 Zfp438	0
chr13	53151706	53175032	328 Nfil3	0
chr2	29478970	29490762	329 Rapgef1	0
chr11	97276377	97298026	330 <i>not annotate</i>	1
chr2	72127807	72149127	331 B230120H23	0
chr17	88996401	89016317	332 Ston1	0
chr6	53547911	53576104	333 Creb5	0
chr4	119695448	119706320	334 Foxj3	0
chr12	70625735	70641176	335 Sos2	0

chr8	4677182	4679088	336 Zfp958	1
chr6	81999376	82021773	337 Fam176a	0
chr17	41005082	41022951	338 9130008F23f	0
chr1	74432986	74443903	339 Ctdsp1	1
chr2	71627162	71652462	340 Itga6	0
chr2	32022125	32039976	341 Prrc2b	1
chr3	79089456	79101576	342 <i>not annotate</i>	1
chr2	165676295	165691310	343 Zmynd8	1
chr8	3402448	3426362	344 Arhgef18	0
chr7	87335641	87354478	345 Sema4b	1
chr1	122012440	122032877	346 Dbi	0
chr4	83733024	83774011	347 Bnc2	0
chr1	135855616	135876075	348 Btg2	0
chr8	110010170	110028094	349 Wwp2	0
chr6	41484401	41513857	350 Ephb6	0
chr15	101007724	101023230	351 Acvr1b	1
chr17	48110555	48114101	352 Foxp4	0
chr2	92262223	92270468	353 Cry2	0
chr9	110987344	111007493	354 Lrrfip2	0
chr3	131151932	131167892	355 <i>not annotate</i>	0
chr7	137109003	137142128	356 Fgfr2	0
chr3	58992536	59009759	357 Gpr87	1
chr3	51837480	51853090	358 Maml3	1
chr13	5824872	5845030	359 Klfb	0
chr7	134620613	134623537	360 Fbrs	0
chr17	53716282	53736927	361 Kat2b	0
chr4	45481332	45503547	362 Shb	1
chr13	38402013	38413588	363 Bmp6	0
chr15	37212308	37242743	364 Grhl2	0
chr17	26719409	26734517	365 Ergic1	0
chr2	35287656	35303029	366 Ggta1	0
chr1	164112876	164128639	367 Ai848100	0
chr1	108754172	108764525	368 Serpinb5	0
chr14	26409605	26428185	369 Zmiz1	1
chr15	90417289	90440437	370 Cpne8	0
chr11	105794782	105809083	371 Cyb561	0
chr6	91596245	91609646	372 Slc6a6	0
chr11	112758209	112788966	373 Sox9	0
chr15	12148833	12162573	374 Mtmr12	0
chr2	102712180	102725682	375 Cd44	0
chr9	121244628	121270505	376 Trak1	1
chr6	128225484	128247661	377 Tead4	0

Table 2-5. Complete list of super-enhancer regulated genes in TACs *in vivo*

chr	start	end	enhancerRank	assignment	overlap: HFSC SE? (1=yes)
chr2	26327248	26413177	1	Notch1	1
chr2	167531288	167717719	2	Cebpb	1
chr4	148168533	148282473	3	Cas2	1
chr11	95009362	95119058	4	Dlx3	0
chr15	85441364	85534582	5	Mirlet7c-2, Mirlet7b	1
chr7	29685677	29757914	6	Actn4	1
chr9	43545542	43614142	7	Pvrl1	1
chr13	63339353	63407473	8	mir23b	1
chr1	88330130	88420834	9	Ptma	1
chr4	140847320	140916861	10	Epha2	0
chr14	70949933	70987251	11	Hr	0
chr1	193658825	193721984	12	Slc30a1	0
chr2	165923137	166018806	13	Ncoa3	0
chr12	100563682	100644239	14	Foxn3	1
chr18	75523484	75552355	15	Smad7	0
chr8	86707078	86728638	16	mir23a	1
chr8	129098406	129144005	17	Irf2bp2	1
chrX	166423413	166446949	18	Mid1	1
chr15	77627545	77689321	19	Myh9	1
chr2	27555097	27629896	20	Rxa	1
chr4	135690401	135705484	21	Id3	1
chr4	133148550	133171158	22	Sfn	1
chr4	82079339	82159844	23	Nfib	1
chr16	10329896	10386319	24	Emp2	0
chr11	100246895	100270609	25	Jup	0
chr5	137047048	137099488	26	Cux1	0
chr9	70680705	70770774	27	Adam10	0
chr2	136888682	136938986	28	Jag1	0
chr5	134879618	134929924	29	Gtf2ird1	0
chr2	165673395	165721899	30	Zmynd8	1
chr10	18557275	18599185	31	Perp	1
chr17	27174531	27213348	32	Itpr3	1
chr5	32421886	32446278	33	Fosl2	0
chr4	117912815	117955506	34	Ptprf	0
chr12	88196238	88236521	35	6430527G18Rik	0
chr9	96595198	96660010	36	Zbtb38	0
chr6	134866488	134883704	37	Cdkn1b	0
chr7	30216750	30276417	38	Sipa1l3	0
chr14	70420329	70468368	39	Egr3	0
chr11	69215265	69233419	40	Kdm6b	1
chr15	59465085	59485570	41	Trib1	0
chr19	57044164	57090229	42	Afap1l2	0
chr15	101796833	101814927	43	Krt79	1
chr4	135723245	135737905	44	E2F2	0
chr13	72761353	72777933	45	Irx2	1

chr1	191592621	191643887	46 Ptpn14	0
chr5	115448778	115464837	47 Sppl3	1
chr18	65724740	65761065	48 Zfp532	1
chr11	16659038	16733762	49 Egfr	1
chr11	98250333	98281651	50 Erbb2	0
chr4	45494673	45526870	51 Shb	1
chr5	135412436	135446792	52 Abhd11	0
chr8	124374110	124428914	53 Slc7a5	0
chr8	87300807	87318815	54 Nfix	1
chr15	97684092	97736047	55 Vdr	1
chr11	121383614	121420063	56 Zfp750	0
chr11	100145367	100157959	57 Krt17	1
chr1	74822534	74864244	58 Wnt10a	0
chr16	30055612	30071339	59 Hes1	0
chr2	25017294	25042171	60 Nrarp	0
chr6	114936748	114957838	61 Vgll4	0
chr6	120997680	121039024	62 Mical3	0
chr11	98785761	98807458	63 Rara	0
chr6	83342015	83386231	64 Tet3	0
chr7	80728755	80771487	65 Chd2	1
chr9	106255783	106289242	66 Dusp7	1
chr15	81971631	81998449	67 Srebf2	0
chr4	84169326	84194357	68 Bnc2	1
chr9	66437678	66490684	69 Usp3	0
chr9	31086137	31110110	70 Aplp2	0
chr1	46906827	46959823	71 Slc39a10	0
chr12	56563709	56597070	72 Nfkbia	1
chr15	100992898	101035375	73 Acvr1b	1
chr2	131907584	131957836	74 Slc23a2	0
chr5	34022021	34042177	75 Fgfr3	0
chr7	87164439	87178081	76 Zfp710	0
chr6	114822880	114866200	77 Vgll4	1
chr11	93994754	94037906	78 Spag9	0
chr7	119389208	119420563	79 Mical2	1
chr7	137349376	137404925	80 Fgfr2	1
chr19	53379917	53400725	81 Mxi1	0
chr2	150638755	150685179	82 Abhd12	0
chr8	83353837	83397056	83 Gab1	1
chr2	32010930	32047319	84 Prrc2b	1
chr6	125280555	125319373	85 Tnfrsf1a	1
chr8	122855013	122901959	86 Gse1	0
chr10	56102431	56152744	87 Gja1	0
chr12	70462557	70478927	88 Arf6	0
chr9	63804133	63841370	89 Smad6	0
chr17	29276876	29321228	90 Cdkn1a	0
chr3	108204736	108229973	91 Celsr2	0

chr10	80864616	80896783	92 Nfic	0
chr6	99459043	99479133	93 Foxp1	1
chr11	121336715	121370003	94 Zfp750	0
chr12	8860763	8888406	95 Sdc1	0
chr18	12041340	12075853	96 Cables1	0
chr14	57895612	57962533	97 Gjb2	0
chr9	42934911	42983026	98 Arhgef12	0
chr11	117676960	117707382	99 Birc5	0
chr15	27814347	27873623	100 Trio	0
chr11	102062179	102084603	101 Hdac5	0
chr11	68876562	68908469	102 Aurkb	0
chr14	26443339	26462664	103 Zmiz1	1
chr9	102611311	102637635	104 Amotl2	0
chr2	30967380	31003673	105 Fnbp1	0
chr15	101156733	101169055	106 Krt80	1
chr5	116865535	116896903	107 Hspb8	0
chr18	60881691	60909034	108 <i>not annotated</i>	1
chr10	80591611	80610005	109 Zbtb7a	0
chr9	43110635	43134104	110 Trim29	0
chr2	152519244	152553455	111 Id1	1
chr7	139956968	139999595	112 Mettl10	1
chr10	19790473	19845421	113 Mtap7	0
chr6	131331841	131347832	114 Ybx3	0
chr10	60254068	60289497	115 Unc5b	0
chr1	90992052	91030764	116 Sh3bp4	0
chr13	37922055	37965774	117 Rreb1	1
chr15	12396852	12446543	118 Pdzd2	0
chr17	84345992	84367149	119 Zfp36l2	0
chr13	63241490	63298438	120 mir23b	1
chr11	121558572	121585541	121 Metrnl	0
chr7	71040955	71075984	122 Klf13	1
chr14	57718438	57747431	123 Gjb2	0
chr19	9054745	9074150	124 Ahnak	1
chr14	26413230	26430723	125 Zmiz1	1
chr4	123314586	123344910	126 Macf1	1
chr11	118905816	118920397	127 Cbx2	0
chr4	149918354	149972815	128 Rere	1
chr1	90128072	90168899	129 Hjurp	0
chr8	128073814	128094654	130 <i>not annotated</i>	0
chr14	73769002	73791390	131 Itm2b	1
chr15	85981179	86013823	132 CerK	0
chr9	121256672	121299368	133 Trak1	1
chr11	76125820	76151799	134 Nxn	1
chr10	59360762	59387464	135 Ddit4	0
chr4	53450572	53465614	136 Slc44a1	0
chr2	156550808	156575945	137 Dlgap4	1

chr16	33832147	33884555	138 Itgb5	0
chr9	44286113	44304971	139 Bcl9l	1
chr4	136826998	136850850	140 Cdc42	0
chr2	145647593	145688882	141 Rin2	1
chr14	120679528	120719447	142 Mbnl2	1
chr10	6481053	6517441	143 Plekhg1	0
chr7	137767286	137793035	144 Tacc2	1
chr5	129074753	129099055	145 Fzd10	0
chr1	137787604	137808649	146 Pkp1	0
chr7	87897951	87932558	147 Iqgap1	0
chr1	167211069	167248938	148 Tiprl	1
chr12	25201647	25249174	149 Grhl1	0
chr10	19877810	19903995	150 Mtap7	0
chr14	32213284	32242587	151 Mettl6	0
chr16	97973683	98000666	152 Ripk4	0
chr14	21538434	21579017	153 Chchd1	0
chr12	70519584	70568536	154 Arf6	1
chr5	22905878	22925828	155 Mll5	1
chr16	76366947	76381863	156 Nrip1	0
chr17	46992409	46995894	157 Tbcc	1
chr7	87334119	87360425	158 Sema4b	1
chr11	97265674	97303332	159 <i>not annotated</i>	1
chr6	98963725	98983115	160 Foxp1	0
chr18	50146617	50192567	161 Tnfaip8	0
chr5	35331659	35357994	162 Rgs12	1
chr4	62157293	62175571	163 Alad	0
chr5	134799595	134829089	164 Gtf2ird1	0
chr8	125569855	125592621	165 Ankrd11	0
chr12	25271873	25286161	166 Grhl1	0
chr6	125417298	125437896	167 Cd9	1
chr11	77648865	77661919	168 Myo18a	0
chr4	148423274	148456419	169 Casz1	1
chr4	83995925	84063932	170 Bnc2	0
chr7	135066103	135079798	171 Fus	0
chr17	5324006	5377252	172 Arid1b	0
chr6	122760231	122777013	173 Foxj2	1
chr2	35516689	35545382	174 Dab2ip	1
chr3	10273350	10299072	175 Fabp5	0
chr13	49054659	49078590	176 Fam120a	0
chr3	87336699	87370578	177 Etv3	0
chr5	104161732	104190104	178 Aff1	1
chr5	36699597	36733345	179 Sorcs2	0
chr19	56988747	57016167	180 Afap1l2	0
chr15	96523232	96541326	181 Slc38a2	0
chr5	34054904	34069924	182 Fgfr3	0
chr9	61208548	61225740	183 Tle3	0

chr7	114802075	114832193	184 Ppfbp2	1
chr2	72073246	72103357	185 B230120H23Rik	1
chr10	80397421	80404563	186 Gadd45b	0
chr19	25449450	25504493	187 Kank1	1
chr6	121109714	121145830	188 Mical3	0
chr12	71769233	71791485	189 Frmd6	0
chr17	56689274	56695122	190 Safb	0
chr4	32324663	32345336	191 <i>not annotated</i>	0
chr10	90631615	90651383	192 Tmpo	0
chr16	4636158	4659719	193 Vasn	0
chr11	121453701	121496892	194 Zfp750	0
chrX	96599332	96630079	195 Pja1	0
chr15	98807203	98824494	196 Tuba1b	0
chr3	130808633	130819756	197 Lef1	0
chr17	87751040	87784551	198 Ttc7	1
chr13	103670027	103697213	199 Mast4	1
chr14	26283875	26309728	200 Zmiz1	1
chr18	25094389	25120051	201 Fhod3	0
chr9	118903002	118931031	202 Ctdspl	0
chr16	23979751	23994337	203 Bcl6	1
chr3	148647096	148653841	204 Lphn2	0
chr10	74572152	74598910	205 Bcr	0
chr17	84098242	84108910	206 Mta3	0
chr1	195339731	195377519	207 Mir205	1
chr4	84102366	84156037	208 Bnc2	1
chr8	97513898	97524173	209 Gpr56	0
chr4	122707377	122749405	210 Mycl1	0
chr3	58992360	59010704	211 Gpr87	1
chr4	135119416	135132144	212 Grhl3	0
chr5	136353721	136380072	213 Ywhag	0
chr3	51837268	51853064	214 Maml3	1
chr4	150119707	150163422	215 Rere	0
chr17	46744409	46762014	216 Ptk7	0
chr11	51453590	51471480	217 N4bp3	0
chr8	125046853	125071264	218 Piezo1	0
chr7	135017489	135031114	219 Fus	0
chr17	15945232	15968440	220 Rgmb	0
chr12	106216501	106255322	221 Glrx5	0
chr7	71000725	71028203	222 Klf13	0
chr2	172681731	172704202	223 Bmp7	0
chr6	128038711	128059194	224 Tspan9	0
chr2	32722659	32735289	225 Fam129b	0
chr12	113814115	113836269	226 Inf2	1
chr1	74334842	74345780	227 Arpc2	1
chr2	156251577	156283927	228 Epb4.1l1	0
chr5	77583718	77629846	229 Hopx	0

chr2	6155936	6192953	230 Usp6nl	0
chr4	88574471	88588217	231 Mir31	0
chr18	35999703	36009412	232 Cxxc5	0
chr2	32750334	32770591	233 Fam129b	0
chr4	59885729	59914869	234 1110054005rik	0
chr17	6947887	6963363	235 Ezc	0
chr15	12474637	12507420	236 Pdxd2	0
chr4	140527255	140546693	237 Atp13a2	0
chr3	100845273	100870324	238 Ptgrn	0
chr7	26421575	26435096	239 B3gnt8	0
chr4	137458239	137487796	240 Ece1	1
chrX	11644688	11669421	241 Bcor	0
chr2	59594452	59618544	242 Pkp4	0
chr16	95933431	95993085	243 Ets2	0
chr12	86792053	86810636	244 Fos	0
chr3	108565238	108599918	245 Gpsm2	1
chr3	79089733	79101362	246 <i>not annotated</i>	1
chr14	31425353	31445595	247 Prkcd	0
chr5	149801745	149812223	248 <i>not annotated</i>	1
chr11	62627066	62640811	249 Trim16	0
chr8	129183165	129192683	250 Irf2bp2	0
chr10	127027322	127053147	251 Lrp1	0
chr12	85514368	85530166	252 Elmsan1	1
chr9	77779514	77814674	253 Elovl5	0
chr7	29634978	29653123	254 Actn4	0
chr9	104246444	104285880	255 Acpp	0
chr1	193016551	193049869	256 Atf3	1
chr2	30548980	30568776	257 Mir3089	1
chr9	30916165	30932238	258 St14	0
chr2	4477415	4490698	259 Frmd4a	0
chr5	50405815	50446689	260 Gpr125	1
chr10	79557914	79570455	261 Stk11	0
chr2	30318256	30327065	262 Ppp2r4	0
chr16	92605585	92632694	263 Runx1	0
chr4	122904738	122921820	264 Heyl	0
chr7	80534265	80560626	265 Chd2	1
chr18	61773429	61796688	266 Csnk1a1	1
chr12	77629610	77638469	267 Plekhg3	0
chr14	47973476	48015755	268 Lgals3	1
chr11	120546137	120571667	269 Aspscr1	0
chr16	25810481	25850726	270 Trp63	1
chr19	61275279	61276059	271 unclear	0
chr6	114911328	114920271	272 Vgll4	0
chr5	137179063	137198750	273 Cux1	0
chr17	35872915	35914816	274 Ddr1	0
chr4	149422058	149436811	275 Mir34a	0

chr7	123326008	123342634	276 not annotated gene	0
chr8	19772268	19785449	277 unclear, none expressed	0
chr2	62219218	62258253	278 Dpp4	0
chr6	38583772	38593339	279 Luc7l2	0
chr2	129429165	129459468	280 Sirpa	0
chr2	29514489	29551626	281 Rapgef1	0
chr14	61598296	61637561	282 Tnfrsf19	0
chr10	18037325	18049775	283 Nhsl1	0
chr1	157056835	157072369	284 Stx6	0
chr5	103864855	103894764	285 Ptpn13	1
chr11	88158831	88193446	286 Msi2	0
chr11	106518665	106541596	287 Tex2	1
chr18	61893887	61908889	288 Grpel2	0
chr2	103518613	103547591	289 Nat10	0
chr19	47388246	47417935	290 Sh3pxd2a	1
chr4	133368765	133385400	291 Rps6ka1	0
chr4	57164034	57178467	292 Ebb4.1l4b	1
chr6	99308740	99343407	293 Foxp1	0
chr18	4994169	5036035	294 Svil	1
chr16	97893206	97941593	295 Ripk4	0
chr4	106499925	106521380	296 Ssbp3	0
chr12	8814352	8836695	297 Sdc1	1
chr15	90876984	90885830	298 Kif21a	0
chr17	71077757	71106019	299 Tgif1	1
chr4	137027133	137051303	300 Hspg2	1
chr11	78175857	78194587	301 Foxn1	0
chr10	77760779	77784200	302 Agpat3	0
chr7	30041494	30061833	303 Spint2	0
chr9	107207369	107231381	304 Mapkapk3	0
chr14	57837972	57872344	305 Gjb2	0
chr4	107490092	107503857	306 Magoh	0
chr2	35426827	35447705	307 Dab2ip	0
chr9	50653921	50676346	308 Ppp2r1b	1
chr1	93972239	94013222	309 Hdac4	1
chr14	121738969	121768460	310 Stk24	0
chr17	35093351	35103479	311 Hspa1b	0
chr7	89119073	89141168	312 Bnc1	1
chr9	37025231	37053763	313 Tmem218	0
chr7	151749036	151760399	314 Ppfia1	0
chr15	102631231	102687433	315 Hoxc13	0
chr6	39670712	39689308	316 Braf	0
chr7	138118771	138126099	317 Htra1	0
chr3	121784235	121825426	318 Arhgap29	0
chr3	97811584	97829716	319 Notch2	0
chr19	5529548	5549275	320 Ovol1	0
chr4	94729341	94744980	321 Jun	0

chr5	125552252	125563743	322 Ncor2	0
chr13	38214825	38238721	323 Dsp	0
chr2	160124355	160180065	324 Mafb	0
chr5	118886557	118915890	325 Med13l	0
chr13	53556771	53562556	326 Msx2	0
chr11	23992364	24028130	327 Bcl11a	0
chr1	72282943	72301822	328 Mreg	0
chr14	76276276	76299616	329 Tpt1	1
chr12	113410129	113425827	330 Mir203	0
chr1	182697935	182712582	331 H3f3a	0
chr10	59420103	59442498	332 Ddit4	0
chr1	173942557	173954410	333 Vangl2	0
chr2	109792349	109827952	334 Lgr4	0
chr7	26051856	26063054	335 Erf	0
chr8	109131808	109156822	336 Cdh1	1
chr1	92961386	92994053	337 Lrrfip1	1
chr6	125522372	125548826	338 Cd9	0
chr5	32484187	32503275	339 Fosl2	0
chr3	89121778	89137503	340 Zbtb7b	0
chr9	119910436	119925938	341 Csrnp1	0
chr4	45464911	45480857	342 Shb	0
chr1	133116903	133139162	343 Rassf5	0
chr1	59479416	59516868	344 Fzd7	0
chr18	13088992	13114871	345 Osbpl1a	0
chr5	115938691	115942567	346 Pxn	1
chr2	59508315	59521485	347 Tanc1	1
chr5	103777765	103806912	348 Ptpn13	0
chr15	100457976	100472200	349 Dazap2	0
chr11	76164454	76199207	350 Nxn	0
chr6	89294790	89309973	351 Plxna1	0
chr18	70723712	70731942	352 Mbd2	0
chr1	74425771	74444730	353 Ctdsp1	1
chr3	95468264	95480124	354 Mcl1	1
chr3	89181876	89193084	355 Zbtb7b	1
chr8	4676962	4679218	356 Zfp958	1
chr11	4089898	4105861	357 Tbc1d10a	0
chr10	79395112	79409810	358 C030046l01Rik	0
chr13	104813642	104835374	359 Nln	0
chr11	36240569	36259604	360 Odz2	1
chr1	94218861	94242414	361 Hdac4	0
chr4	140795024	140817231	362 Epha2	0
chr3	121150402	121172977	363 Cnn3	0
chr11	76009527	76025826	364 Nxn	0
chr2	59657831	59681200	365 Tanc1	0
chr2	110013502	110054714	366 Lgr4	0
chr12	53603909	53606242	367 Arhgap5	0

chr12	113351530	113360800	368 Mir203	0
chr4	9015556	9052556	369 Chd7	0
chr4	116760877	116778895	370 Ptch2	0
chr15	37112587	37148314	371 Grhl2	0
chr5	113566715	113584375	372 2900026A02Rik	1
chr1	137656930	137667754	373 Lad1	0
chr6	112967260	112989027	374 Setd5	0
chr2	173079151	173093079	375 Pmepa1	0
chr4	129177726	129195161	376 Marcksl1	0
chr6	31063724	31077239	377 Mir29a	0
chr11	116476617	116494646	378 Rhbdf2	0
chr8	123072872	123088488	379 Gse1	0
chr10	67619515	67641588	380 Arid5b	0
chr12	88116079	88143303	381 6430527G18Rik	0

Table 2-6. Complete list of super-enhancer regulated genes in HFSCs *in vitro*

chr	start	end	enhancerRank	assignment	overlap	HFSC SE in vivo (1=yes)
chr10	18573248	18615344	1	Perp		1
chr6	86496089	86591802	2	Asprv1		0
chr19	9092653	9183149	3	Ahnak		1
chr11	100137847	100167906	4	Krt17		1
chr11	112917539	112979470	5	Sox9		0
chr8	37198807	37257644	6	D8Ert82e		0
chr5	124115124	124159588	7	Clip1		0
chr11	121390763	121468234	8	Zfp750		0
chr2	32720380	32784522	9	Fam129b		0
chr4	123263906	123345032	10	Macf1		1
chr2	128362391	128399844	11	Gm14005		0
chr6	134745640	134777691	12	Dusp16		0
chr8	129423079	129457127	13	Irf2bp2		0
chr6	86168774	86246478	14	Tgfa		0
chr10	37049829	37093505	15	Marcks		0
chr2	167599297	167666544	16	Cebpb		1
chr10	93985482	94034668	17	Tmcc3		0
chr19	25404647	25483574	18	Kank1		1
chr1	156895782	156939567	19	Ier5		0
chr6	112955967	112989945	20	Setd5		0
chr17	32028138	32081734	21	Sik1		0
chr13	111642859	111721231	22	Plk2		0
chr2	119069412	119093304	23	Spint1		0
chr6	120084617	120143655	24	B4galnt3		0
chr10	44417458	44477228	25	Prdm1		0
chr13	38234806	38264217	26	Dsp		1
chr10	116169610	116235774	27	Cnot2		0
chr5	22890955	22935105	28	Mll5		1
chr18	61777854	61804107	29	Csnk1a1		1
chr10	18036394	18055276	30	Nhs1		0
chr14	47946272	48000927	31	Lgals3		1
chr17	31960450	31985541	32	Sik1		1
chr8	67093477	67168407	33	Sc4mol		0
chr18	20339135	20388510	34	Dsg3		0
chr19	38059198	38115395	35	Myof		0
chr1	88328882	88384885	36	Ptma		1
chr18	21353883	21384929	37	Rnf138		0
chr2	152606672	152648906	38	Bcl2l1		0
chr14	99976871	100036102	39	Klf5		0
chr12	80589428	80662570	40	Zfp36l1		1
chr17	31863828	31892806	41	Sik1		0
chr9	43563133	43610398	42	Pvr1		1
chr11	16689318	16752915	43	Egfr		1
chr1	137743254	137766531	44	Pkp1		0

chr1	121398078	121437979	45 Ralb	0
chr13	103636067	103701165	46 Mast4	1
chr1	92945362	93003044	47 Lrrfip1	1
chr2	103036739	103084617	48 Ehf	0
chr12	80124182	80152835	49 Plekhh1	0
chr10	18067850	18110356	50 Nhsl1	1
chr2	132407366	132442206	51 Gpcpd1	0
chr4	88572306	88607222	52 Mir31	0
chr8	93902687	93937025	53 Fto	1
chr12	8795606	8841033	54 Sdc1	1
chr7	73716355	73748041	55 Lass3	0
chr8	71535910	71564516	56 Atp6v1b2	0
chr12	74826211	74892963	57 Hif1a	0
chr11	80297585	80348427	58 Myo1d	0
chr10	37168960	37226921	59 Marcks	0
chr8	83363648	83395690	60 Gab1	1
chr5	104161123	104209224	61 Aff1	1
chr9	70709743	70751665	62 Adam10	0
chr7	80717736	80769867	63 Chd2	1
chr15	101795836	101815408	64 Krt8	1
chr16	26400083	26448885	65 Cldn1	0
chr10	44270437	44302946	66 Prdm1	0
chr17	13988870	14029418	67 Mlt4	1
chr1	163815934	163863040	68 Al848100	0
chr18	82657616	82695597	69 Mbp	0
chr17	46991490	47017794	70 Tbcc	1
chr10	59361828	59386645	71 Ddit4	0
chr6	125356923	125398554	72 Cd9	0
chr17	7007608	7040772	73 Ezr	0
chr11	20765500	20799628	74 1110067d22Rik	0
chr10	40228879	40244982	75 Cdk19	0
chr10	24670061	24706316	76 Arg1	0
chr10	6958192	6987884	77 Ppp1r14c	1
chr6	97795707	97836104	78 Mitf	0
chr12	70517316	70563385	79 Arf6	1
chr8	86710274	86729186	80 mir23a	1
chr16	95461708	95508098	81 Kcnj15	1
chr2	148253388	148305785	82 Thbd	0
chr2	129066940	129090527	83 Slc20a1	0
chr17	71056378	71106575	84 Tgif1	1
chr18	20140065	20165442	85 Dsc3	0
chr2	136873941	136939037	86 Jag1	0
chr6	97228033	97270080	87 Frmd4b	0
chr12	8860284	8893218	88 Laptm4a	0
chr6	113018139	113053353	89 Setd5	0

chr5	32713875	32745875	90 Ppp1cb	0
chr11	97146532	97172132	91 Npepps	1
chr8	25528293	25553979	92 1810011O10Rik	0
chr10	21548538	21574457	93 Sgk1	1
chr18	65195165	65215583	94 Nedd4l	1
chr8	58896104	58924258	95 intergenic	0
chr4	45494132	45527434	96 Shb	1
chr12	25271920	25285968	97 Grhl1	0
chr17	26729003	26759496	98 Ergic1	1
chr11	67334771	67378126	99 Gas7	0
chr7	29704277	29739072	100 Actn4	1
chr8	119850122	119869116	101 Cmp1	0
chr3	10257372	10295818	102 Fabp5	0
chr5	43432630	43474013	103 Cpeb2	0
chr7	114821447	114872033	104 Ppfibp2	1
chr8	36910711	36942583	105 Cldn23	0
chr4	86329419	86375092	106 Plin2	0
chr8	129188142	129213157	107 Irf2bp2	1
chr6	135228631	135277607	108 Emp1	0
chr1	137779178	137806257	109 Pkp1	0
chr18	12768749	12790962	110 Ttc39c	0
chr5	77562671	77596899	111 Hopx	0
chr5	135430840	135466852	112 Cldn4	0
chr11	68670998	68688578	113 Ndel1	0
chr8	129126614	129153129	114 Irf2bp2	0
chr3	102927768	102963979	115 Bcas2	1
chr3	101937871	102001240	116 Vangl1	0
chr2	140651777	140676379	117 Flrt3	0
chr12	81303114	81346582	118 Actn1	1
chr12	25202566	25251040	119 Grhl1	0
chr15	97688106	97731309	120 Vdr	1
chr16	31569733	31604787	121 Dlg1	0
chr11	86423241	86468120	122 Mir21	0
chr8	35636127	35699609	123 B930018H19Rik	0
chr10	83676912	83713202	124 intergenic	0
chr2	103495027	103547658	125 Nat10	0
chr1	147782128	147808951	126 intergenic	0
chr12	120602862	120638372	127 Macc1	0
chr2	60526713	60550475	128 Rbms1	0
chr13	32994580	33039505	129 Serpinb6b	0
chr18	32776174	32810017	130 Wdr36	0
chr2	61122250	61149986	131 Rbms1	0
chr16	97955323	98000678	132 Ripk4	0
chr8	125511944	125552878	133 Ankrd11	1
chr14	63431786	63479966	134 Wdfy2	0

chr9	110583412	110613001	135 Ccdc12	0
chr10	40029217	40066715	136 Cdk19	0
chr5	32636193	32649801	137 Fosl2	1
chr7	87886690	87934919	138 Iqgap1	0
chr2	104681168	104706169	139 Prrg4	0
chr10	22894773	22924580	140 unclear	0
chr4	135988902	136018804	141 Luzp1	0
chr10	118418113	118441840	142 Cand1	0
chr7	3134595	3158451	143 unclear	0
chr16	56830280	56874643	144 Tmem45a	0
chr15	101151266	101171521	145 Krt80	1
chr15	85487432	85516068	146 Mirlet7c-2, Mirlet7b	1
chr11	86815489	86844278	147 Gdpd1	0
chr15	99880448	99928277	148 Dip2b	1
chr10	85745522	85776235	149 Timp3	0
chr13	5834809	5845989	150 Klf6	1
chr17	32106995	32142846	151 Rrp1b	0
chr6	31210901	31238411	152 Mklm1	0
chr1	193606996	193641891	153 Lpgat1	0
chr11	103233262	103262648	154 Arhgap27	0
chr8	86122681	86146308	155 Dnajb1	1
chr11	121336067	121349276	156 Zfp750	0
chr18	65765457	65801683	157 Zfp532	0
chr5	31927813	31950701	158 Bre	0
chr6	129162475	129185049	159 Clec2d	1
chr15	38381417	38404135	160 Azin1	1
chr18	36559601	36578196	161 Pfdn1	0
chr2	84378769	84393172	162 Ctnnd1	0
chr12	86688871	86740186	163 Tmed10	0
chr7	25414001	25432300	164 Lypd3	0
chr8	126783259	126815848	165 Galnt2	1
chr2	110012662	110040905	166 intergenic	0
chr15	59228743	59250055	167 Nsmce2	0
chr15	38313331	38362426	168 Azin1	0
chr3	54905636	54928011	169 Spg20	0
chr1	77454389	77470890	170 Eph4	0
chr13	47256446	47276020	171 Rnf144b	0
chr6	125415813	125441073	172 Cd9	1
chr12	100568321	100616917	173 Foxn3	1
chr12	72971193	72992378	174 Daam1	0
chr10	41932918	41993796	175 Foxo3	0
chr2	84542712	84559999	176 Zdhhc5	0
chr2	6158658	6195118	177 Usp6nl	0
chr11	106498562	106539730	178 Tex2	1
chr8	3407187	3431420	179 Arhgef18	1

chr1	135987417	136003516	180 Btg2	1
chr18	20631536	20658568	181 Dsg3	0
chr12	28677553	28689554	182 intergenic	0
chr10	67597887	67641399	183 Arid5b	0
chr19	21177322	21203399	184 Zfand5	1
chr2	150654107	150687824	185 Gins1	0
chr7	140972924	140994353	186 Dhx32	0
chr11	112475714	112502466	187 Sox9	0
chr7	20400939	20423359	188 Bcl3	0
chrX	13078745	13108406	189 Ddx3x	0
chr19	37416730	37431802	190 Kif11	0
chr7	137807741	137827866	191 Tacc2	0
chr8	10645747	10678366	192 unclear	0
chr15	51499190	51520372	193 intergenic	0
chr1	109382194	109405128	194 SerpinB2	0
chr13	12896585	12917425	195 Prl2c4	0
chr5	104021455	104054255	196 Ptpn13	0
chr9	70096668	70123222	197 Myo1e	1
chr2	102976045	102993275	198 Ehf	0
chr19	21104478	21128241	199 Zfand5	0
chr18	20293481	20317585	200 Dsc3	0
chr2	13324634	13335974	201 Rsu1	0
chr8	129362254	129380574	202 Irf2bp2	0
chr11	100237285	100253033	203 Jup	0
chr6	108477267	108488133	204 Bhlhe40	0
chr6	70755611	70776249	205 Rpia	0
chr15	51296521	51317722	206 Utp23	0
chr6	51006789	51032656	207 intergenic	1
chr16	92900453	92931393	208 Runx1	0
chr9	41896173	41918827	209 Sorl1	0
chr18	39893555	39917932	210 Nr3c1	0
chr9	66053142	66088437	211 Dapk2	0
chr10	96082170	96096571	212 Btg1	0
chr19	57254892	57279178	213 Ablim1	0
chr8	36960651	36984546	214 Cldn23	0
chr8	120006857	120018230	215 Plcg2	0
chr9	44853841	44870389	216 Mpzl3	0
chr2	84457874	84477852	217 Ctnnd1	0
chrX	137030118	137064702	218 Tsc22d3	0
chr18	21119176	21133317	219 Rnf138	0
chr18	64835692	64878521	220 Atp8b1	0
chr8	129040157	129075678	221 Irf2bp2	0
chr6	65137292	65145820	222 Hpgds	0
chr5	73954220	73971131	223 Dcun1d4	0
chr14	26283662	26310419	224 Zmiz1	1

chr2	117604879	117630494	225 4930412B13Rik	0
chr11	102911045	102920403	226 Nmt1	0
chr16	92988784	93014621	227 Runx1	0
chr19	42066190	42098244	228 Ubtd1	0
chr8	75799128	75815511	229 Large	0
chr6	108391346	108408185	230 Bhlhe40	0
chr11	112627725	112650380	231 Sox9	0
chr12	86790435	86802198	232 Fos	0
chr12	53917138	53938517	233 Arhgap5	0
chr14	103887424	103909842	234 Scel	0
chr10	17471191	17499411	235 Cited2	0
chr16	97891818	97919094	236 Ripk4	0
chr11	97276333	97304476	237 Arhgap23	1
chr4	123082701	123104324	238 Macf1	1
chr6	113609826	113641232	239 Irak2	0
chr1	162178478	162211856	240 Cacybp	0
chr16	55714413	55738597	241 Nfkbiz	0
chr2	143671514	143693669	242 Dstn	0
chr7	123631390	123669288	243 Pik3c2a	0
chr2	107065632	107075868	244 2700007P21rik	0
chr19	47385297	47406602	245 Sh3pxd2a	1
chr12	53875168	53889556	246 Arhgap5	0
chr7	82539626	82572899	247 Akap13	0
chr18	61902094	61912116	248 Grpel2	0
chr18	67458237	67484807	249 Impa2	0
chr8	97659781	97700619	250 Kif3c	0
chr1	191593699	191640091	251 Ptpn14	0
chr18	65895590	65909152	252 Zfp532	0
chr12	56562183	56580490	253 Nfkbia	0
chr19	44304112	44324157	254 Scd3	0
chr15	58075809	58105951	255 Fbxo32	0
chr8	27918333	27946533	256 Zfp703	0
chr11	76277570	76309026	257 Timm22	0
chr17	53708864	53737329	258 Kat2b	1
chr2	127450531	127489720	259 Mal	0
chr10	85633416	85663993	260 Timp3	0
chr10	27690747	27710136	261 Ptpk	0
chr15	59372034	59404457	262 Nsmce2	0
chr6	129110368	129135336	263 Clec2d	0
chr19	41063066	41086839	264 Zfp518a	0
chr5	124486776	124503708	265 Vps37b	0
chr10	121328948	121349593	266 Srgap1	0
chr4	137407499	137426681	267 Ece1	0
chr2	28378733	28386364	268 Ralgs	1
chr8	109084723	109107206	269 Cdh1	0

chr15	100992191	101015419	270 Acvr1b	1
chr1	185728561	185758957	271 1700056E22Rik	0
chr8	10414825	10437662	272 Irs2	0
chr3	95496090	95512728	273 Mcl1	0
chr12	114031229	114037779	274 Cep170b	0
chr18	4959068	4978948	275 Svll	0
chr6	142285388	142292126	276 Slco1a5	0
chr1	184167434	184187326	277 Degs1	0
chr13	98299865	98322589	278 Rgnef	0
chrX	73077415	73092978	279 Pls3	0
chr9	34930532	34972064	280 Dcps	0
chr15	61125884	61142495	281 myc	0
chr10	80125589	80143308	282 Mknk2	0
chr12	114260067	114279759	283 Pacs2	0
chr16	26233670	26253821	284 Cldn1	0
chr12	87296718	87353346	285 1700019e19Rik	0
chr12	88116544	88143268	286 Irf2bpl	0
chr17	88008478	88020292	287 Epcam	0
chr5	44155932	44202308	288 Fbxl5	0
chr10	67700300	67713165	289 Arid5b	1
chr10	24159546	24187322	290 Ctgf	1
chr11	5385464	5413558	291 Xbp1	0
chr9	74923447	74940669	292 Myo5a	0
chr13	6189890	6200006	293 Klf6	0
chr15	36771025	36786534	294 Ywhaz	0
chr10	3155257	3172781	295 Cnksr3	0
chr7	151748395	151765891	296 Ppfia1	0
chr10	41838072	41862128	297 Foxo3	0
chr9	70681366	70696673	298 Adam10	0
chr19	32329148	32349838	299 Sgms1	0
chr12	81927718	81964798	300 Zfp36l2	1
chr16	92598210	92627870	301 Runx1	0
chr8	27856222	27869363	302 Zfp703	0
chr10	98698578	98711156	303 Dusp6	0
chr2	165941641	165974917	304 Sulf2	0
chr12	36336613	36359169	305 Ahr	0
chr6	114810358	114844929	306 Vgll4	1
chr1	180968690	180979614	307 Smyd3	0
chr1	38005313	38029567	308 Txnnc9	0
chr5	136353163	136370008	309 Hspb1	0
chr12	88207213	88238115	310 Irf2bpl	0
chr9	50276861	50288378	311 1600029D21Rik	0
chr6	98896883	98906544	312 Foxp1	0
chr19	24237855	24255569	313 Tjp2	0
chr11	120844787	120877721	314 Csnk1d	0

chr9	104245910	104286021	315 Acpp	0
chr5	142900140	142922058	316 Foxk1	1
chr11	45629429	45646517	317 Clint1	0
chr11	45972701	45992240	318 Nipal4	0
chr1	69479076	69515524	319 Ikzf2	0
chr2	167508386	167520124	320 Cebpb	0
chr7	117427116	117435613	321 Sbf2	0
chr10	126998804	127035065	322 Lrp1	0
chr14	102180456	102205944	323 Lmo7	0
chr6	149204810	149213095	324 2810474O19Rik	0
chr19	55288138	55307331	325 Acsf5	0
chr2	32009525	32039188	326 Prrc2b	1
chr16	30503450	30529058	327 Lsg1	0
chr2	128220730	128249892	328 Gm14005	0
chr6	91431631	91442118	329 Chchd4	0
chr4	139076544	139114953	330 Iffo2	1
chr2	137419224	137435350	331 Jag1	0
chr15	37121141	37132769	332 Grhl2	0
chr19	32365386	32397939	333 Sgms1	0
chr4	133039540	133050848	334 Fam46b	0
chr12	14292444	14312245	335 Gm16497	0
chr11	115807745	115832896	336 Itgb4	1
chr19	56988222	57015816	337 Afap1l2	0
chr6	67385013	67412225	338 Tacstd2	0
chr2	170132304	170148314	339 Zfp217	0
chr3	108204789	108229347	340 Psrcl	0
chr1	132657434	132673442	341 AA986860	0
chr9	40574250	40616798	342 Hspa8	0
chr17	54277436	54308148	343 intergenic	0
chr6	72462341	72503544	344 Capg	0
chr17	27174589	27212810	345 Itpr3	1
chr3	95528615	95539220	346 Ecm1	0
chr11	70383467	70401272	347 Mink1	1
chr16	77737466	77756406	348 mir125b-2	0
chr12	81133103	81150468	349 Zfp36l1	0
chr8	119635591	119662053	350 Gan	0
chr17	26670329	26693400	351 Ergic1	0
chr10	116954867	116970040	352 intergenic	0
chr3	95916720	95941344	353 Otud7b	0
chr18	62328188	62364556	354 Adrb2	0
chr7	26660925	26689000	355 Cyp2b10	0
chr10	116119454	116146335	356 Cnot2	0
chr11	51884860	51894766	357 Ppp2ca	0
chr11	22963312	22980103	358 Cct4	0
chr19	4408497	4431396	359 Rhod	0

chr1	137821348	137841829	360 Pkp1	0
chr14	79902902	79934811	361 Elf1	0
chr1	184016569	184025664	362 Enah	0
chr12	36549478	36560287	363 Ahr	0
chr18	62251670	62264033	364 Adrb2	0
chr3	79333122	79364863	365 Fnip2	0
chr2	85349426	85375584	366 4833423E24Rik	0
chr2	173082161	173107286	367 Pmepa1	0
chr11	4197017	4210460	368 Lif	0
chr19	57048696	57070777	369 Afap1l2	0
chr2	79376057	79408103	370 Ssfa2	1
chr19	32254242	32274048	371 Sgms1	0
chr15	59651476	59677687	372 Trib1	0
chr5	30022108	30038556	373 Dnajb6	0
chr17	29561616	29597519	374 Pim1	0
chr2	107162188	107187134	375 Kcna4	0
chr1	71436078	71449514	376 Abca12	0
chr4	56487838	56506261	377 Ikbkap	0
chr6	145915010	145928268	378 Bhlhe41	0
chr12	36386870	36402178	379 Ahr	0
chr6	140488942	140498092	380 Aebp2	0
chr8	82062438	82086844	381 Otud4	0
chr1	76636701	76661676	382 intergenic	0
chr9	77266059	77289456	383 Lrrc1	0
chr9	76400620	76416237	384 Fam83b	0
chr3	122160493	122179795	385 Bcar3	0
chr17	71437150	71445117	386 Myl12a	0
chr1	43200012	43227285	387 Fhl2	0
chr9	102663789	102682424	388 Amotl2	0
chr5	73294896	73313233	389 Slain2	0
chr16	44225292	44242209	390 Gm608	0
chr12	85562564	85588421	391 Elmsan1	0
chr14	120690574	120726012	392 Mbnl2	1
chr7	103376909	103395324	393 Odz4	0
chr3	148732478	148749451	394 Lphn2	0
chr2	167533621	167558765	395 Cebpb	0
chr6	54799724	54819470	396 Znrf2	0
chr16	5118261	5137439	397 Ppl	1
chr12	77641022	77660270	398 Plekhg3	0
chr3	141980165	142009926	399 Pdlim5	0
chr9	70767038	70776281	400 Adam10	0
chr16	95879687	95905602	401 Ets2	1
chr1	127377974	127424943	402 Actr3	0
chr2	24287714	24311161	403 Psd4	0
chr11	59216110	59228693	404 Snap47	0

chr3	94857757	94872446	405 Psmc4	0
chr2	37602202	37613661	406 Strbp	0
chr2	26402327	26413419	407 Notch1	0
chr16	29909646	29917911	408 Hes1	0
chr11	72282094	72300728	409 Spns2	0
chr3	95474372	95481376	410 Mcl1	1
chr9	76540695	76550720	411 Fam83b	0
chr16	55769350	55791216	412 Nfkbiz	0
chr15	77011776	77051493	413 Rbfox2	1
chr13	63340608	63355814	414 mir23b	1
chr15	66807161	66831105	415 Ndrp1	0
chr18	78026266	78039966	416 Pstpip2	0
chr9	116219954	116241441	417 Tgfb2	0
chr15	61437381	61453015	418 myc	0
chr15	59553618	59572555	419 Trib1	0
chr1	74341306	74346345	420 Arpc2	1
chr5	77536721	77549438	421 Hopx	0
chr6	120746031	120752746	422 Atp6v1e1	0
chr16	18644671	18660198	423 Sept5	0
chr12	120449084	120470068	424 Itgb8	1
chr1	173399214	173409446	425 F11r	0
chr12	77558322	77581086	426 Plekhg3	0
chr7	141686137	141695604	427 Adam12	0
chr4	57164290	57180575	428 Epb4.1l4b	1
chr3	89120603	89135881	429 Efna1	0
chr6	121143148	121155442	430 Pex26	0
chr10	77880311	77892072	431 Cstb	0
chr12	77959066	77969624	432 Fntb	0
chr6	121010582	121019263	433 Mical3	0
chr19	5014807	5019776	434 Rin1	0
chr12	113351597	113361218	435 Mir203	0
chr4	107222786	107240238	436 Glis1	0
chr11	80572706	80606334	437 Myo1d	0
chr11	86873747	86884126	438 Gdpd1	0
chr17	35931607	35952224	439 Ier3	0
chr7	80676037	80692000	440 Chd2	1
chr8	25615293	25632930	441 1810011O10Rik	0
chr1	181052398	181072601	442 Smyd3	0
chr6	83341405	83362564	443 Bola3	0
chr6	42362983	42377147	444 EphA1	0
chr5	150175919	150195118	445 unclear	0
chr8	87180235	87192247	446 Ier2	0
chr2	6077943	6087819	447 Proser2	0
chr10	21492547	21512261	448 Sgk1	0
chr12	3316931	3330869	449 Rab10	0

chr8	19132719	19151357	450 Defb14	0
chr2	30097348	30126143	451 Lrrc8a	0
chr10	127358693	127365125	452 unclear	0
chr7	87968632	87988872	453 Iqgap1	0
chr8	109149277	109172207	454 Cdh1	1
chr13	29716594	29732907	455 E2F3	0
chr8	37701660	37708175	456 Dlc1	0
chr5	73791445	73804490	457 Cwh43	0
chr10	69403851	69427624	458 Ank3	0
chr17	43063418	43080984	459 Cd2ap	0
chr4	111552432	111582537	460 Slc5a9	0
chr11	83893581	83916109	461 Dusp14	0
chr8	113334036	113350297	462 Sf3b3	0
chr13	3767263	3782516	463 Calml3	0
chr8	47950232	47957261	464 Irf2	0
chr8	46609081	46617173	465 Sorbs2	0
chr8	73172418	73206727	466 Jund	0
chr6	120211299	120228470	467 B4galnt3	1
chr10	12650476	12677913	468 Stx11	0
chr5	63192512	63207841	469 Arap2	0
chr8	96880988	96902375	470 Herpud1	0
chr3	41312590	41327858	471 Phf17	0
chr2	141090977	141107018	472 Flrt3	0
chr6	134620150	134652359	473 Dusp16	0
chr9	102611256	102629709	474 Amotl2	0
chr12	77982613	78007361	475 Max	0
chr4	89014565	89030406	476 Cdkn2b	0
chr3	116651478	116667882	477 Palmd	1
chr9	78469183	78482749	478 Cd109	0
chr2	94572036	94580460	479 intergenic	0
chr15	27493086	27510374	480 Fam105b	0
chr11	96152691	96174182	481 Hoxb9	0
chr10	111108333	111132329	482 Nap1l1	0
chr2	128276570	128297713	483 Gm14005	0
chr19	10004969	10030590	484 Fth1	0
chr10	76092340	76106284	485 Col6a2	0
chr12	76926301	76934990	486 Syne2	0
chr6	48152454	48178159	487 Zfp746	0
chr11	85079257	85093048	488 Ppm1d	0
chr10	102106482	102134290	489 intergenic	0
chr9	66836937	66874432	490 Tpm1	0
chr2	103101927	103119818	491 Ehf	0
chr6	145940935	145968608	492 Bhlhe41	0
chr18	38341979	38356754	493 Pcdh1	0
chr2	130313227	130328322	494 Ptpra	0

chr1	137651805	137668499	495 Phlda3	0
chr13	38209719	38221437	496 Dsp	0
chr10	117152827	117167290	497 Mdm2	0
chr18	5395856	5415637	498 Zfp438	1
chr9	75264622	75283212	499 Mapk6	0
chr15	36946265	36961636	500 Zfp706	0
chr12	77906120	77920493	501 Fntb	0
chr14	41760133	41770700	502 Tspan14	0
chr3	122199549	122229096	503 Bcar3	0
chr17	21605258	21617622	504 Zfp53	0
chr11	62626823	62640729	505 Trim16	0
chr11	22522896	22545215	506 B3gnt2	0
chr9	122012001	122021167	507 Snrk	0
chr15	59340904	59356207	508 Nsmce2	0
chr6	108646841	108664248	509 Bhlhe40	0
chr2	102784227	102800674	510 Cd44	0
chr9	106278835	106297528	511 Dusp7	1
chr6	61182369	61199164	512 Ccser1	0
chr11	121492336	121515216	513 Tbcd	0
chr1	185684333	185693582	514 Dusp10	0
chr6	41496987	41538330	515 Ephb6	1
chr7	135065612	135079598	516 Prss8	0
chr13	33653590	33679384	517 intergenic	0
chr15	62511987	62546615	518 intergenic	0
chr1	10243261	10248787	519 Arfgef1	0
chr11	98529356	98540718	520 Psmc3	0
chr13	38162801	38190708	521 Dsp	0
chr3	97821144	97840227	522 Notch2	0
chr8	77562013	77590936	523 Hmox1:Mcm5	0
chr8	42079918	42096908	524 Mtus1	0
chr2	91081426	91090942	525 Pacsin3	0
chr2	27558292	27578244	526 Rxra	1
chr16	17153709	17191650	527 Ydjc	0
chr9	43128355	43139998	528 Trim29	0
chr3	151774000	151791626	529 Fubp1	0
chr17	44716857	44727025	530 Runx2	0
chr9	43092964	43112003	531 Trim29	0
chr6	37646993	37657479	532 Trim24	0
chr5	31897917	31913200	533 Mrpl33	0
chr5	144271667	144280033	534 Rac1	1
chr13	3819980	3832830	535 Net1	0
chr1	108342213	108360051	536 Phlpp1	0
chr2	115433133	115442941	537 BC052040	0
chr3	93308126	93322112	538 S100a10	0
chr13	34281015	34305697	539 Psmg4	0

chr12	78025724	78030706	540 Max	0
chr4	80519999	80541949	541 Lurap1l	0
chr12	80452698	80486386	542 Zfp36l1	0
chr15	74614072	74620972	543 Ly6d	0
chr5	73734740	73764669	544 Ociad1	0
chr13	74899585	74910712	545 Cast	0
chr10	67500395	67505827	546 Arid5b	0
chr6	50351522	50374237	547 Osbpl3	0
chr1	53894551	53913358	548 Stk17b	0
chr1	194963586	194972674	549 Irf6	0
chr5	73230318	73249551	550 Slain2	0
chr5	92917286	92929840	551 Scarb2	0
chr4	134832110	134858027	552 Clic4	0
chr3	65725929	65734411	553 Ccnl1	0
chr16	95933480	95952098	554 Ets2	0
chr9	31658959	31690290	555 Barx2	1
chr17	44681488	44693712	556 Runx2	0
chr6	34663323	34686101	557 Cald1	0
chr11	61510257	61522573	558 Fam83g	1
chr4	107158456	107168696	559 Glis1	0
chr14	21424119	21430456	560 Usp54	0
chr15	59297048	59316999	561 Nsmce2	0
chr13	72761185	72778280	562 Irx2	1
chr16	32852856	32865593	563 Fytd1	0
chr8	25576505	25596027	564 1810011O10Rik	0
chr7	105706140	105713710	565 2210018M11Rik	0
chr5	31865948	31884546	566 Mrpl33	0
chr7	31542856	31555506	567 Dmkn	0
chr7	91319191	91338664	568 Abhd17c	0
chr8	129396234	129409064	569 Irf2bp2	0

References

- Adam, R.C. *et al.* (2015) Pioneer factors govern super-enhancer dynamics in stem cell plasticity and lineage choice. *Nature* 521, 366-270
- Ambrosi, C. *et al.* (2017) Dynamics and Context-Dependent Roles of DNA Methylation. *J Mol Biol* pii: S0022-2836, 30083-30089
- Banerji, J. *et al.* (1981) Expression of a β -globin gene is enhanced by remote SV40 DNA sequences. *Cell* 27, 299–308
- Baubec, T. *et al.* (2015) Genomic profiling of DNA methyltransferases reveals a role for DNMT3B in genic methylation. *Nature* 520, 243-247
- Benoit, Y.D. *et al.* (2012) Polycomb repressive complex 2 impedes intestinal cell terminal differentiation. *J. Cell Sci.* 125, 3454-3463
- Bergman, Y. and Cedar, H. (2013) DNA methylation dynamics in health and disease. *Nat. Struct. Mol. Biol.* 20, 274-281
- Beronja, S. *et al.* (2010) Rapid functional dissection of genetic networks via tissue-specific transduction and RNAi in mouse embryos. *Nat Med.* **16**, 821-827. doi: 810.1038/nm.2167. Epub 2010 Jun 1036. (2010).
- Blackledge, N.P. *et al.* (2014) Variant PRC1 complex-dependent H2A ubiquitylation drives PRC2 recruitment and polycomb domain formation. *Cell* 157, 1445-1459
- Blanpain, C. *et al.* (2004) Self-renewal, multipotency, and the existence of two cell populations within an epithelial stem cell niche. *Cell* 118, 635-648
- Blanpain, C. *et al.* (2006) Canonical notch signaling functions as a commitment switch in the epidermal lineage. *Genes Dev* 20, 3022-3035
- Blanpain, C. and Fuchs, E. (2009) Epidermal homeostasis: a balancing act of stem cells in the skin. *Nat Rev Mol Cell Biol* 10, 207-217
- Blanpain, C. and Fuchs, E. (2014) Stem cell plasticity. Plasticity of epithelial stem cells in tissue regeneration. *Science* 344, 1242281
- Bock, C. *et al.* (2012) DNA methylation dynamics during in vivo differentiation of blood and skin stem cells. *Mol. Cell* 47, 633-647
- Bröske, A.M. *et al.* (2009) DNA methylation protects hematopoietic stem cell multipotency from myeloerythroid restriction. *Nat. Genet.* 41, 1207-1215

- Buczacki, S.J. *et al.* (2013) Intestinal label-retaining cells are secretory precursors expressing Lgr5. *Nature* 495, 65-69
- Buenrostro, J.D. *et al.* (2013) Transposition of native chromatin for fast and sensitive epigenomic profiling of open chromatin, DNA-binding proteins and nucleosome position. *Nat Methods* 10, 1213-1218
- Campbell, C.E. *et al.* (2008) The transcription factor Nfix is essential for normal brain development. *BMC Dev Biol* 8, 52
- Cantor, A.B. *et al.* (2008) Antagonism of FOG-1 and GATA factors in fate choice for the mast cell lineage. *J. Exp. Med.* 205, 611-624
- Challen, G.A. *et al.* (2011) Dnmt3a is essential for hematopoietic stem cell differentiation. *Nat. Genet.* 44, 23-31
- Challen, G.A. *et al.* (2014) Dnmt3a and Dnmt3b have overlapping and distinct functions in hematopoietic stem cells. *Cell Stem Cell* 15, 350-364
- Chang, C. Y. *et al.* (2013) NFIB is a governor of epithelial-melanocyte stem cell behaviour in a shared niche. *Nature* 495, 98-102
- Chen, T. *et al.* (2012) An RNA interference screen uncovers a new molecule in stem cell self-renewal and long-term regeneration. *Nature* 485, 104-108
- Chi, A.S. and Bernstein, B.E. (2009) Developmental biology. Pluripotent chromatin state. *Science* 323, 220-221
- Creyghton, M. P. *et al.* (2010) Histone H3K27ac separates active from poised enhancers and predicts developmental state. *Proc Natl Acad Sci U S A* 107, 21931-21936
- Das Neves, L. *et al.* (1999) Disruption of the murine nuclear factor I-A gene (Nfia) results in perinatal lethality, hydrocephalus, and agenesis of the corpus callosum. *Proc Natl Acad Sci USA* 96, 11946-11951
- Driller, K. *et al.* (2007) Nuclear factor I X deficiency causes brain malformation and severe skeletal defects. *Molecular and Cellular Biology* 27, 3855-3867
- Ellis, T. *et al.* (2001) The transcriptional repressor CDP (Cutl1) is essential for epithelial cell differentiation of the lung and the hair follicle. *Genes Dev* 15, 2307-2319
- Ernst, J. *et al.* (2011) Mapping and analysis of chromatin state dynamics in nine human cell types. *Nature* 473, 43-49
- Ezhkova, E. *et al.* (2009) Ezh2 orchestrates gene expression for the stepwise differentiation of tissue-specific stem cells. *Cell* 136, 1122-1135

- Ezhkova, E. *et al.* (2011) EZH1 and EZH2 cogovern histone H3K27 trimethylation and are essential for hair follicle homeostasis and wound repair. *Genes Dev.* 25, 485-498
- Folgueras, A.R. *et al.* (2013) Architectural niche organization by LHX2 is linked to hair follicle stem cell function. *Cell Stem Cell* 13, 314-327
- Frye, M. and Benitah, S.A. (2012) Chromatin regulators in mammalian epidermis. *Semin. Cell. Dev. Biol.* 23, 897-905
- Gertz, J. *et al.* (2013) Distinct properties of cell-type-specific and shared transcription factor binding sites. *Mol. Cell* 52, 25-36
- Gosselin, D. *et al.* (2014) Environment drives selection and function of enhancers controlling tissue-specific macrophage identities. *Cell* 159, 1327-1340
- Gronostajski, R.M. *et al.* (1985) Site-specific DNA binding of nuclear factor I: analyses of cellular binding sites. *Molecular and Cellular Biology* 5, 964-971
- Gründer, A. *et al.* (2002) Nuclear factor I-B (Nfib) deficient mice have severe lung hypoplasia. *Mechanisms of Development* 112, 69-77
- He, Y.F. *et al.* (2011) Tet-mediated formation of 5-carboxylcytosine and its excision by TDG in mammalian DNA. *Science* 333, 1303-1307
- Heintzman, N.D. *et al.* (2009) Histone modifications at human enhancers reflect global cell-type-specific gene expression. *Nature* 459, 108-112
- Heinz, S. *et al.* (2010) Simple combinations of lineage-determining transcription factors prime cis-regulatory elements required for macrophage and B cell identities. *Mol. Cell* 38, 576-589
- Heinz, S. *et al.* (2015) The selection and function of cell type-specific enhancers. *Nat Rev Mol Cell Biol.* 16, 144-154
- Hennighausen, L. *et al.* (1985) High-affinity binding site for a specific nuclear protein in the human IgM gene. *Nature* 314, 289-292
- Hidalgo, I. *et al.* (2012) Ezh1 is required for hematopoietic stem cell maintenance and prevents senescence-like cell cycle arrest. *Cell Stem Cell* 11, 649-662
- Hnisz, D. *et al.* (2013) Super-enhancers in the control of cell identity and disease. *Cell* 155, 934-947
- Hnisz, D. *et al.* (2015) Convergence of developmental and oncogenic signaling pathways at transcriptional super-enhancers. *Mol. Cell* 58, 362-370

- Hodges, E. *et al.* (2011) Directional DNA methylation changes and complex intermediate states accompany lineage specificity in the adult hematopoietic compartment. *Mol. Cell* 44, 17-28
- Hon, G.C. *et al.* (2014) 5mC oxidation by Tet2 modulates enhancer activity and timing of transcriptome reprogramming during differentiation. *Mol. Cell* 56, 286-297
- Horsley, V. *et al.* (2008) NFATc1 balances quiescence and proliferation of skin stem cells. *Cell* 132, 299-310
- Hsu, Y.C. *et al.* (2011a) Dynamics between stem cells, niche, and progeny in the hair follicle. *Cell* 144, 92-105
- Hsu Y.C. *et al.* (2011b) Mesenchymal nuclear factor I B regulates cell proliferation and epithelial differentiation during lung maturation. *Dev Biol* 354, 242–252
- Hsu, Y.C. *et al.* (2014) Transit-amplifying cells orchestrate stem cell activity and tissue regeneration. *Cell* 157, 935-949
- Hwang, W.W. *et al.* (2014) Distinct and separable roles for EZH2 in neurogenic astroglia. *Elife* 3:e02439
- Ito, M. *et al.* (2005) Stem cells in the hair follicle bulge contribute to wound repair but not to homeostasis of the epidermis. *Nat. Med.* 11, 1351–1354
- Ito, S. *et al.* (2011) Tet proteins can convert 5-methylcytosine to 5-formylcytosine and 5-carboxylcytosine. *Science* 333, 1300-1303
- Jones, K.A. *et al.* (1987) A cellular DNA-binding protein that activates eukaryotic transcription and DNA replication. *Cell* 48, 79–89
- Jones, P.A. (2012) Functions of DNA methylation: islands, start sites, gene bodies and beyond. *Nat. Rev. Genet* 13, 484-492
- Juan, A.H. *et al.* (2011) Polycomb EZH2 controls self-renewal and safeguards the transcriptional identity of skeletal muscle stem cells. *Genes Dev.* 25, 789-794
- Junion, G. *et al.* (2012) A transcription factor collective defines cardiac cell fate and reflects lineage history. *Cell* 148, 473-486
- Kadaja, M. *et al.* (2014) SOX9: a stem cell transcriptional regulator of secreted niche signaling factors. *Genes Dev.* 28, 328-341
- Kandyba, E. *et al.* (2013) Competitive balance of intrabulge BMP/Wnt signaling reveals a robust gene network ruling stem cell homeostasis and cyclic activation. *Proc Natl Acad Sci U S A* 110, 1351-1356

- Keyes, B.E. *et al.* (2013) Nfatc1 orchestrates aging in hair follicle stem cells. *Proc. Natl. Acad. Sci. U S A* 110, E4950-4959
- Khavari, D.A. *et al.* (2010) DNA methylation and epigenetic control of cellular differentiation. *Cell Cycle* 9, 3880-3883
- Kim, T.H. *et al.* (2014) Broadly permissive intestinal chromatin underlies lateral inhibition and cell plasticity. *Nature* 506, 511-515
- Klose R.J. and Bird, A.P. (2006) Genomic DNA methylation: the mark and its mediators. *Trends Biochem Sci.* 31, 89-97
- Ko, M. *et al.* (2011) Ten-Eleven-Translocation 2 (TET2) negatively regulates homeostasis and differentiation of hematopoietic stem cells in mice. *Proc. Natl. Acad. Sci. U S A.* 108, 14566-14571
- Kruse, U., and Sippel, A.E. (1994) Transcription factor nuclear factor I proteins form stable homo- and heterodimers. *FEBS Letters* 348, 46–50
- Kunimoto, H. *et al.* (2012) Tet2 disruption leads to enhanced self-renewal and altered differentiation of fetal liver hematopoietic stem cells. *Sci. Rep.* 2, 273
- Lara-Astiaso, D. *et al.* (2014) Immunogenetics. Chromatin state dynamics during blood formation. *Science* 345, 943-949
- Lavin, Y. *et al.* (2014) Tissue-resident macrophage enhancer landscapes are shaped by the local microenvironment. *Cell* 159, 1312-1326
- Leegwater, P.A. *et al.* (1985) Recognition site of nuclear factor I, a sequence-specific DNA-binding protein from HeLa cells that stimulates adenovirus DNA replication. *Embo J* 4, 1515–1521
- Li, J. *et al.* (2012) Progressive alopecia reveals decreasing stem cell activation probability during aging of mice with epidermal deletion of DNA methyltransferase 1. *J Invest Dermatol.* 132, 2681-2690
- Li, Z. *et al.* (2011) Deletion of Tet2 in mice leads to dysregulated hematopoietic stem cells and subsequent development of myeloid malignancies. *Blood* 118, 4509-4518
- Lien, W.H. *et al.* (2011) Genome-wide maps of histone modifications unwind in vivo chromatin states of the hair follicle lineage. *Cell Stem Cell* 9, 219-232
- Lien, W.H. *et al.* (2014) In vivo transcriptional governance of hair follicle stem cells by canonical Wnt regulators. *Nat. Cell Biol.* 16, 179-190

- Liu, Z. *et al.* (2014) Enhancer activation requires trans-recruitment of a mega transcription factor complex. *Cell* 159, 358-373
- Lo Celso, C. *et al.* (2004) Transient activation of beta-catenin signalling in adult mouse epidermis is sufficient to induce new hair follicles but continuous activation is required to maintain hair follicle tumours. *Development* 131, 1787-1799
- Lopez-Garcia, C. *et al.* (2010) Intestinal stem cell replacement follows a pattern of neutral drift. *Science* 330, 822-825
- Lovén, J. *et al.* (2013) Selective inhibition of tumor oncogenes by disruption of super-enhancers. *Cell* 153, 320-334
- Lu, C. P. *et al.* (2012) Identification of stem cell populations in sweat glands and ducts reveals roles in homeostasis and wound repair. *Cell* 150, 136-150
- Luyten, A. *et al.* (2014) Active enhancers are delineated de novo during hematopoiesis, with limited lineage fidelity among specified primary blood cells. *Genes Dev.* 28, 1827-1839
- Maunakea, A.K. *et al.* (2010) Conserved role of intragenic DNA methylation in regulating alternative promoters. *Nature* 466, 253-257
- Maunakea, A.K. *et al.* (2013) Intragenic DNA methylation modulates alternative splicing by recruiting MeCP2 to promote exon recognition. *Cell Res.* 23, 1256-1269
- Maurano, M.T. *et al.* (2012) Systematic localization of common disease-associated variation in regulatory DNA. *Science.* 337, 1190–1195
- McGrath, J. A. *et al.* (1995) Mutations in the 180-kD bullous pemphigoid antigen (BPAG2), a hemidesmosomal transmembrane collagen (COL17A1), in generalized atrophic benign epidermolysis bullosa. *Nat Genet* 11, 83-86
- Meisterernst, M., *et al.* (1988) A quantitative analysis of nuclear factor I/DNA interactions. *Nucleic Acids Res* 16, 4419–4435.
- Meisterernst, M., *et al.* (1989) Structural and functional organization of a porcine gene coding for nuclear factor I. *Biochemistry* 28, 8191–8200.
- Mellén, M. *et al.* (2012) MeCP2 binds to 5hmC enriched within active genes and accessible chromatin in the nervous system. *Cell* 151, 1417-1430
- Meredith, D.M. *et al.* (2013) Program specificity for Ptf1a in pancreas versus neural tube development correlates with distinct collaborating cofactors and chromatin accessibility. *Mol. Cell. Biol.* 33, 3166-3179

- Mermod, N. *et al.* (1989) The proline-rich transcriptional activator of CTF/NF-I is distinct from the replication and DNA binding domain. *Cell* 58, 741–753.
- Messina, G., *et al.* (2010) Nfix Regulates Fetal-Specific Transcription in Developing Skeletal Muscle. *Cell* 140, 554–566
- Mochizuki-Kashio, M. *et al.* (2011) Dependency on the polycomb gene Ezh2 distinguishes fetal from adult hematopoietic stem cells. *Blood* 118, 6553–6561
- Moran-Crusio, K. *et al.* (2011) Tet2 loss leads to increased hematopoietic stem cell self-renewal and myeloid transformation. *Cancer Cell* 20, 11–24
- Moriyama, M. *et al.* (2008) Multiple roles of Notch signaling in the regulation of epidermal development. *Dev Cell* 14, 594–604
- Morrison, S.J., and Spradling, A.C. (2008) Stem cells and niches: mechanisms that promote stem cell maintenance throughout life. *Cell* 132, 598–611
- Nagata, K. *et al.* (1982) Adenovirus DNA replication in vitro: identification of a host factor that stimulates synthesis of the preterminal protein-dCMP complex. *Proc Natl Acad Sci USA* 79, 6438–6442
- Neri, F. *et al.* (2017) Intragenic DNA methylation prevents spurious transcription initiation. *Nature* 543, 72–77
- Nguyen, H. *et al.* (2009) Tcf3 and Tcf4 are essential for long-term homeostasis of skin epithelia. *Nat. Genet.* 41, 1068–1075
- Nowak, J.A. *et al.* (2008) Hair follicle stem cells are specified and function in early skin morphogenesis. *Cell Stem Cell* 3, 33–43
- Nowock, J. *et al.* (1985) The TGGCA protein binds to the MMTV-LTR, the adenovirus origin of replication, and the BK virus enhancer. *Nucleic Acids Res* 13, 2045–2061
- Park, D.H. *et al.* (2014) Activation of neuronal gene expression by the JMJD3 demethylase is required for postnatal and adult brain neurogenesis. *Cell Rep.* 8, 1290–1299
- Parker, S. C. *et al.* (2013) Chromatin stretch enhancer states drive cell-specific gene regulation and harbor human disease risk variants. *Proc Natl Acad Sci U S A* 110, 17921–17926
- Pathania, R. *et al.* (2015) DNMT1 is essential for mammary and cancer stem cell maintenance and tumorigenesis. *Nat. Commun.* 6, 6910

- Pereira, J. *et al.* (2010) Ezh2, the histone methyltransferase of PRC2, regulates the balance between self-renewal and differentiation in the cerebral cortex. *Proc. Natl. Acad. Sci. U S A.* 107, 15957-15962
- Pimkin, M. *et al.* (2014) Divergent functions of hematopoietic transcription factors in lineage priming and differentiation during erythro-megakaryopoiesis. *Genome Res.* 24, 1932-1944
- Pongubala, J.M. *et al.* (2008) Transcription factor EBF restricts alternative lineage options and promotes B cell fate commitment independently of Pax5. *Nat. Immunol.* 9, 203-215
- Qi, X. *et al.* (2013) Antagonistic regulation by the transcription factors C/EBP α and MITF specifies basophil and mast cell fates. *Immunity* 39, 97-110
- Quivoron, C. *et al.* (2011) TET2 inactivation results in pleiotropic hematopoietic abnormalities in mouse and is a recurrent event during human lymphomagenesis. *Cancer Cell* 20, 25-38
- Rada-Iglesias, A. *et al.* (2011) A unique chromatin signature uncovers early developmental enhancers in humans. *Nature* 470, 279-283
- Rada-Iglesias, A. *et al.* (2012) Epigenomic annotation of enhancers predicts transcriptional regulators of human neural crest. *Cell Stem Cell* 11, 633-648
- Rhee, H. *et al.* (2006) Lhx2 maintains stem cell character in hair follicles. *Science* 312, 1946-1949
- Rompolas, P. *et al.* (2012) Live imaging of stem cell and progeny behaviour in physiological hair-follicle regeneration. *Nature* 487, 496-499
- Rompolas, P. *et al.* (2013) Spatial organization within a niche as a determinant of stem-cell fate. *Nature* 502, 513-518
- Roulet, E. *et al.* (2000) Experimental analysis and computer prediction of CTF/NFI transcription factor DNA binding sites. *Journal of Molecular Biology* 297, 833-848
- Scadden, D.T. (2014) Nice neighborhood: emerging concepts of the stem cell niche. *Cell* 157, 41-50
- Schaffer, A.E. *et al.* (2010) Nkx6 Transcription Factors and Ptf1a Function as Antagonistic Lineage Determinants in Multipotent Pancreatic Progenitors. *Dev. Cell* 18, 1022-1029
- Schramek, D. *et al.* (2014) Direct in vivo RNAi screen unveils myosin IIa as a tumor suppressor of squamous cell carcinomas. *Science* 343, 309-313

- Schübeler, D. (2015) Function and information content of DNA methylation. *Nature* 517, 321-326
- Schwartz, Y.B. and Pirrotta, V. (2013) A new world of Polycombs: unexpected partnerships and emerging functions. *Nat. Rev. Genet.* 14, 853-864
- Sen, G.L. *et al.* (2008) Control of differentiation in a self-renewing mammalian tissue by the histone demethylase JMJD3. *Genes Dev.* 22, 1865-1870
- Sen, G.L. *et al.* (2010) DNMT1 maintains progenitor function in self-renewing somatic tissue. *Nature* 463, 563-567
- Sharif, J. *et al.* (2007) The SRA protein Np95 mediates epigenetic inheritance by recruiting Dnmt1 to methylated DNA. *Nature* 450, 908-912
- Shaw, T. and Martin, P. (2009) Epigenetic reprogramming during wound healing: loss of polycomb-mediated silencing may enable upregulation of repair genes. *EMBO Rep.* 10, 881-886
- Shen, X. *et al.* (2008) EZH1 mediates methylation on histone H3 lysine 27 and complements EZH2 in maintaining stem cell identity and executing pluripotency. *Mol. Cell* 32, 491-502
- Siersbaek, R. *et al.* (2014) Transcription factor cooperativity in early adipogenic hotspots and super-enhancers. *Cell Rep* 7, 1443-1455
- Smith, Z.D. and Meissner, A. (2013) DNA methylation: roles in mammalian development. *Nat Rev Genet.* 14, 204-220
- Soeda, T., *et al.* (2010) Sox9-expressing precursors are the cellular origin of the cruciate ligament of the knee joint and the limb tendons. *Genesis* 48, 635-644
- Soufi, A. *et al.* (2012) Facilitators and impediments of the pluripotency reprogramming factors' initial engagement with the genome. *Cell* 151, 994-1004.
- Soufi, A. *et al.* (2015) Pioneer transcription factors target partial DNA motifs on nucleosomes to initiate reprogramming. *Cell* 161, 555-568
- Spradling, A., Drummond-Barbosa, D. & Kai, T. (2001) Stem cells find their niche. *Nature* 414, 98-104
- Spruijt, C.G. *et al.* (2013) Dynamic readers for 5-(hydroxy)methylcytosine and its oxidized derivatives. *Cell* 152, 1146-1159

- Stadler, M.B. *et al.* (2011) DNA-binding factors shape the mouse methylome at distal regulatory regions. *Nature* 480, 490-495
- Stange, D. E. *et al.* (2013) Differentiated Troy+ chief cells act as reserve stem cells to generate all lineages of the stomach epithelium. *Cell* 155, 357-368
- Steele-Perkins, G. *et al.* (2003) Essential role for NFI-C/CTF transcription-replication factor in tooth root development. *Molecular and Cellular Biology* 23, 1075–1084
- Steele-Perkins, G. *et al.* (2005) The transcription factor gene Nfib is essential for both lung maturation and brain development. *Molecular and Cellular Biology* 25, 685–698
- Suzuki, H.I. *et al.* (2017) Super-Enhancer-Mediated RNA Processing Revealed by Integrative MicroRNA Network Analysis. *Cell* 168, 1000-1014
- Tahiliani, M. *et al.* (2009) Conversion of 5-methylcytosine to 5-hydroxymethylcytosine in mammalian DNA by MLL partner TET1. *Science* 324, 930-935
- Tavares, L. *et al.* (2012) RYBP-PRC1 complexes mediate H2A ubiquitylation at polycomb target sites independently of PRC2 and H3K27me3. *Cell* 148, 664-678
- Tian, H. *et al.* (2011) A reserve stem cell population in small intestine renders Lgr5-positive cells dispensable. *Nature* 478, 255-259
- Trowbridge, J.J. *et al.* (2009) DNA methyltransferase 1 is essential for and uniquely regulates hematopoietic stem and progenitor cells. *Cell Stem Cell* 5, 442-449
- Tsai, C.C. *et al.* (2012) Oct4 and Nanog directly regulate Dnmt1 to maintain self-renewal and undifferentiated state in mesenchymal stem cells. *Mol. Cell* 47, 169-182
- Tsumura, A. *et al.* (2006) Maintenance of self-renewal ability of mouse embryonic stem cells in the absence of DNA methyltransferases Dnmt1, Dnmt3a and Dnmt3b. *Genes Cells* 11, 805-814
- van Es, J. H. *et al.* (2012) Dll1+ secretory progenitor cells revert to stem cells upon crypt damage. *Nat Cell Biol* 14, 1099-1104
- Vidal, V.P. *et al.* (2005) Sox9 is essential for outer root sheath differentiation and the formation of the hair stem cell compartment. *Curr. Biol.* 15, 1340-1351
- Wamstad, J.A. *et al.* (2012) Dynamic and coordinated epigenetic regulation of developmental transitions in the cardiac lineage. *Cell* 151, 206-220
- Wang, X. *et al.* (2008) AP-2 factors act in concert with Notch to orchestrate terminal differentiation in skin epidermis. *J Cell Biol* 183, 37-48

- Whitlock, N. V. *et al.* (2002) Compound heterozygosity for non-sense and mis-sense mutations in desmoplakin underlies skin fragility/woolly hair syndrome. *J Invest Dermatol* 118, 232-238
- Whyte, W.A. *et al.* (2013) Master transcription factors and mediator establish super-enhancers at key cell identity genes. *Cell* 153, 307-319
- Wilson, N.K. *et al.* (2010) Combinatorial transcriptional control in blood stem/progenitor cells: genome-wide analysis of ten major transcriptional regulators. *Cell Stem Cell* 7, 532-544
- Wu, H. *et al.* (2010) Dnmt3a-dependent nonpromoter DNA methylation facilitates transcription of neurogenic genes. *Science* 329, 444-448
- Wu, X. *et al.* (2011) Skin stem cells orchestrate directional migration by regulating microtubule-ACF7 connections through GSK3beta. *Cell* 144, 341-352
- Yan, J. *et al.* (2013) Transcription factor binding in human cells occurs in dense clusters formed around cohesin anchor sites. *Cell* 154, 801-813
- Yan, K.S. *et al.* (2012) The intestinal stem cell markers Bmi1 and Lgr5 identify two functionally distinct populations. *Proc. Natl. Acad. Sci. U S A* 109, 466-471
- Zaret, K.S. and Carroll, J.S. (2011) Pioneer transcription factors: establishing competence for gene expression. *Genes Dev.* 25, 2227-2241
- Zhang, L. *et al.* (2012) Thymine DNA glycosylase specifically recognizes 5-carboxylcytosine-modified DNA. *Nat Chem Biol.* 8, 328-330
- Zhang, R.R. *et al.* (2013) Tet1 regulates adult hippocampal neurogenesis and cognition. *Cell Stem Cell* 13, 237-245
- Ziller, M.J. *et al.* (2013) Charting a dynamic DNA methylation landscape of the human genome. *Nature* 500, 477-481